Application of Adsorption for Removal of Emerging Pollutants from Drinking Water

A Thesis Submitted to the College of Graduate Studies and Research in

Partial Fulfillment of the Requirements for the Degree of

Master of Science

In the Department of Chemical and Biological Engineering

University of Saskatchewan

Saskatoon, Saskatchewan

Canada

By

Mohamadmahdi Kowsari

PERMISSION TO USE

In presenting this thesis in partial fulfillment of the requirements for a Master of Science degree from the University of Saskatchewan, I agree that the Libraries of this University may make it freely available for inspection. I further agree that permission for copying of this thesis in any manner, in whole or in part, for scholarly purposes may be granted by the professors who supervised my thesis work, in their absence, by the Graduate Chair of the program or Dean of the College in which my thesis work was done. It is understood that any copying, publication, or use of this thesis or parts thereof for financial gain shall not be allowed without my written permission. It is also understood that due recognition shall be given to me and to the University of Saskatchewan in any scholarly use which may be made of any material in my thesis.

Requests for permission to copy or to make other use of material in this thesis in whole or in part should be addressed to:

Head of the Department of Chemical and Biological Engineering

College of Engineering, 57 Campus Drive

University of Saskatchewan

Canada S7N 5A9

ABSTRACT

The potential human health issues resulting from the continuous consumption of drinking water containing low concentration levels of persistent emerging pollutants has raised some concerns. The presence of emerging pollutants in surface water bodies and ground-water in Canada together with absence of proper drinking water treatment processes in remote places has created the need for an effective and simple process for removal of emerging pollutants from drinking water. Low seasonal temperatures in regions such as Saskatchewan demand a removal process that is effective at temperatures lower than room temperature. Adsorption with granular activated carbon is a well-established and effective method for removal of organic compounds from drinking water. There are a large number of reports on removal of organic compounds by activated carbon in literature however, the effectiveness of adsorption of emerging pollutants with granular activated carbon is not clear. Effectiveness of ozone treatment for oxidation of emerging pollutants is reported in literature however, effectiveness of regeneration of adsorbents saturated with emerging pollutants with ozone has not been investigated extensively.

In the present work, effectiveness of adsorption with granular activated carbon for removal of emerging pollutants is investigated. Three model compounds of Ibuprofen, 2,4-dichlorophenoxyacetic acid, and Bisphenol A reported at considerable concentration levels in Saskatchewan water bodies were selected as model compounds. Bituminous coal based and coconut shell based granular activated carbons with basic point of zero charge were selected as adsorbents. Isotherm adsorption of model compounds on adsorbents was conducted at 280, 288, and 296 K. The Gibbs free energy, enthalpy, and entropy of adsorption were calculated using isotherm model parameters. Nitric acid pre-treatment was applied to reduce the point of zero charge of adsorbents. Adsorption isotherms were conducted with the acid treated adsorbents.

Adsorption removal of model compounds in tap water was studied. Effectiveness of regeneration of saturated adsorbents with ozone was investigated.

In terms of quality of fit to the isotherm adsorption data, Langmuir model was better than Freundlich model indicating monolayer adsorption of model compounds in all experiments. Higher Langmuir monolayer adsorption capacity (Q_{max}) of bituminous coal based adsorbent than coconut shell adsorbent for adsorption of model compounds was attributed to the higher porosity of bituminous coal based adsorbent. Adsorption of model compounds (i.e. IBP and BPA) present in molecular form in the pH condition of the experiments were more dependent on adsorbent surface functional groups e.g. carboxyl and carbonyl groups. The Q_{max} of adsorption of 2,4-D present in anionic form was proportional with the specific surface area of adsorbent. Adsorption at temperatures lower than room temperature was effective. Adsorbent with acidic point of zero charge was more effective in removal of model compounds than adsorbent with basic point of zero charge. Adsorption of BPA was higher in tap water in comparison to Millipore water due to the more neutral surface of adsorbent in tap water. Higher pH of tap water than Millipore water and the ionic interaction between the adsorbent and dissolved solids present in tap water caused the more neutral surface of adsorbent. Regeneration of adsorbents with ozone failed in restoration of adsorption capacity of adsorbents and excessive ozonation destroyed the pore structure of adsorbents.

ACKNOWLEDGEMENTS

My best acknowledgement goes to my supervisor, Dr. Jafar Soltan who gave me the opportunity to be a member of his research group and study my research of interest under his supervision. He helped me discover my potentials and encouraged me to develop my research skills. His profound knowledge of chemical engineering together with his patience helped me succeed in all stages of my education.

I also want to express my warmest appreciation to the members of my graduate advisory committee, Dr. Catherine Niu and Dr. Arcadio Rodriguez-Prado for their many invaluable comments and feedbacks.

I want to extend my thanks to Mr. Richard Blondin, Ms. Heli Eunike, and Mr. Dragan Cekic for their kind assistance and valuable knowledge helping me through my experimental works. I would like to appreciate the kind assistant of my research group members, Dr. Ebrahim Rezaei Geshnizgani, Mr. Carlos Guzman Perez, Mr. Mostafa Aghbolaghy, and Ms. Azam Sadeghi.

The financial support provided by the Department of Chemical and Biological Engineering of University of Saskatchewan, National Sciences and Engineering Research Council (NSERC) of Canada, and Shastri Foundation is greatly acknowledged.

I send my warmest gratitude to my kind parents and my lovely siblings, who have encouraged and supported me through all stages of my life unconditionally.

In particular, I would like to thank my sweet soul mate, Bryn Rees, for her love, encouragement, and support.

DEDICATION

*This research is dedicated to **Dr. Taha Kowsari** my brother and **Dr. Jafar Soltan** my supervisor, who this research could not be accomplished without their boundless care and support!*

TABLE OF CONTENTS

LIST OF TABLES

LIST OF FIGURES

NOMENCLATURE

Greek Letters:

$\Delta G°$	Standard Gibbs free energy of adsorption (kJ/mol)
$\Delta H°$	Standard enthalpy of adsorption (kJ/mol)
$\Delta S°$	Standard entropy of adsorption (J/mol.K)
σ_m	Cross-sectional area of a N_2 molecule equal to 0.162 (nm^2/molecule)

English Letters:

1/n	Freundlich adsorption affinity
2,4-D	2,4-Dichlorophenoxyacetic acid ($C_8H_6Cl_2O_3$)
b	Langmuir intensity of adsorption (L/g)
BC	Washed, sieved, and dried Filtrasorb®400
BET	Brunauer-Emmett-Teller
BJH	Barrett-Joyner-Halenda
BPA	Bisphenol A ($C_{15}H_{16}O_2$)
C_0	Initial concentration of solute in liquid phase (mg/L)
C_e	Equilibrium concentration of solute in liquid phase (mg/L)
CS	Washed Sieved, and dried AquaSorb®CS

D_{ave}	Average pore width (nm)
EP	Emerging pollutant
GAC	Granular activated carbon
IBP	Ibuprofen ($C_{13}H_{18}O_2$)
K'_c	Apparent equilibrium constant
$K°_c$	Standard equilibrium constant
K_F	Freundlich relative adsorption maximum capacity ($mg^{(n-1)/n}.L^{1/n}.g^{-1}$)
Log K_{OW}	Octanol-water partition coefficient
n^a_m	N_2 monolayer maximum capacity
N-BC	Acid treated BC
N-CS	Acid treated CS
pKa	Acid dissociation constant
PZC	Point of zero charge
q_e	Solute concentration on adsorbent at equilibrium (mg/g)
Q_{max}	Langmuir monolayer maximum adsorption capacity (mg/g)
rpm	Round per minute
S_{BET}	Adsorbent specific surface area (m^2/g)

S-BC	BC saturated with IBP, 2,4-D, and BPA
S-CS	CS saturate with IBP, 2,4-D, and BPA
$S_{External}$	(Adsorbent specific surface area) – (Surface area of micropores) (m^2/g)
SEM	Scanning Electron Microscope
S_{Micro}	Micropores surface area (pore size range of 0.4-2 nm) (m^2/g)
UV-Vis	Ultraviolet and visible light
V	Volume of the solution (L)
V_{BET}	Adsorbent specific pore volume (cm^3/g)
W	Weight of adsorbent (g)

CHAPTER ONE

INTRODUCTION

Occurrence of emerging pollutants (EPs) in surface water bodies and ground-waters has been reported in the past decades [1]. Long term consumption of drinking water containing low concentration of these compounds can cause health issues [2]. Surface water bodies and ground waters are the resources for drinking water and the influent of the drinking water treatment plants [3]. Some of EPs are persistent in nature and hard to remove. Poor removal of these compounds in inefficient drinking water treatment plants or lack of drinking water treatment plants in rural areas will lead to presence of these compounds in drinking water. The need for development of effective process for removal of these emerging pollutants for treatment of tap water is becoming a reality. Granular activated carbon (GAC) filtration is an effective and established method for removal of organic compounds from drinking water [4-6]. Extent of adsorption of various compounds on activated carbon depends on physical and chemical characteristics of adsorbent, adsorbate, and water matrix [6]. The EP molecules have complex structures and it is hard to predict their adsorption behaviour on GAC. This research aims to clarify effectiveness of removal of EPs using GAC.

1.1. Research Motivation and Experimental Considerations

The mixture of EPs in concentration levels up to 35 μg/L in the upstream of South Saskatchewan River in Medicine Hat has been reported [7]. EPs pass untreated through secondary stage of conventional wastewater treatment plants. Effluent of wastewater treatment plants is released into the rivers at upstream and downstream drinking water treatment plants use the same river water as the influent. In addition, runoff of farming irrigation in Saskatchewan unavoidably releases agrochemicals into surface waters and ground waters [8]. EPs present in sewage leak into aquifers from stabilization lagoons and septic tanks. Rural communities usually are not served by sophisticated drinking water treatments plants or they directly consume ground water using water wells. Thus, removal of the EPs present in the water before consumption is necessary to avoid the consequent health issues.

Considering the low average temperature of tap water in cold regions such as 283 K for Saskatoon and the effect of temperature on water treatment processes [9], it is necessary to have a treatment process that is efficient in removal of EPs at temperatures ranging from below the room temperature to close to freezing temperature of water. GAC filtration is a well-established method for removal of organic compounds. On the other hand, EP molecules often contain aromatic rings [10] in their structure which is favourable for adsorption on GAC. However, removal of EPs at temperatures in the range of 280 to 296 K is not reported in the literature. To gain a better understanding of the effect of temperature on adsorption of the model compounds of this research on GAC, determining thermodynamic parameters is important [11].

Coconut shell based and bituminous coal based GACs are commonly used in water treatment processes. There is more research done on removal of EPs using bituminous coal based carbons in literature than coconut shell based carbons [12]. While, coconut shell based carbons are

extensively used in water treatment and they are cheaper than bituminous coal based carbons [13]. Calgon Carbon Corporation produces high quality bituminous coal based carbons and Jacobi Carbons Company produces high quality coconut shell based carbons. Therefore, FILTRASORB®400 a bituminous coal based GAC from Calgon Carbon and AquaSorb®CS a coconut shell based GAC from Jacobi Carbons were chosen for this study. For more convenience the acronyms of BC and CS will be used to name these two adsorbents instead of bituminous coal based and coconut shell based, respectively. Both carbons are steam activated and recommended for removal of organic compounds from drinking water by suppliers [14, 15].

In order to study the effectiveness of removal of EPs using GAC, model compound EPs are needed to be chosen. Reviewing the occurrence of EPs reported in literature and regional reports, Ibuprofen an anti-inflammatory drug (IBP) [7, 16], 2,4-dichlorophenoxyacetic acid a herbicide (2,4-D) [6, 8], and Bisphenol A, a chemical used in production of plastics (BPA) [7, 17], are among the most frequently detected compounds. Sosiak et al. [7] reported IBP concentration levels up to 1.7 μg/L at upstream of North Saskatchewan River. The same study reported BPA concentration levels up to 1.5 μg/L in the upstream of Oldman River in Alberta. These three EPs were chosen as model compounds to study their adsorption on GAC, representing three different categories of EPs.

It is difficult to predict adsorption behaviour of complex molecules of EPs. Different functional groups influence adsorption of the molecule differently [18] therefore; it is more practical to consider the most influencing parameter in adsorption characteristics of the molecule and relate the adsorption behaviour to those major parameters. One of the most influencing parameters on adsorption of organic compounds on GAC is the electrostatic charge of the adsorbent and adsorbate [19]. Comparing the adsorption uptake of an adsorbent with the same porosity and

different surface electrostatic charge will help with the better understanding of the effect of activated carbon surface charge and the adsorbate molecule charge on adsorption. Nitric acid pre-treatment is a popular pre-treatment method to oxidize the surface of the activated carbon and consequently change the surface charge of the activated carbon [20].

Presence of compounds other than the adsorbate in solution influences adsorption of the adsorbate [4]. Removal of the EPs for drinking water usage occurs in tap water matrix. Adsorption of organic compounds on GAC in pure water has been investigated in literature to some extent [6, 21, 22]. However; effect of tap water matrix of Saskatoon on adsorption has not been investigated adequately. To have a better insight into the adsorption of EPs on GAC in operating conditions with tap water, there is a need to compare the adsorption behaviour of these compounds on the same adsorbents but with different water matrices.

Regeneration of saturated adsorbent can restore the adsorption capacity of the adsorbent. Various regeneration methods have different levels of effectiveness in restoration of adsorption capacity of the adsorbents. Literature confirms effectiveness of mineralization and degradation of EPs with ozone [23-25]. Literature also reports effective catalytic activity of GAC in ozonative removal of EPs present in pure water [26]. However, effect of ozonation in regeneration of GAC saturated with EPs is not clear and needs to be investigated [27]. It is helpful to investigate the effectiveness of ozonation in regeneration of GAC saturated with model compounds of this research representing different categories of EPs.

1.2. Research Objectives

Based on motivation of this research, the main objective of the research was identified. The main objective of this research is to study the applicability of adsorption with GAC for removal of EPs

from drinking water using mentioned model compounds and adsorbents and to evaluate the effectiveness of ozonation for regeneration of saturated GAC. In order to achieve this goal following sub-objectives were identified:

- to conduct batch adsorption of IBP, 2,4-D, and BPA on BC and CS in Milli-Q water at temperatures ranging from 280 to 296 K, to determine the best isotherm model of adsorption, and subsequently determine thermodynamic parameters using isotherm model parameters
- to investigate the effect of point of zero charge of adsorbents, pre-treated with nitric acid on adsorption of selected model compounds in Milli-Q water
- to study adsorption of model compounds in tap water at 296 K
- to investigate the effectiveness of ozonation regeneration of spent activated carbon, saturated with the selected model compounds

1.3. Scope of This Research

This thesis contains seven chapters with the contents explained as below:

- Background: This chapter presents the occurrence of EPs in surface waters and their negative effects on human health. This chapter also presents the utilization of GAC adsorption process in water treatment, reviews literature for usage of GAC in removal of similar contaminants, and briefly reviews the thermodynamics of adsorption of organic compounds on GAC in literature. The derivation of formulas and isotherm models of this research are presented as well. Acid pre-treatment of activated carbon and regeneration of spent activated carbon with ozone are also reviewed.

- Experimental: This chapter describes the materials used in this research and the procedures used. The experimental procedures and methods of analysis are provided thereafter. Repeatability of the experiments comes at the end of this chapter.
- Characterization of Adsorbents: This chapter provides the results of porosity characterizations carried out and the point of zero charges of adsorbents measured. In addition the author summarizes the most relevant physic-chemical properties of adsorbents that are going to be used in the next chapters.
- Adsorption of Model Compounds on Fresh Adsorbents: This chapter presents the results of adsorption of model compounds of this research on fresh adsorbents at three temperatures of 280, 288, and 296 K in Milli-Q water. Afterward it presents the thermodynamic analysis based on the isotherm parameters acquired.
- Adsorption of Model Compounds on Pre-treated Adsorbents: This chapter presents the analysis of the results of adsorption of model compounds on nitric acid pre-treated adsorbents at 296 K in Milli-Q water.
- Semi-batch Regeneration of Adsorbents with Ozone: This chapter presents the results of regeneration of adsorbents saturated with model compounds.
- General Conclusions and Recommendations for Future Works: This chapter summarizes the most important findings of this research and proposes the recommendations for future work.

1.4. Contribution of This Work

This research studies adsorption of three model compounds on two GACs commonly used in water treatment industry. Thermodynamic analysis of adsorption at temperature range of 280 to

296 K indicated that effect of entropy of adsorption on spontaneity of adsorption is more pronounced than the exothermic or endothermic nature of the adsorption.

Adsorption of model compounds on adsorbents with lower point of zero charge but the same porosity in Milli-Q water was examined. The pronounced difference among the maximum adsorption capacity of model compounds with different acid dissociation constants indicated the significant effect of electrostatic forces on adsorption of model compounds on GAC. It is believed that the presence of oxygen containing surface functional groups of adsorbents, formed during the acid pre-treatment of the adsorbents affected the adsorption of model compounds in molecular form drastically. This indicates the importance of presence of functional groups in the structure of model compounds.

Adsorption of model compounds in tap water with the same adsorbents was studied. It was seen that adsorption of the deprotonated model compounds decreased in comparison with the adsorption in Milli-Q water. However, maximum adsorption capacity of model compound in molecular form did not decrease drastically. This showed that the effect of electrostatic forces is the dominant controlling factor in adsorption in tap water.

GACs were saturated with the model compounds. Saturated adsorbents were regenerated with ozone. Adsorption of model compounds on ozone treated samples was examined. Nearly no uptake of the model compounds on both saturated adsorbents was observed. This indicated that aside from the type of model compound and source of GAC, the regeneration of the saturated adsorbent with ozone has the same effect and is not successful in restoration of the adsorption capacity of the adsorbent.

CHAPTER TWO

BACKGROUND

This chapter will explain the theoretical concepts of the models and formulas used in this research while reviewing the literature and presenting the related research. Next chapters will be referenced to this chapter for the derivation of formulas and/or definitions of concepts are explained in detail.

2.1. Occurrence of Emerging Pollutants in Surface Waters

Presence of emerging pollutants (EPs) in surface waters and sources of drinking water has raised health concerns. Presence of EPs even at low concentration levels over a long period of time can have detrimental effects on human health. EPs are persistent compounds and can readily pass through various drinking water treatment processes. A large number of EPs exist in surface waters due to discharge of waste stream of industrial processes, municipal conventional secondary treated effluents (containing; pharmaceuticals, personal care products, and household cleaning chemicals), stabilization lagoons and septic tanks leakages, and farming irrigation runoff (containing; pesticides and herbicides) [28]. Natural and synthetic organic contaminants were detected in samples taken from two rivers studied in South Saskatchewan River basin [29].

Three model compounds representing different categories of EPs were selected for this research. Ibuprofen is a non-steroidal anti-inflammatory drug, commonly found in surface waters at high

concentrations [7]. 2,4-dichlorophenoxyacetic acid is a herbicide applied to control broad-leaved weeds in gardens and farming and is commonly preferred in the world because of its low cost and selectivity. It is poorly biodegradable and is present in high concentration levels in surface waters coming from irrigation runoff of farming operations [6]. Bisphenol A is a chemical widely used in production of polycarbonates, epoxy resins, and other plastics. BPA is an antioxidant, non-biodegradable, and highly resistant to chemical degradation and is reported at high concentration levels in surface waters [5]. Chemical characteristics of IBP, 2,4-D, and BPA are presented in Table 2-1.

Table 2-1. Physical and chemical characteristics of IBP, 2,4-D, and BPA molecules.

Model compound	**Molecular formula**	**Molecular weight (g/mol)**	**Log K_{OW}**	**pKa**	**Water solubility (mg/L) at 298 K**	**Reference**
IBP	$C_{13}H_{18}O_2$	206.23	3.97	4.9	21	[2, 28, 30, 31]
2,4-D	$C_8H_6Cl_2O_3$	221.04	2.81	2.6	900	[32-34]
BPA	$C_{15}H_{16}O_2$	228.30	3.32	9.6-10.2	120	[5, 35]

All three model compounds have relatively similar molecular weights. The Log of octanol-water partition coefficient (Log K_{ow}) indicates the hydrophobicity of an organic molecule determined with measurement of distribution of the organic solute between a non-polar phase (octanol) and polar phase (water) [36]. The logarithm of ratio of concentration of organic solute in octanol to concentration of organic solute in water (Equation 2-1) is considered as the partition coefficient [37].

$$\log K_{OW} = \log \frac{C_{s,o}}{C_{s,w}} \qquad (2\text{-}1)$$

Where $C_{s,o}$ is concentration of organic solute in octanol and $C_{s,w}$ is concentration of organic solute in water. A molecule with higher Log K_{ow} has more tendency to be adsorbed on non polar

surfaces such as activated carbon. The partition coefficient is often related to solubility in aqueous phase, as the higher the partition coefficient the lower the solubility of the compound in aqueous phase [38].

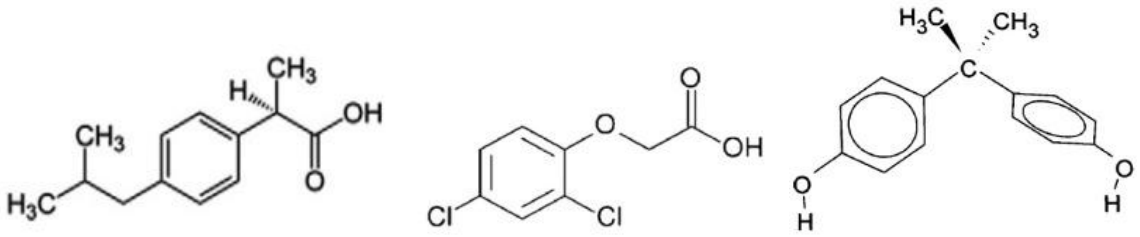

(a) (b) (c)

Figure 2-1. Molecular structure of IBP (a), 2,4-D (b), and BPA (c).

IBP has a molecular dimension of 1.03 (length) × 0.52 (width) × 0.43 nm (height) [10]. Length of BPA molecule from one hydroxyl group of aromatic ring to another is 0.94 nm, width of the molecule is 0.53 nm, and the height of benzenic ring is 0.43 nm [5]. From this information one can infer that length of 2,4-D does not exceed 1.1 nm.

There is an equilibrium associated with dissociation of an acid (equation 2-2). Considering HA being the weak acid in equation 2-2, it dissociates into H^+ and A^-. Ka in equation 2-3 is the equilibrium constant correlating the concentration of dissociated species and the concentration of weak acid in aqueous phase.

$$HA \rightleftharpoons H^+ + A^- \quad (2\text{-}2)$$

$$Ka = \frac{[H^+][A^-]}{[HA]} \quad (2\text{-}3)$$

pH is defined to be –Log $[H]^+$ therefore, it is possible to rewrite equation (2-4) and derive equation (2-5). In equation (2-5) in order to have pH = pKa, concentration of A^- must be equal to concentration of weak acid. This indicates that at pH value equal to pKa, half of the initial concentration of weak acid is dissociated and rest of it is still in molecular form.

$$pKa = -\log Ka = -\log \frac{[H^+][A^-]}{[HA]} \quad (2\text{-}4)$$

$$pKa = -\log[H^+] - \log \frac{[A^-]}{[HA]} = pH - \log \frac{[A^-]}{[HA]} \quad (2\text{-}5)$$

According to literature, the pKa of IBP is associated with the H^+ of carboxyl group. IBP is in molecular form before dissociation and is negatively charged after dissociation [16]. In case of 2,4-D, pKa is related to H^+ of carboxyl group as well [39]. Thus, 2,4-D is in molecular form and neutral before dissociation but after dissociation it is negatively charged [40]. Deprotonation of BPA is attributed to separation of H^+ of phenolic groups therefore; BPA is in molecular and neutral form before deprotonation and negatively charged after dissociation [5].

2.2. Granular Activated Carbon Filtration

Activated carbon filtration is used in water treatment to remove dissolved organic contamination by physical separation [13]. It is one of the most established technologies used in purification of water contaminated with organic pollutants [32]. This process is relatively inexpensive and highly efficient for removal of contamination from drinking water [41]. One of the most important advantages of activated carbon filtration over other treatment processes is that it does not release by-products into the effluent stream [42].

Activated carbon in water treatment is used in forms of powdered and granular activated carbon. Powdered activated carbon should be separated from the effluent as residual process solids and

cannot be recovered or reactivated while granular activated carbon can be replaced or regenerated. GAC treatment is an approach for removal of organic compounds regularly found at concentrations of concern. GAC has larger particle size in comparison with powdered activated carbon and does not cause a high pressure drop therefore; it is typically used in fixed-bed columns [13]. Water treatment companies producing filters for removal of organic contaminant from tap water use GAC as the adsorbent. GAC is the practical choice as it can be replaced or reactivated, it does not cause a pressure drop in fixed bed columns, and it is not suspended in stream and consequently it is not needed to be separated from the effluent.

GAC is synthesized from carbonaceous material including coal, lignin, coconut shell, and wood [42, 43]. Every source has its own advantages and disadvantages. Bituminous coal based and coconut shell based GACs are recommended for drinking water treatment [13]. Coconut shell based activated carbons are made of coconut shell which is an agricultural by-product and is available in large quantities with a lower price than bituminous coal [44]. Coconut shell GACs has higher mechanical strength than bituminous coal based GACs [45]. This allows treatment of large volume of water with less abrasion in comparison with bituminous coal based GACs. Bituminous coal based GACs has higher ash content than coconut shell based GACs [46]. Coconut shell based GAC has a more micro-porous structure than the bituminous coal based GAC [47]. Tsai et al. [48] stated that bituminous coal based carbons have higher amounts of acidic groups in their structure than the coconut shell based GAC. The literature does not adequately investigate the effectiveness of adsorption of one EP on two GAC of coconut shell based and bituminous based with the same experimental conditions. This knowledge gap represents a challenge to evaluate the effectiveness of various characteristics of these two GAC on adsorption of EPs.

Batch Adsorption Isotherm Modeling

Adsorption isotherm modeling can be used to compare the adsorption of model compounds on different adsorbents and to find thermodynamic parameters of adsorption. When an aqueous phase containing a dissolved organic compound (solute) comes in contact with GAC pellets (adsorbent), transfer of the solute from aqueous phase to the surface of adsorbent (and also the reverse process) occurs (equation 2-6), due to the higher affinity of the organic compound to the surface of GAC than water and the higher concentration of solute in bulk of the liquid. Solute molecules will be transferred between the interface of the adsorbent and the bulk of the liquid until an equilibrium is attained. At equilibrium, equal amounts of solute will be adsorbed and desorbed; consequently the concentration of solute in bulk of aqueous phase and on GAC surface will remain constant.

solute in aqueous phase ⇋ solute on GAC surface (2-6)

$$K_c' = \frac{Concentration\ of\ solute\ on\ GAC\ surface}{Concentration\ of\ solute\ in\ aqueous\ solution} \quad (2\text{-}7)$$

K_c' is the apparent equilibrium constant, for each equilibrium concentration of solute in liquid phase. The correlation showing the concentration of solute on GAC as a function of concentration of solute in bulk of the aqueous phase, at constant temperature, is called the adsorption isotherm [9].

Adsorption isotherm modeling allows comparison of adsorption using model parameters. Adsorption isotherm model parameters give information about the maximum adsorption capacity, surface and energy sites distribution heterogeneity, and adsorption intensity. Freundlich

and Langmuir adsorption isotherm models describe the adsorption of organic compounds on GAC in water better than other models [10, 48, 49]. These two models are:

Freundlich model: $$q_e = K_F C_e^{1/n} \quad (2\text{-}8)$$

Langmuir model: $$q_e = \frac{Q_{max} b C_e}{1 + b C_e} \quad (2\text{-}9)$$

In Equation (2-8) K_F (mg $^{(n-1)/n}$.$L^{1/n}$.g^{-1}) is Freundlich relative adsorption maximum capacity and 1/n indicates adsorption affinity or surface heterogeneity. In Equation (2-9); Q_{max} (mg/g) is the Langmuir monolayer maximum adsorption capacity and b (L/mg) is a direct measure of adsorption intensity [6, 10, 48, 50]. The uptake of the solute on adsorbent is calculated using equation (2-9).

$$q_e = \frac{(C_0 - C_e) \cdot V}{W} \quad (2\text{-}10)$$

Where C_0 and C_e (mg/L) are the initial and equilibrium concentration of the solute, respectively, V (L) is the volume of the solution, and W (g) is weight of the adsorbent. q_e is found in mg of solute per gram of adsorbent (mg/g) [10].

There are differences between these two models. The Freundlich model better simulates adsorption processes on heterogeneous adsorbent surface; where the lower the value of 1/n the higher the heterogeneity of the surface of adsorbent [16, 51]. While the Langmuir is a better fit for monolayer adsorption on adsorption sites with uniform energy [49]. The Freundlich model is more applicable for adsorption at high concentration range while the Langmuir is more applicable at low concentration ranges [52]. In a Freundlich isotherm, the uptake approaches infinity with the increase in solute concentration. The adsorption processes observed in practical

systems do not follow this behaviour, but rather the uptake capacity exhibit a limited value.[51]. In order to fit the models to experimental data and find the model parameters, the model can be written in linear form:

Linear Langmuir model: $$\frac{C_e}{q_e} = \frac{1}{Q_{max}b} + \frac{C_e}{Q_{max}} \quad (2\text{-}11)$$

Linear Freundlich model: $$\ln q_e = \ln K_F + \frac{1}{n}\ln C_e \quad (2\text{-}12)$$

The C_e/q_e is plotted against C_e and the slope of the straight line fit to the data represents $1/Q_{max}$. Having Q_{max} it is possible to find b from the intercept of the line. To find the Freundlich parameters from the equilibrium experimental data, ln q_e is plotted against ln C_e. The slope of the straight line fitted to the data will be 1/n and the intercept will be ln K_F.

Parameters Influencing Adsorption of EPs on GAC

There are a variety of factors that affect the adsorption of a solute in aqueous phase on GAC. The characteristics of the adsorbent, solution, and EP affect the adsorption process at a constant temperature [6]. There are some parameters that influence adsorption more than others. According to literature attractive (London) dispersion forces and donor-acceptor interactions [53], adsorbent porosity [47, 54], and electrostatic forces [53] are among the most influencing parameters affecting the adsorption of EPs on GAC at a constant temperature. Major water component species and temperature are also influencing parameters on adsorption in operating conditions relevant to this research. Effect of dispersion forces and donor-acceptor interactions, adsorbent porosity, and electrostatic forces on adsorption of EPs is briefly reviewed below. Effect of tap water major components and temperature will be reviewed afterwards.

Effect of Attractive London Dispersive Forces and Donor-acceptor Interactions on Adsorption of EPs on GAC

London dispersive forces are Van der Waals forces between non-polar species. Bigger London dispersive forces are exerted to larger size molecules such as EPs [55]. Therefore, attraction forces between large uncharged EP molecules and non-polar graphene layers of GAC can be attributed to London dispersion forces [56]. Adsorption of EPs on GAC is influenced by dispersion forces through π-π electron interactions of aromatic rings [57]. Presence of polar functional groups on the surface of graphene layers of GAC or in structure of the organic molecules of EPs can increase or decrease the dispersion forces [5, 28]. Guedidi et al. indicate that oxygen-containing functional groups on the surface of graphene layers withdraw electrons from the aromatic rings resulting in less dispersive forces [28].

Oxygen atoms of oxygen-containing functional groups of graphene layers have lone pair electrons in their valance orbital. Oxygen atoms (electron donor) of oxygen-containing functional groups such as carbonyl groups [28] can donate the lone pair electrons to an EP (electron acceptor) molecule with electron deficiency in their structure [58]. This indicates that presence of oxygen-containing functional groups on GAC surface can decrease dispersive interactions and at the same time increase adsorption through formation of donor-acceptor complexes with the solute molecules. To find out the effect of dispersive forces and electron donor-acceptor interactions on model compounds of this research, literature needs to be reviewed and experiments need to be conducted.

Guedidi et al. [28] attributed the adsorption of IBP at pH 3 to formation of donor-acceptor complexes of IBP with carbonyl groups of the GAC surface; however, they reject adsorption of IBP through π-π interaction of IBP aromatic ring and graphene layers. Guedidi et al. related

higher uptake of IBP to the higher amount of carbonyl, quinone, and lactonic groups on GAC surface.

Guifang et al. [59] studied adsorption of BPA on nitric acid treated activated carbons. They observed significant reduction in uptake of BPA after nitric acid treatment of adsorbents. They mentioned that formation of carboxylic and hydroxyl groups on surface of carbon during nitric acid treatment withdrew the electrons from basal planes of graphene. They speculated that this decreased π-π dispersion interactions. Bautista et al. [60] found that adsorption of BPA on their three activated carbon adsorbents followed the π-π interaction as the most dominant mechanism. Zhu et al. [61] stated that phenolic compounds can be adsorbed to the carboxylic groups of the carbon surface through formation of hydrogen bonds which is believed to be the primary reason for adsorption of BPA and not the π-π interactions.

Effect of Adsorbent Porosity on adsorption of EPs on GAC

EP molecules have high molecular weights and consequently large molecular structures. Therefore, the pore size of adsorbent can influence adsorption of EPs. Higher pore volume and surface area of adsorbent lead to higher adsorption capacity thus pore volume and surface area of an adsorbent play key role in adsorption of a compound. Microporous or mesoporous structure of an adsorbent affects the adsorption uptake. It has been observed that mesoporous carbons are effective adsorbents for the removal of bulky molecules [47], on the other hand it has been observed that microporous adsorbents have higher adsorption uptake for several EPs [28]. Effect of porosity of GAC on adsorption of EPs of this research is briefly reviewed below.

Mestre et al. [10] indicated that activated carbons with a higher pore volume exhibited a higher IBP adsorption capacity. They noted that carbons with smaller mean micropore half-width

yielded a higher adsorption affinity. Guedid et al. noted that IBP adsorption occurred in micropores with a diameter below 0.6 nm. Gun'ko et al. [18] mentioned that IBP molecules form dimmers with the carboxylic groups in their structure that hinder entering micropores. However, adsorption of those dimmers in pores with diameter larger than 1 nm was completely possible. They [18] also found that IBP was adsorbed in a monomer form at low concentrations while in higher concentrations the formation of a dimmer contributed to the uptake of IBP.

Sui et al. [62] studied the adsorption of BPA on a mesoporous carbon and a commercial powdered activated carbon. The mesoprous GAC and powdered activated carbon had a Barrett-Joyner-Halenda (BJH) average pore diameters of 4.87 and 3.06 nm, respectively. The mesopore volume and surface area of mesoporous carbon was higher than the powdered carbon. They indicated that the higher pore volume and surface area of the mesoporous carbon were the most important factors influencing the uptake of BPA. Tsai et al. [48] reported lower uptake of BPA on an activated carbon of their own, compared to a different activated carbon, indicating that the difference was due to the pore volume.

Effect of Electrostatic Interactions on Adsorption of EPs on GAC

The surface polarity of the graphene layers together with the positive or negative charge of solute molecule can cause attraction or repulsion of solute molecules. The charge of an adsorption site of GAC in aqueous phase may be represented as:

$$-\mathrm{XOH_2^+} \rightleftharpoons -\mathrm{XOH} \rightleftharpoons -\mathrm{XO^-} \qquad (2\text{-}13)$$

Where $-XOH_2^+$ represents protonated adsorption site, –XOH a neutral adsorption site and $-XO^-$ a deprotonated adsorption site. Protonated and deprotonated adsorption sites determine the surface charge of the adsorbent. There is a pH value at which the concentration of these two

groups is equal. This pH value is known as point of zero charge (PZC), where the total charge on the surface becomes zero [63]. With an increase in solution pH, polar adsorption sites lose protons and the surface of the adsorbent will be more negatively charged. Depending on the pH of the solution and the pKa of the solute, the solute can be positive, neutral, or negatively charged. Having the same charge for the solute and adsorbent or the opposite charges, repulsion or attraction forces would be present between the solute and adsorbent [64]. When either the adsorbent or the solute, or both are in neutral condition, the electrostatic forces are minimal [34].

Exposure of activated carbon to atmosphere will cause the oxidation of the carbon surface. This phenomenon is called ‘aging’ [65]. Aging mainly increases the carbonyl functional groups while simultaneously decreases the amount of basic groups which causes reduction in PZC of carbon [28]. Boehm et al. [65] also emphasized that surface oxides formed through aging of GAC have acidic characteristics.

Mestre et al. [10] studied adsorption of IBP on a GAC. They indicated that the carbon with lower PZC has a larger number of oxygen containing functional groups. A reduction of 3-5% in maximum adsorption capacity of IBP was observed with increase of pH from 5 to 6 for their activated carbon with PZC of 9.9. They attributed this observation to the increase in negatively charged adsorption sites on the GAC surface. This reduction was accentuated for an activated carbon with a PZC equal to 7.5 due to repulsive forces between the more negatively charged surface of the carbon and deprotonated IBP molecules. Dubey et al. [16] studied adsorption of IBP on a GAC. They indicated the adsorption to be physisorption. The maximum uptake of IBP occurred at pH 2 mainly involving the carboxylic group in the IBP molecule.

Bakhtiari et al. [40] studied dissociation of 2,4-D. They reported that about 50% of 2,4-D was dissociated at pH of about 3 and 2,4-D was completely dissociated at pH 5. At approximate pH 3.5 close to 90% of 2,4-D was dissociated. Gupta et al. [66] studied the effect of pH on adsorption of 2,4-D on the GAC of their research. They observed that the maximum adsorption uptake decreased 1-2% when the pH increased from pH 3 to 8. Salman and Hameed [50] observed a reduction of about 10 mg/g in the maximum uptake of 2,4-D on bituminous coal based GAC of their research with pH increase from 3 to 8. Aksu and Kabasakal [6] indicated that adsorption of 2,4-D on GAC was highly dependent on the pH of the solution. They observed the uptake of 2,4-D to be constant from pH 2 to 3; however it decreased from 98.1 to 83.0 mg/g by increasing the pH from 2 to 8 when the PZC of the GAC was 8.2. They observed that 2,4-D was completely dissociated between pH 4 and 8.

Sui et al. [62] studied adsorption of BPA on a mesoporous activated carbon. Adsorption of BPA was to a high degree constant between pH 2 to 10 due to the pKa of BPA being 9.6 to 10.2. BPA was deprotonated at pH values higher than 10 and formed bisphenolate anions. Bautista et al. [5] observed that the first deprotonation of BPA starts at pH 8 and the second one at pH 9. The most favourable condition for adsorption of BPA was noted to be when the surface of the carbon is in neutral condition and the BPA molecule is not deprotonated.

Effect of Major Components of Tap Water on Adsorption of EPs on GAC

Adsorption of EPs in operating conditions of a drinking water treatment plant occurs in tap water. There are species present in the tap water. These species compete with EPs in adsorption on GAC [42]. This competition in adsorption reduces the maximum adsorption capacity of EPs. The major components of tap water can also affect the ionic strength of the solution and

consequently affects the adsorption of EPs [5]. It is necessary to know the effect of major species of tap water on adsorption of the target solute.

Bautista et al. [5] noted that a presence of electrolytes in solution has a positive effect on adsorption of organic molecules in molecular form, due to the positively charged surface of the carbon. They observed an uptake increase of molecular BPA on GAC in presence of sodium hydroxide to be due to the aforesaid reason. Pastrana-Martinez et al. [67] studied adsorption of Fluroxypyr on GAC in absence and presence of water hardness. Maximum uptake of Fluroxypyr on GAC was lower in the presence of hardness in comparison with pure water, however, maximum uptake increased with increasing hardness when the equilibrium concentration of Fluroxypyr was below 6 mg/L. They observed that water salinity screens the electrostatic repulsion forces between charged Fluroxypyr molecules, when non-electrostatic solute-adsorbent was predominant.

2.3. Thermodynamics of Adsorption

Finding thermodynamic parameters of adsorption helps differentiating the physical adsorption from chemical adsorption, and helps predicting the adsorption behaviour in relevant conditions and different temperatures. Finding the equilibrium constants at different temperatures allows calculation of change in standard Gibbs free energy, standard entropy, and standard enthalpy.

Adsorption of model compounds on adsorbent can be represented with the reversible equilibrium function of Equation (2-6). The apparent equilibrium constant of K'_c in Equation (2-7) is defined as the concentration of solute on adsorbent divided by the concentration of solute in liquid phase. In order to obtain the standard thermodynamic equilibrium constant (K°_c) the activity should be used instead of concentration of model compound (Equation 2-14).

$$K_C^\circ = \frac{a_s}{a_e} = \frac{v_s}{v_e} \cdot \frac{C_s}{C_e} \quad (2\text{-}14)$$

In Equation (2-14) a_s and a_e are the activity of solute on adsorbent and in solution respectively, v_s and v_e are activity coefficients of solute on adsorbent and in solution respectively, and C_s and C_e are the concentrations of solute on adsorbent and in solution. For this purpose, the apparent equilibrium constant (K'_c) values for different initial concentrations of the model compounds are obtained by extrapolation when the initial concentration of model compound in solution at equilibrium approaches zero. This value is equal to the inverse of the intercept of C_s/C_e versus C_e curve, and in turn is the intercept of the linear form of the Langmuir model. Knowing the intercept of the linear form of the Langmuir curve to be $1/(Q_{max}.b)$, the standard equilibrium constant (K°_c) will be $Q_{max}.b$ [6, 67-69]. Finding the standard equilibrium constant for any temperature, the standard free energy (ΔG°) will be calculated from Equation 2-15.

$$\Delta G^\circ = - RT \, . \ln K^\circ_c \quad (2\text{-}15)$$

$$\Delta G^\circ = \Delta H^\circ - T\Delta S^\circ \quad (2\text{-}16)$$

R in Equation (2-15) is the gas constant 0.008314 (kJ/K.mol) and T is the absolute temperature in Kelvin. Knowing the relationship between standard Gibbs free energy, standard enthalpy, and standard entropy and substituting Equation (2-15) in Equation (2-16) the values for ΔH° and ΔS° of adsorption can be calculated from the slope and intercept of the Van't Hoff plot of $\ln K^\circ_c$ versus 1/T [28, 70].

$$\ln K_c^\circ = \frac{\Delta S^\circ}{R} - \frac{\Delta H^\circ}{RT} \quad (2\text{-}17)$$

From Equation (2-17), the standard enthalpy change ΔH° (kJ/mol) is negative of the slope of the trend-line, multiplied by R; and the standard entropy ΔS° (kJ/mol.K) is intercept of the trend-line multiplied by R.

Thermodynamics of Adsorption of EPs

Guedidi et al. [28] determined the thermodynamic parameters of adsorption of IBP at q_e=100 mg/g and pH=3 on fresh microporous-mesoporous commercial GAC, GAC treated with hydrogen peroxide with simultaneous sonication, and GAC thermally treated at 973 K (Table 2-2). Adsorption of IBP on all three activated carbons had a positive ΔH° indicating endothermic adsorption. The ΔH° values were lower for adsorbents with higher surface oxygen-containing groups, which was attributed to the effect of exothermic interaction of some of surface oxygen-containing groups with IBP. The small negative ΔG° value for three carbons indicated a spontaneous physisorption [71]. Guedidi et al. attributed the more negative ΔG° value for adsorption of IBP on the sonicated sample to the presence of high energy adsorption sites of particular oxygenated groups formed by sonication of adsorbent. Guedidi et al. assumed those oxygenated groups to be carbonyl or lactonic groups. The positive ΔS° indicated increase of disorder at solid-liquid interface because of probable desorption of water and methanol molecules from IBP molecules before adsorption of IBP on adsorbent. They also concluded the competition in adsorption on GAC between solvent and IBP molecules, due to a positive value of standard entropy.

Mestre et al. [10] observed a slight increase in adsorption uptake of IBP by GAC when the temperature increased from 298 to 313 K, which confirms the endothermic adsorption process and consequently a positive value for ΔH°. Dubey et al. [16] determined the thermodynamic parameters of adsorption of IBP on a novel mesoporous activated carbon, synthesized from an

invasive weed. They found the adsorption to be endothermic with increase in randomness on surface of adsorbent.

Gupta et al. [66] estimated thermodynamic parameters of adsorption of 2,4-D on a carbonaceous adsorbent prepared from raw material procured from industrial waste slurry. The negative ΔG° and ΔH° indicated the spontaneous and exothermic nature of adsorption, respectively. They deduced the physical adsorption in the presence of weak attraction forces was due to the low enthalpy value. They assumed that the negative value of entropy indicating the decrease in disorder to be due to binding of molecules with the surface of adsorbent. Aksu and Kabasakal [6, 69] found the thermodynamic parameters of adsorption of 2,4-D on a H-type bituminous coal based GAC (Table 2-2). They described the adsorption to be feasible and spontaneous because of negative ΔG°. They suggested the endothermic nature of adsorption and the increase in randomness due to the positive values for enthalpy and entropy, respectively. They concluded the higher adsorption at higher temperature to be due to enlargement of pore size or activation of surface of adsorbent or creation of new adsorption sites as a result of bond rupture. They also assumed the increase in intraparticle diffusion enhanced the mobility and penetration of 2,4-D into pores at higher temperature. Adsorption of 2,4-D on a mineral clay was carried out by Nejati et al. [72] and the thermodynamic parameters were determined (Table 2-2). Negative values of ΔG° and ΔH° were mentioned to indicate the spontaneous adsorption and exothermic process, respectively suggesting physisorption with weak attraction forces. They related the positive value of entropy to increase in randomness at the interface of the solid and liquid phases.

Liu et al. [59] studied the adsorption of BPA on fresh activated carbon (Westvaco Corp., America) and the nitric acid treated form of the same carbon. They found the adsorption on both carbons to have a physisorption mechanism due to an activation energy less than 40 kJ/mol.

They mentioned the physisorption to be an exothermic process. The experiments at temperatures from 288 to 318 K indicated the reduction in uptake and logically an exothermic adsorption, which was in agreement with their induction about the exothermic nature of physisorption. Sui et al. [62] studied adsorption of BPA on a mesoporous carbon prepared from hexagonal SBA-15 mesoporous silica. They observed a decrease in adsorption of BPA with increase of the temperature from 283 to 313 K, confirming an exothermic process.

Table 2-2. Thermodynamic parameters of adsorption of model compounds on various adsorbents

Model compound	Adsorbent	Temperature range	ΔG° (kJ/mol)	ΔS° (J/mol.K)	ΔH° (kJ/mol)	Reference
IBP	Activated Carbon	298-318	-3	198	57	[16]
2,4-D	Carbonaceous adsorbent	298-318	-21	-60	-2	[66]
2,4-D	GAC	298-318	-7	73	15	[6]
2,4-D	Layered double hydroxide	298-333	-5	2	-5	[72]

2.4. Acid Pre-treatment of Activated Carbon

In order to create acidic oxide groups on GAC surface, various liquid oxidants are used in this investigation. Among the liquid oxidants, nitric acid is often used since its oxidizing properties can be controlled by temperature and concentration [65]. Nitric acid treatment increases the amount of acidic surface oxygen-containing functional groups leading to reduction of PZC of GAC [73]. Nitric acid treatment of GAC at room temperature does not have a significant influence on porosity of GAC and is a suitable method for reduction of PZC without influencing GAC porosity [74].

Yu et al. [74] investigated nitric acid treatment of coconut shell base GAC. They treated fresh GAC with 65% concentrated nitric acid at 303 K for 3 hours. They did not observe a significant

difference in morphology of carbon after treatment in SEM images except removal of inorganic fine particles or ashes. Ash content analysis indicated close to 50% reduction of ash after acid treatment which confirmed the SEM results. Acid treatment caused about 20% decrease of pore volume and surface area of micropores, and the total surface area. They concluded that moderate change of temperature up to 363 K does not have a significant influence on pore structure modification. They mentioned that nitric acid oxidation increased the amount of oxygen-containing functional groups. Acid treatment at room temperature decreased the amount of carbonyl or phenol groups on surface of GAC while it increased the amount of carboxylic groups.

Chen et al. [75] treated a coal based GAC with different concentrations of nitric acid at 363 K for 10 hours. They found that amount of carboxylic groups increase monotonically with the increase of concentration of nitric acid. It was also found that the amount of carbonyl groups increases and reaches their maximums when the nitric acid concentration is 2 N and decreases with further increase in concentration of nitric acid. It was observed that the amount of surface oxygen-containing functional groups increases significantly after treatment and has the same trend as carboxyl functional groups. A slight increase in total surface area was observed after 0.1 N nitric acid treatment. This was explained to be due to pore opening caused by removal of ashes and impurities. They also explained the increase in microporous surface area and volume due to anchoring of oxygen-containing functional groups inside the larger pores by oxidation with nitric acid. However, decrease in total surface area was observed with further increase in nitric acid concentration. They described the decrease in micropore surface area and volume by collapse of pore walls and carboxylic groups stretching to the walls of slit-shaped pores and consequently lack of access to them. The presence of oxygen-containing surface groups makes the surface of

carbon more hydrophilic, causing it to attract water clusters that block the pore entrances. This represents an example when the structure of microporous activated carbons is usually made up of slit-shaped pores [10].

Houshmand and Daud [76] studied nitric acid treatment of palm-shell-based GAC at 298 K with 2 and 8 N nitric acid and 2 and 8 hours of treatment. Total surface area and micropore volume of all oxidized samples decreased in comparison with the fresh sample. They identified pore destruction and pore blockage to be the main reasons for the reduction in surface area and pore volume of the samples. They concluded that decrease in surface area must have occurred due to increase in concentration of surface oxygen-containing functional groups. Liu et al. [77] investigated the nitric acid treatment of coconut shell GAC. They treated the carbon at 363 K with 6 N nitric acid for 12 hours. Result of their experiments indicated a slight reduction in total surface area. Studying surface chemistry of the acid treated sample showed that increase in acidity is mainly due to formation of carboxylic acid and phenolic functional groups on surface of carbon. Oxidation processes including nitric acid treatment not only introduced acidic surface functional groups but also destroyed basic functional groups [28]. Shamsi Jazeyi et al. [20] studied treatment of a commercial GAC with 6 N boiling nitric acid for 3 hours. Results of their analysis indicated a slight increase in total surface area, total pore volume, and micropore volume and reduction of ash content to almost half of the ash content of the fresh carbon. They briefly concluded that nitric acid treatment at that temperature introduced carboxylic acid groups into the surface of GAC.

2.5. Activated Carbon Regeneration with Ozone

Ozone has a high oxidation potential which makes it a good choice for oxidation of organics in aqueous phase. The effectiveness of ozonation in removal of EPs in water has been confirmed in

literature [2, 78]. Ozone regeneration therefore could be a good candidate for GAC regeneration as ozone can be injected to packed bed columns of GAC and it is capable of driving oxidation of organic molecules in aqueous phase.

The effect of regeneration of GAC with ozone has not been investigated extensively and needs to be clarified and examined for more adsorbents and a larger number of adsorbates, so that its effectiveness of the regeneration with ozone is clarified [27, 79-81]. Ozonative regeneration of GAC saturated with IBP, 2,4-D, and BPA has not been reported in the literature. Regeneration of coconut shell based GAC has not been investigated; however there are a number of reports on GAC regeneration and pre-treatment with ozone which give an insight into the regeneration of GAC with ozone.

Alvarez et al. [79] used in situ ozone injection for regeneration of bituminous coal based GAC. One sample saturated with secondary effluent of wastewater treatment plant and another sample saturated with gallic acid (phenolic compound present in wastewater effluents of food processing plants). They found that regeneration of GAC saturated with gallic acid was not successful. It was observed that regeneration with ozone failed to remove all the gallic acid from the GAC and it destroyed adsorption sites and plugged the pores. They found that excessive ozone treatment caused significant reduction in surface area and pore volume. Increase in mesopore volume also suggested that ozone has widened the micropores. The ozone reacted mainly with the GAC itself and oxidized the surface and destroyed the porosity.

Alvarez et al. [27] in another research compared ozone regeneration with thermal regeneration of GAC exhausted with phenol. They applied ozone treatment to fresh GAC. It was found that longer ozone treatment time decreased the phenol uptake. A significant increase in carboxylic

group concentration was observed after ozone treatment. They indicated that formation of surface oxygen-containing groups was the reason behind the inhibition of adsorption of phenol. The surface area was restored to some extent; however extended ozone treatment decreased the surface area. Ozone treatment of phenol saturated samples led to removal of physically adsorbed phenol molecules in the first 20 minutes.

Yaghmaeian et al. [81] used in situ ozone treatment for regeneration of amoxicillin saturated NH_4Cl pre-treated activated carbon. They observed that ozone regeneration with low dosage of 1.4 mg-O_3/min can completely restored the adsorption capacity of the NH_4Cl pre-treated activated carbon saturated with amoxicillin.

Valdes and Zaror [80] utilized ozone treatment as a pre-treatment method and indicated reduction in BET surface area of fresh GAC pre-treated with 5 g/h of ozone. Ozone pre-treatment slightly increased the mesopore surface area. The extended oxidation led to destruction of pore walls. A 20-30% reduction of mass was also observed after 60 min of 5 g/h ozone treatment. The same behaviour was observed for benzothiazole saturated GAC. Pre-treated GAC showed a reduction in adsorption maximum capacity and intensity for adsorption of benzothiazole which was explained to be due to reduction in π-electron density on graphene layers. They mentioned high concentration of oxygenated acidic surface groups near the π-electron sites decreased the surface Lewis basicity causing electron withdrawing effect. They believed that this weakened the π-π dispersive interactions between the π-electrons of aromatic ring of benzothiazole, and π-electrons of carbon basal plane and consequently reduced the adsorption capacity.

Rivera-Utrilla and Sanchez-Polo [53] pre-treated a bituminous coal based GAC with 5 g/h of ozone. They reported a significant reduction in adsorption capacity of naphthalenesulphonic acids on ozone treated bituminous coal based activated carbon. This was described to be due to the decrease in π-π dispersive interactions between the basal planes of carbon and aromatic rings of adsorbate molecules. They also mentioned the repulsive forces at pH values close to the point of zero charge of carbon, as a reason for the reduction of capacity of adsorption, as the PZC of carbon decreased with ozone treatment.

CHAPTER THREE

EXPERIMENTAL

This chapter presents the materials used in this research and their characteristics, either provided by the supplier or being measured with experimental works. Experimental procedures are explained in detail and equipment used in this research is introduced. Analytical methods used to measure the characteristics of the adsorbents and other parameters involved in this research are explained in the last part of this chapter.

3.1. Materials

Model Compounds

All chemicals were ordered in high purity and used as received in experiments. BPA and IBP were obtained from Sigma-Aldrich Company with purity of ≥98% and ≥99%, respectively. 2,4-D was supplied by Alfa Aesar with purity of 98%. Stock solutions were prepared with Milli-Q water in 1 L volumetric flasks, for Milli-Q water experiments. For experiments with tap water matrix, tap water with characteristics presented in Table 3-1 was used for preparation of stock solutions. For the case of IBP, in order to increase the solubility and achieve higher concentrations 75 mL of methanol (7% w/w; methanol/Milli-Q water) was used in preparation of stock solution both for Milli-Q water matrix and tap water matrix [10]. Stock solutions were prepared fresh for every batch of experiments the day prior to the experiments. To avoid

introduction of any electrolyte and changing the ionic strength of the solution buffer or acid/base was not added to the stock solutions and pH was not adjusted [82]. For more consistency the new stock solution initial concentration were measured and if it was in an acceptable range of concentration (±0.5 mg/L), it was mixed with the remaining of the previous stock solution to keep the concentration of the stock solutions as accurate and consistent as possible.

Adsorbents

Filtrasorb®400 was supplied by Calgon Carbon Corporation. Filtrasorb®400 comes in 12×40 mesh size. Supplier recommends the BC for removal of dissolved organic compounds from water and wastewater. Filtrasorb®400 is made from bituminous coal through a process known as re-agglomeration. Activation of Filtrasorb®400 is controlled to produce a significant volume of both low and high energy adsorption sites for effective adsorption of a broad range of high and low molecular weight organic contaminants [14]. Filtrasorb®400 was washed with distilled water and dried in oven at 383 K overnight. Dried Filtrasorb®400 was labelled ‘BC’ and it was kept in desiccator to be used in experiments.

AquaSorb®CS granular activated carbon is manufactured from coconut shell based charcoal. The AquaSorb®CS used was the mesh size of 8×30. In order to keep the conformity between the sizes of adsorbents used in this research, this product was sieved with 12×40 mesh to have the same size as BC activated carbon. The final product was washed with distilled water and dried in oven at 383 K overnight. The dried AquaSorb®CS was labelled ‘CS’ and kept in desiccator to be used in experiments.

Water Matrices

Milli-Q water with resistivity of 18.2 MΩ.cm or conductivity of 0.055 micro-Siemens/cm at 298 K was used as Milli-Q water in experiments to prepare stock solutions. Tap water from laboratory tap water supply was used as drinking water matrix. It was collected over the time for more conformity. Major characteristics of tap water influencing the adsorption process were obtained from Saskatoon water treatment plant website (Table 3-1).

Table 3-1. Characteristics of Saskatoon tap water and tap limits [83]

Typical Characteristic	Tap water	Tap water limits
Other characteristics		
Colour (Apparent Colour Unit)	2	15
Conductivity (micro-Siemens/cm)	438	none
pH	7.94	9
Temperature (°C)	10.1	none
Turbidity (Nephelometric Turbidity Unit)	0.2	1
Inorganic Constituents		
Aluminum (mg Al/L)	0.013	0.2
Arsenic (mg As/L)	0.0002	0.010
Barium (mg Ba/L)	0.046	1.0
Boron (mg B/L)	0.02	5.0
Cadmium (mg Cd/L)	0.00001	0.005
Calcium (mg Ca/L)	40	none
M-Alkalinity (mg $CaCO_3$/L)	130	500
P-Alkalinity (mg $CaCO_3$/L)	<1	none
Carbonate (mg CO_3/L)	<1	none
Bicarbonate (mg HCO_3/L)	159	none
Total Hardness (mg $CaCO_3$/L)	168	800
Chloride (mg Cl/L)	11	250
Chlorine Residual (mg Cl_2/L)	1.96	3.0[A]
Chromium (mg Cr/L)	<0.0005	0.05
Copper (mg Cu/L)	0.0017	1.0
Cyanide (mg CN/L)	<0.001	0.2
Fluoride (mg F/L)	0.61	1.5
Iron (mg Fe/L)	0.0035	0.3
Lead (mg Pb/L)	<0.0001	0.01
Magnesium (mg Mg/L)	17	200
Manganese (mg Mn/L)	<0.0008	0.05

[A] As chloramine

Mercury (mg Hg/L)	<0.00001	0.001
Potassium (mg K/L)	3.2	none
Selenium (mg Se/L)	0.0005	0.01
Silver (mg Ag/L)	<0.00005	none
Sodium (mg Na/L)	24	300
Sulphate (mg SO_4/L)	84	500
Uranium (mg U/L)	0.0012	0.02
Zinc (mg Zn/L)	0.0008	5.0
Nutrient Constituents		
Ammonia (mg N/L)	0.30	none
Nitrate & Nitrite (mg NO_3/L)	1.10	45
Total Kjeldahl Nitrogen (mg N/L)	0.62	none
Soluble Ortho Phosphate (mg P/L)	<0.01	none
Total Phosphate (mg P/L)	<0.01	none
Organic Constituents		
Biological oxygen demand 5 days (mg/L)	NR*	none
Dissolved organic carbon (mg C/L)	3.0	none
Total dissolved solids (mg/L)	340	1500
Total suspended solids (mg/L)	<1	none
Volatile suspended solids (mg/L)	<1	none
Total trihalomethanes (µg/L)	36	100

3.2. Experimental Procedures

Isotherm Studies at 296 K

Isotherm experiments were the major part of experimental works for this research. Isotherm experiments at 296 K were carried out in the laboratory where the temperature is controlled at 296 K. The temperature was also measured with mercury thermometer to verify temperature fluctuations. Samples were prepared in 250 mL conical flasks (Erlenmeyer) with a rubber stopper to prevent any loss of samples due to evaporation. 200 mL of solution containing the model compound was added to the conical flasks with 50 mL of headspace for better mixing. The solution was prepared by diluting with the same water matrix of the stock solution. An orbital shaker was used to carry out isotherm experiments. The speed was set to 130 rpm for all

* not required or not applicable by provincial permit to operate

isotherm experiments. The same amount of adsorbent was used for the entire experiments to keep conformity throughout isotherm adsorption experiments.

The concentration of model compounds in contact with adsorbents at equilibrium should not reach zero because it does not allow fitting the data to the models. In order to determine the right amount of adsorbent applicable to all the isotherm experiments, an experiment with the minimum concentrations considered for IBP, 2,4-D, and BPA was conducted. In this experiment 40 mg (0.2 mg/L) of BC and CS was used for each adsorption sample. The maximum uptake of this amount of activated carbon at equilibrium for adsorption of IBP, 2,4-D, and BPA according to literature had to be lower than the amount of IBP, 2,4-D, and BPA available in solution [6, 10, 59, 82]. In each conical flask 200 mL of solutions (10 mg/L for IBP and 15 mg/L for 2,4-D and BPA) was put in contact with 40 mg of BC and CS. The equilibrium concentration of model compounds was measured until the change in concentration of model compounds was less than 2% of initial concentration of model compound in solution. Figure 3-1 shows the concentration of each model compound in solution at equilibrium (C_e). Results show that model compounds concentrations chosen and adsorbent concentration (0.2 g/L) are applicable as the lowest limit for concentration range of model compound and concentration of adsorbents, respectively in isotherm adsorption experiments.

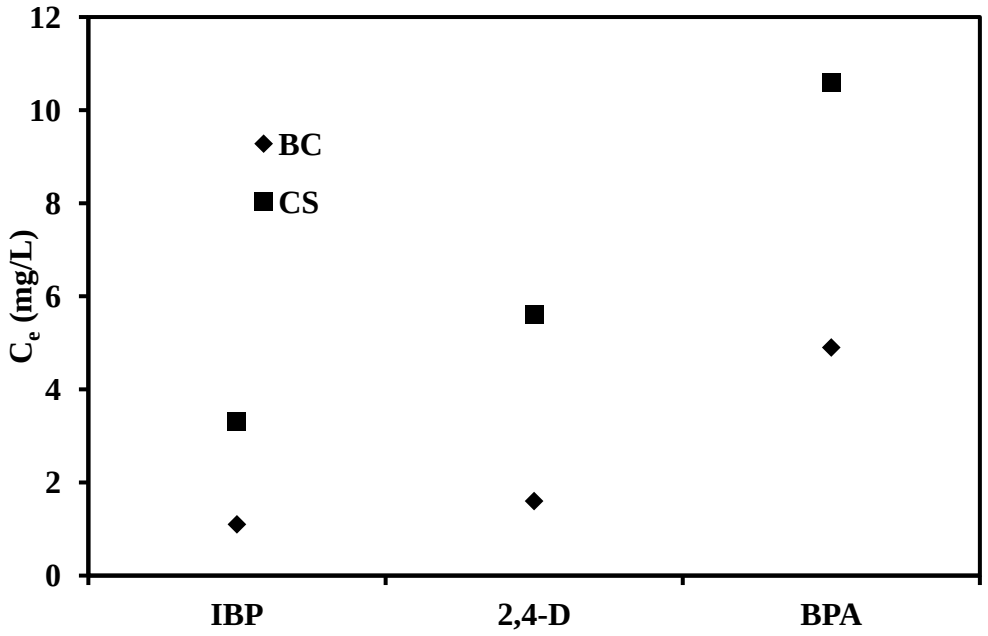

Figure 3-1. Equilibrium concentration of model compounds in contact with 0.2 g/L (40 mg) of BC and CS

To ensure that the samples have reached the equilibrium and no more significant adsorption will occur, several samples were prepared for each model compound and each adsorbent. The time when the change in concentration of model compound in liquid phase became less than 2% of the initial concentration of model compound was considered as equilibrium time. Samples were prepared in the same condition as other isotherm samples. This experiment was duplicated and the average of the concentrations versus time is shown in Figure 3-2 and Figure 3-3.

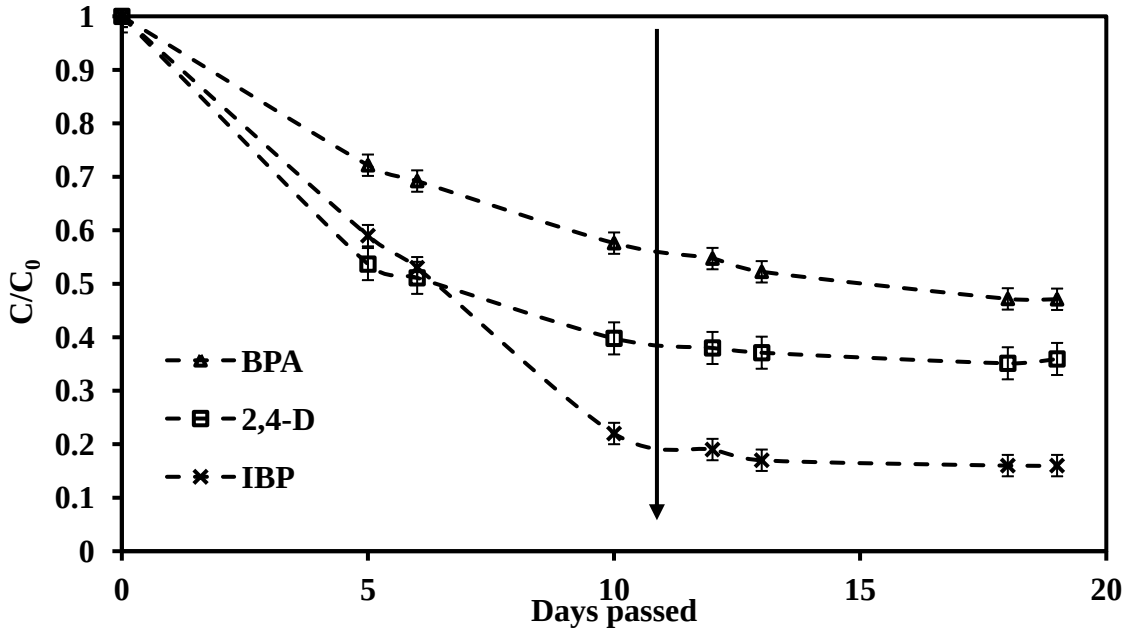

Figure 3-2. Profile of concentration of model compounds in solution as a function of time for adsorption on BC

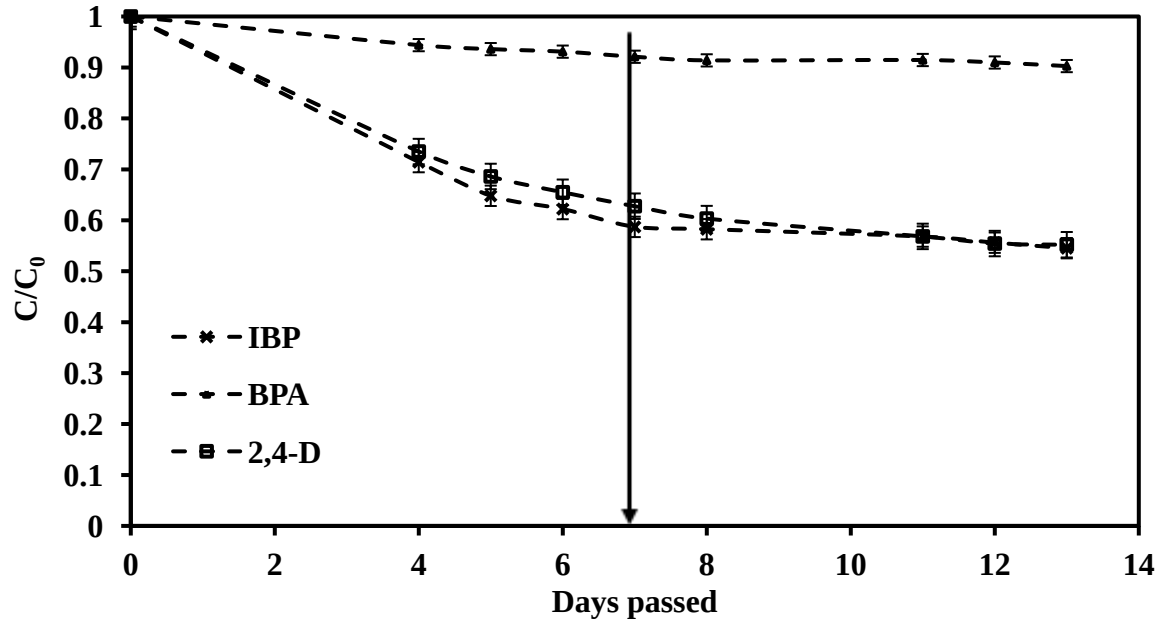

Figure 3-3. Profile of concentration of model compounds in solution as a function of time for adsorption on CS

According to the results of concentration profile, 11 days was chosen as time to reach equilibrium for the entire experiments to keep conformity and consistency.

Adsorption Isotherm Studies at 288 and 280 K

Isotherm studies at 280 and 288 K were conducted to measure the thermodynamic parameters of adsorption including Gibbs free energy, enthalpy, and entropy of adsorption. For this purpose the model parameters of the appropriate isotherm model at 296 K must be obtained. For this purpose, four concentrations of each model compound that covered the entire range of concentration at 296 K were chosen for isotherm experiments. Concentrations of 100, 80, 60, and 30 mg/L were chosen for 2,4-D and BPA. The concentrations of 50, 40, 25, and 10 mg/L were chosen for IBP. In order to use temperatures close to those in cold regions (e.g., Saskatchewan), for thermodynamic analysis two temperatures of 280 and 288 K were chosen. The same glassware as the ones used at 296 K isotherm experiments were used for experiments at 280 and 288 K. A shaker was placed inside a temperature controlled chamber to provide mechanical mixing of samples. The same speed of 130 rpm was set on this shaker. Milli-Q water and stock solution of pollutants were placed in chamber one day prior to preparation of samples to reach the temperature of the chamber. Necessary tools and glassware were carried to the chamber every time to prepare the samples inside the chamber to avoid the fluctuations in temperature of samples. After preparation of samples inside chamber, samples were put on shaker for 11 days until the equilibrium was reached. Samples were moved to the lab for immediate measurement of concentration.

Point of Zero Charge Measurement

Mass titration method was used to measure the point of zero charge (PZC) of adsorbents [64]. Three pH values, assumed to bracket the PZC, were selected. A pH meter was calibrated at the beginning of the experiments. 300 mL of Milli-Q water was added to a beaker. The pH of the solution was adjusted to the desirable pH using NaOH and HNO_3. Five solutions with

concentration of 0.2, 1, 3, 10, and 15% (w/w%; carbon/water) were prepared. For this purpose 30, 150, 450, 1500 and 2250 mg of carbon were weighed and added to test tubes for each pH. 15 mL of solution was measured and transferred using a micropipette to each test tube containing a specific weight of adsorbent. The test tube was quite full and it was immediately sealed with Parafilm® to avoid reaction of the solution with CO_2 present in the air [82]. Samples were shaken for 24 hours. pH meter was calibrated again and pH of each sample was measured immediately after removal of the seal while the pH meter was tightly fitting the test tube diameter (16 mm) and immersed, as there were no air to react with the solution. The pH was recorded and plots were prepared. The pH of the plateau of the plots indicates the PZC [10].

Indigo Method for Liquid Ozone Concentration Measurement

Liquid ozone concentration measurement in regeneration experiments was carried out using an ozone microsensor probe. The Indigo Method was employed to calibrate the microsensor. The minimum detectable concentration with the indigo method is 10-20 µg/L using a spectrophotometer which makes this method a suitable choice for the experiments in the mg/L concentration level. In acidic solution, ozone rapidly decolorizes indigo and the decrease in absorbance of solution is linear with the increase in concentration of ozone in solution, with a proportionality constant of 0.42±0.01 (1/cm.mg.L) [84]. To conduct the Indigo Method, indigo stock solution was prepared by adding 1 mL of concentrated phosphoric acid to 500 mL of distilled water in a 1 L volumetric flask. 770 mg of potassium indigo trisulfonate ($C_{16}H_7N_2O_{11}S_3K_3$) was added to the solution while stirring. The flask was filled to the mark with Milli-Q water. Indigo reagent was prepared using a 1 L volumetric flask filled with 100 mL of indigo stock solution, 7 mL of concentrated phosphoric acid, and 10 g of sodium dihydrogen phosphate (NaH_2PO_4).

Milli-Q water was ozonated in a reactor and samples were taken from the bottom spigot to measure the concentration of ozone and calibrate the probe. For this purpose, a method for concentrations higher than 0.3 mg/L of O_3 was employed. 40 mL of indigo reagent was added to two 100 mL volumetric flasks. One of the flasks was filled to the mark with Milli-Q water considered as blank sample, and the other one was filled to the mark with ozonated water. At the same time, the concentration of ozone measured with the probe was recorded to prepare the calibration curve. Absorbance of each sample at 600±10 nm was measured using the sample with Milli-Q water as blank. The difference in absorbance of the blank sample and the sample containing indigo and ozone was named ΔA. Using f=0.42 (1/cm.mg.L), Indicating b as the path length of spectrophotometer cell to be 1 cm and V as the volume of ozonated water to be 60 mL in this experiment [84]. The actual concentration of ozone was calculated with following formula:

$$O_3\left(\frac{mg}{L}\right) = \frac{100\times\Delta A}{f\times b\times V} \qquad (3.1)$$

Using this method and changing the liquid ozone concentration the calibration curve was prepared (Figure 3-8).

Adsorbents Acid Pre-treatment

10 g of each adsorbent (BC and CS) was weighed and soaked in 2 N nitric acid for three days at 296 K. The acid solution was replaced with distilled water in the third day [74]. Samples were washed with distilled water every day until the pH of the solutions became stable [76].

The samples were filtered and washed with distilled water. Acid treated samples were dried in oven at 383 K for 12 hours [75]. Acid treated samples were bottled immediately and the bottles

were sealed and placed inside desiccators for future use. BC and CS acid treated samples were labelled N-BC and N-CS, respectively.

Adsorbent Regeneration with Ozone

Initially 1 g of BC and CS was weighed. 200 mg of each model compound was added to two 1 L beakers resulting in 600 mg/L of the model compounds in each bottle. 1 L of Milli-Q water was added to each beaker. 75 mL of methanol was added to each solution to increase the solubility of model compounds. The solution was stirred for 10 days. On the 10^{th} day adsorbents were filtered and dried at 296 K for 2 days. The adsorbent was not heated so that the model compounds were not evaporated. 100 mg of each adsorbent was used per test isotherm experiment to make sure that the adsorbent does not have any uptake of the pollution and prove the saturation of the adsorbents. Three samples each one containing 100 mg of adsorbent and a solution containing one model compound was prepared. 10 days after preparation of samples, the concentration of the model compounds was measured and there was no change in the concentration of model compounds in solution, verifying the saturation of adsorbents. Saturated adsorbents were weighed. Each adsorbent was divided into 3 equal aliquots. Each aliquot had a weight of about 0.3 g. Each aliquot was ozonated in Milli-Q water for a specific period of time. A mixture of oxygen and ozone with flow rate of 0.5 L/min and ozone concentration of 18 g/m^3 was bubbled into the liquid. Dissolved liquid ozone concentration of 3.5 to 4.5 mg/L was achieved and set for all experiments, and ozonation times of 15, 30, and 60 min were chosen for ozonation regeneration [27, 79, 80]. Ozonated samples were filtered immediately and dried at 383 K overnight and kept in a desiccator.

3.3. Analytical Methods

Model Compounds Concentration Measurement

Concentration of IBP, 2,4-D, and BPA was determined by UV-Vis spectrometry. For this purpose a MECASYS Optizen POP spectrophotometer was used. Literature reports detection of IBP, 2,4-D, and BPA at 222, 282, and 275.5 nm wavelength, respectively in Milli-Q water [5, 6, 28, 69]. In order to find the precise wavelength attributed to maximum absorbance under the condition of this research a short range of wavelength (190-300 nm) for absorbance of solutions containing model compounds was scanned. The desirable peaks were detected at the expected wavelength with a minor shift. To make sure that the shift in wavelength of peak will not affect the results for all experiments a short neighbourhood of the peak was scanned and the maximum was considered. This scan was also repeated for lower concentrations that were supposed to be used for calibration lines, for conversion of absorbance of model compounds to their concentration. Absorbance curves of model compounds are available in Appendix A. The absorbance curves for different of dilutions of IBP with Milli-Q water are presented in Figure 3-4.

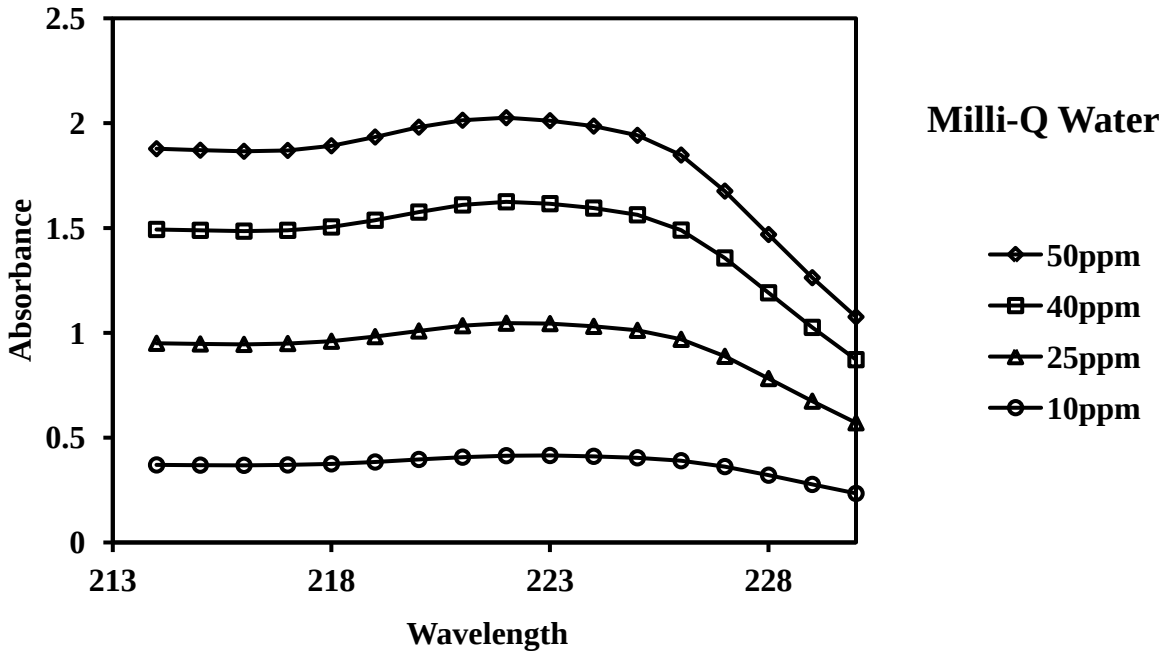

Figure 3-4. Absorbance curve of IBP (7%, w/w; Methanol/Milli-Q water), maximum absorbance occurring at 222 nm

For samples with tap water, the blank sample was also tap water so that the right difference in absorbance was measured. Maximum absorbance of IBP in tap water was higher than in Milli-Q water. Therefore, a different calibration curve was used to convert the absorbance of IBP to its concentration in tap water. The maximum absorbance wavelength for IBP shifted from 222 nm in Milli-Q water to 223 nm in tap water matrix.

For 2,4-D and BPA the absorbance of the solution prepared with tap water matrix had quite the same absorbance as the solution prepared with Milli-Q water matrix.

Model Compounds Concentration Measurement Calibration Lines

Four calibration curves were prepared based on the maximum absorbance curves of the model compounds. IBP had two calibration curves because the absorbance of IBP was different in tap water matrix than in Milli-Q water. The calibration curves showed a linear relationship between the absorbance and the concentration of the model compounds. Therefore the equation of the

linear trend-line obtained using Microsoft Excel, was used to convert the absorbance to concentration. Calibration curves are available in Appendix A. A calibration curve for IBP in Milli-Q water is presented in Figure 3-5.

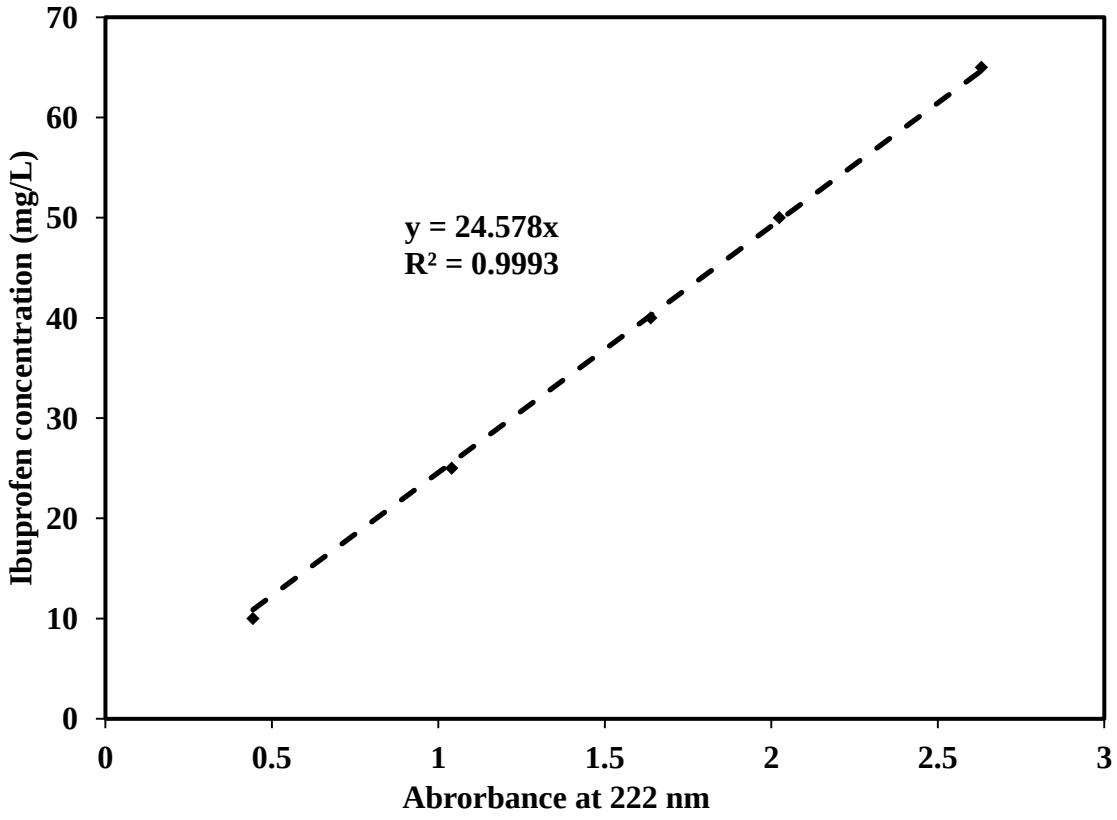

Figure 3-5. IBP (7%, w/w; Methanol/Milli-Q water) concentration measurement calibration line

pH and Temperature Measurement

The pH of the samples was measured using a double-junction Cole-Parmer 12-mm glass body pH electrode. Depending on the range of pH of the samples standard buffers of 4, 7, and 10 bracketing the target range of pH were used for each experiment to calibrate the pH meter before measurements. The room controlled temperature was setup at 296 K and it was also measured with a mercury thermometer. For the lower temperatures of 288 K and 280 K the experiments were carried out in environmental chamber from Conviron Company. The chamber was able to

maintain the temperature in the range of 278-318 K. The chamber was equipped with CMP4030 temperature controller (software version of 5.0).

Liquid Ozone Concentration Measurement and Calibration

In order to measure the concentration of ozone in liquid phase for adsorbent regeneration experiments, dissolved ozone concentration was measured using an ozone microsensor (MS-O3, AMT Analysenmesstechnik GmbH) with a response time of less than 5 seconds. The Indigo Method was employed to measure the actual concentration of ozone in liquid phase and calibrate the microsensor. This method is explained in detailed previously. Using the results of this method and the concentration obtained by the microsensor a calibration curve (Figure 3-6) was prepared.

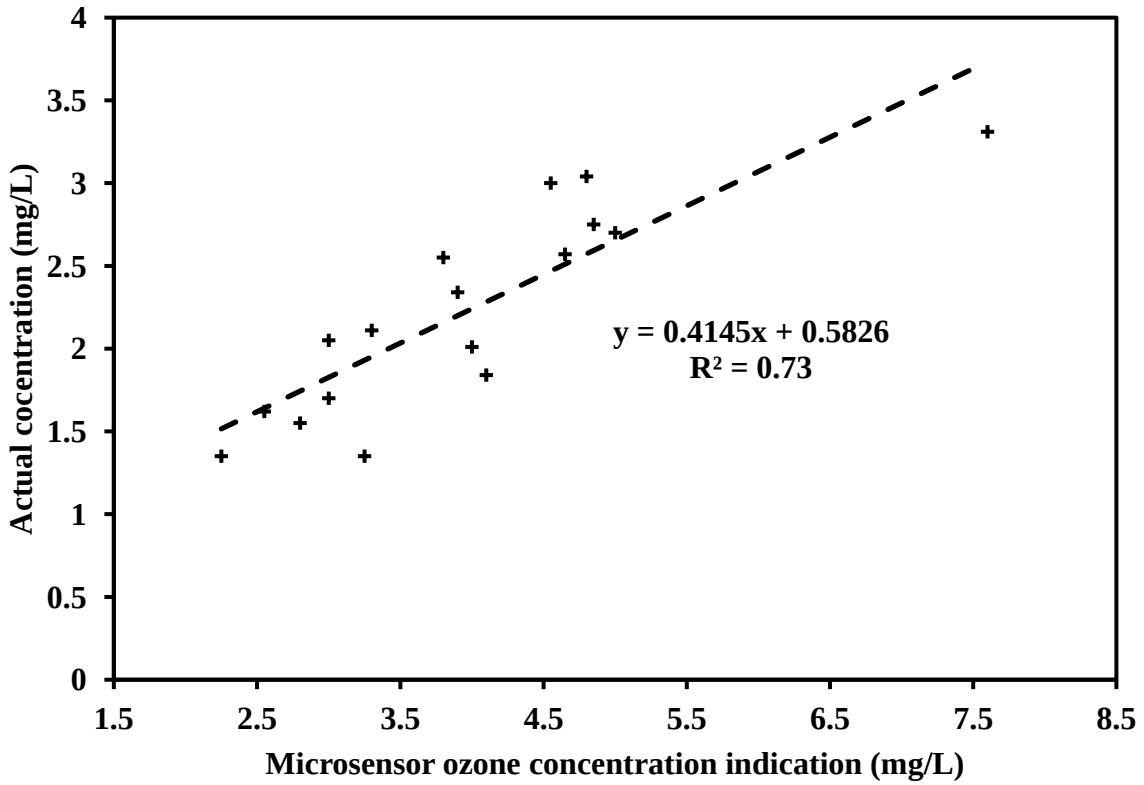

Figure 3-6. Liquid ozone measurement microsensor calibration curve obtained using Indigo Method

Adsorbent Characterization

Surface area and pore volume of adsorbents were measured using a Micromeritics ASAP 2020 equipment. Physisorption of N_2 at 77 K was performed at different partial pressures to plot the isotherm of adsorption and desorption of N_2 on adsorbent. Point of zero charge (PZC) of the adsorbents was measured using mass titration method.

3.4. Repeatability of Experimental Measurements and Procedures

The concentration of fresh stock solutions was measured every time a stock solution was prepared. The standard deviation of the stock solutions divided by the target initial concentration was calculated to be 0.7%, 1.12%, and 0.58% for IBP, 2,4-D, and BPA stock solutions, respectively. The weight of adsorbent for each isotherm experiment was between 40-41mg (0.2-0.205 mg/L) considering all model compound present in solution adsorbed, it can affect the maximum adsorption capacity of model compounds about 2.5%. Several isotherm samples were repeated by random. The standard deviation of the results was in the range of 5% of concentration of the stock solutions. The chamber temperature controller exhibited an accuracy of ±0.1. The ozone microsensor presented a tolerance of ±0.1 mg/L. The pH meter possessed a tolerance of ±0.1. The repetition of absorbance of the same sample with different vials at different time with spectrophotometer exhibited a standard deviation of 0.005.

Isotherm experiments samples were duplicated and the average of the concentrations was used to find the model parameters. Triplicate of the samples were prepared in case the average of concentration of the first sample and the duplicate did not provide a good fit to the model. Duplicate of the PZC measurement samples were also prepared to verify the results.

CHAPTER FOUR

CHARACTERIZATION OF ADSORBENTS

The adsorbents porosity and point of zero charge (PZC) were characterized, following the experimental procedures described in chapter three. In this chapter results of characterization of adsorbents are presented. The techniques used to analyze the results are also presented.

4.1. Measurement of Adsorbent Surface Area and Pore Volume

In order to characterize the porosity of the BC, N-BC, CS, and N-CS, N_2 physical adsorption and desorption at 77 K was carried out using ASAP 2020 system. The micro, meso, and macroporosity of the adsorbents in this research are classified as 0.4-2 nm micropore in conformity to literature [85], 2-50 nm as mesopore, and >50 nm to be the macropore range [5, 49]. Before characterization with N_2, samples were dried overnight at 383 K in an oven to remove moisture from the pores. About 0.2 g of each adsorbent was used for characterization. The degassing of sample was carried out to remove physisorbed species from the surface of sample including, moisture and contamination. This step is also called activation, as it prepares the surface of the adsorbent for adsorption of N_2 molecules [85].

Adsorption and desorption of N_2 on the surface of adsorbent occurs at different partial pressures (p/p_0) of nitrogen, where p_0 is the saturation vapour pressure of N_2. The adsorption of N_2 starts when the relative pressure is 0 until the saturation pressure of N_2 occurs. Afterwards desorption

takes place until the relative pressure reaches 0. Isotherm data for adsorption and desorption of N_2 on adsorbents are present in the Appendix B. The isotherm data at predetermined relative pressures for the adsorption and desorption of N_2 on CS is presented in Figure 4-1.

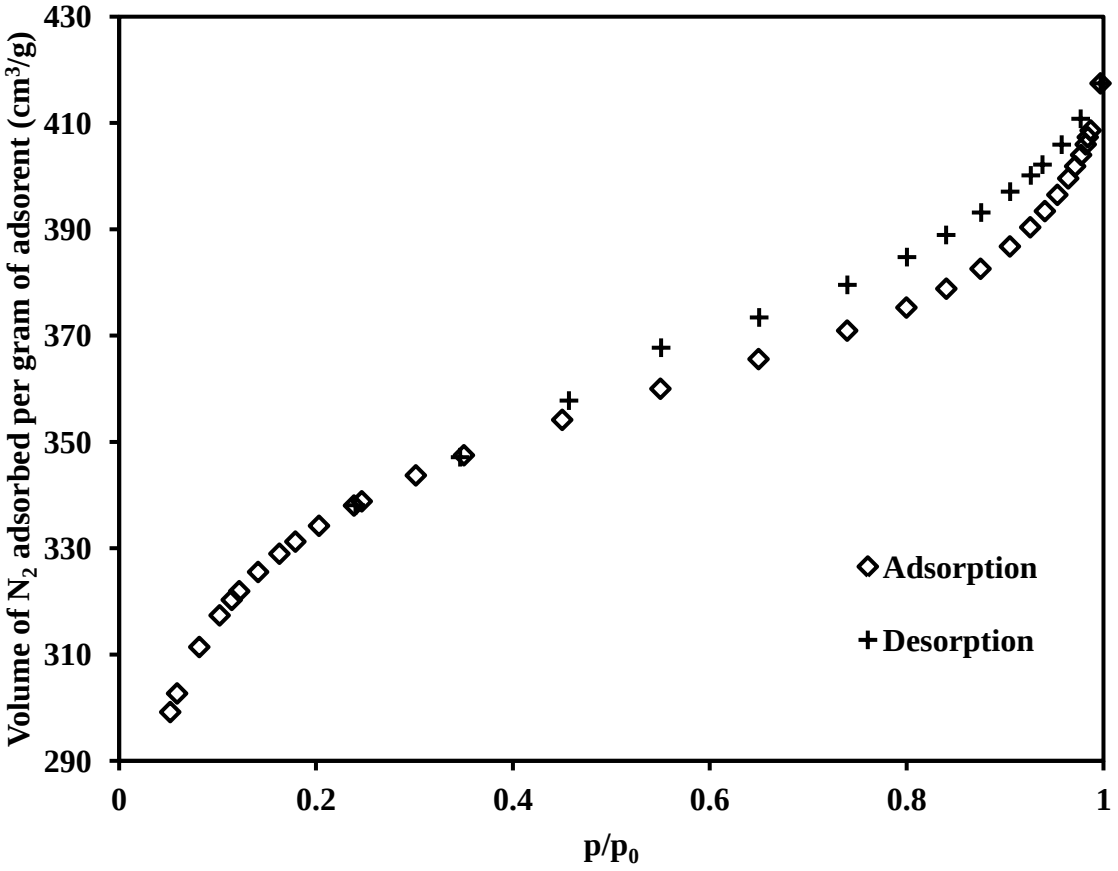

Figure 4-1. Isotherm data of adsorption and desorption of N_2 on CS at 77 K

Calculation of Specific Surface Area and Single-Point Pore Volume by BET Equation

Specific surface area and pore volume of adsorbents were calculated using the Brunauer-Emmett-Teller (BET) equation. This equation is a well-established model commonly used for the calculation of specific surface area using isotherm data [86]. The BET equation is based on a multilayer adsorption. The BET equation after the assumption of number of layers approaching infinity is simplified as below:

$$\frac{p/p_0}{n^a\left(1-\frac{p}{p_0}\right)} = \frac{1}{n_m^a C} + \left(\frac{C-1}{n_m^a C}\right)\left(\frac{p}{p_0}\right) \quad (4\text{-}1)$$

The equation is valid for $p/p_0<0.35$ to estimate the monolayer [87]. In equation 4-1 n^a (cm^3/g) is the amount adsorbed, n^a_m (cm^3/g) is the amount adsorbed at the statistical monolayer, and C is a constant related to energy of adsorption. Plotting $(p/p_0)/[n^a(1-p/p_0)]$ against p/p_0 for the range of $0.05<p/p_0<0.35$, C and n^a_m can be found from the slope and intercept of the resulting straight line [85]. The linear plot for BC using isotherm data is presented in Figure 4-2. The trend-lines fitting the data for adsorption on CS, N-BC, and N-CS are available in Appendix B.

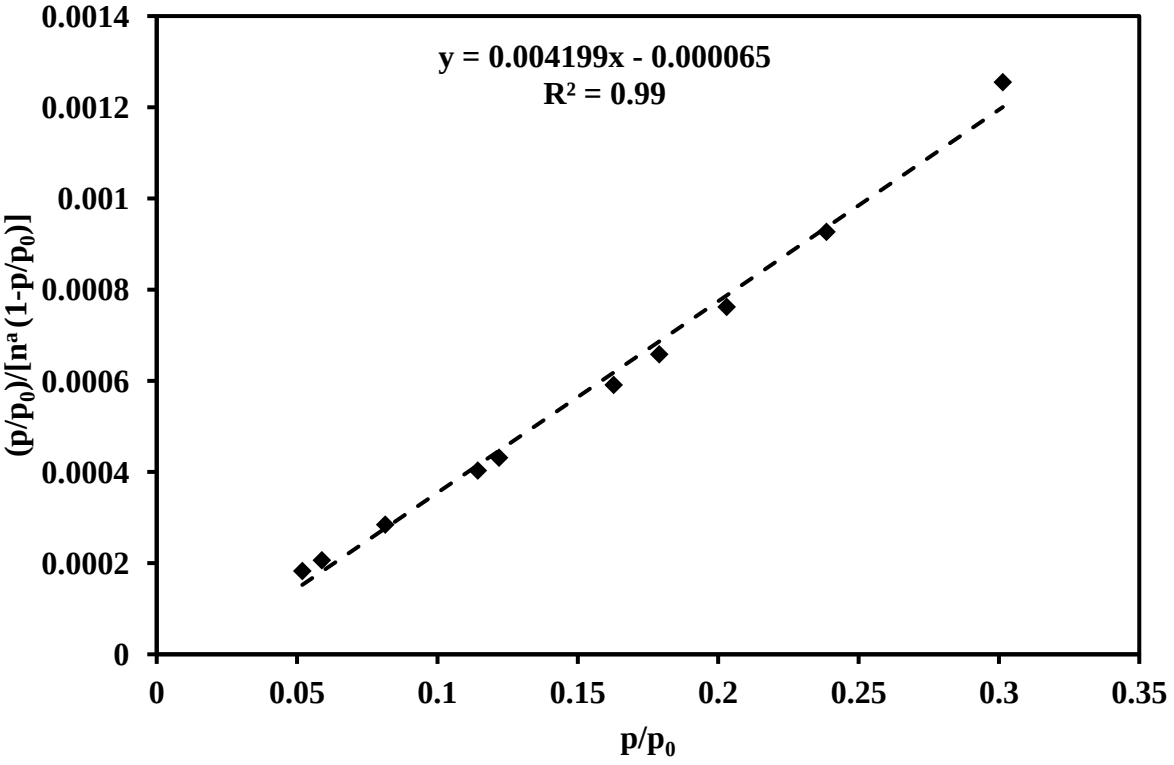

Figure 4-2. Linear trend-line fit to the isotherm data from adsorption of N_2 on BC using BET equation

Using the trend-line equation slope and intercept the C and co n^a_m were determined for all adsorbents. Having the n^a_m (cm^3/g) as the monolayer maximum capacity and using the cross-

sectional area of a N_2 molecule when it is adsorbed on the surface of carbon in monolayer to be σ_m equal to 0.162 (nm^2/molecule) [87] it is possible to calculate the specific surface area of adsorbent. The number of molecules in a mole (Avogardro's number) equals to 6.03×10^{23} and the volume of one mole of gas at standard temperature and pressure is 22,400 cm^3 [13] therefore, the specific surface area for the adsorbents can be calculated from the equation below:

$$S_{BET} = \frac{n_m^a}{22{,}400} \times 6.03 \times 10^{23} \times 10^{-20} \times \sigma_m = 0.269 \times n_m^a \times \sigma_m \qquad (4\text{-}2)$$

The molecular weight of N_2 is 28.02 (g/mol) and the density of N_2 at 77 K is 0.809 (g/cm^3) [85]. At standard temperature and pressure, one mole of an ideal gas has a volume of 22,400 cm^3. Using this information, the single point pore volumes of adsorbents were calculated using the isotherm data at p/p_0=0.984, using the equation 4-3:

$$V(cm^3/g) = \left[\frac{n_m^a}{22{,}400} \times 28.02\right] / 0.809 \qquad (4\text{-}3)$$

Assuming the shape of pores to be cylinders with diameter of D and length of L, the average diameter of pores will be calculated using specific surface area and pore volume of the adsorbents with the equation (4-4).

$$D_{ave}(nm) = \frac{4KV}{S} \qquad (4\text{-}4)$$

The average pore diameter is calculated using equation 4-4, with the single point pore volume (cm^3/g) at p/p_0=0.984 and specific surface area (m^2/g) obtained from the BET equatio. K in equation 4-4 is a constant equal to 1000 to convert the units. Results of calculation of specific surface area, single point pore volume, and average pore diameter for all adsorbents (BC, N-BC, CS, and N-CS) are presented in Table 4-1.

Table 4-1. BET specific surface area and single point pore volume of adsorbents

Adsorbent	**BC**	**N-BC**	**CS**	**N-CS**
S_{BET} (m^2/g)	1053	1085	982	1001
V_{BET} at p/p_0=0.984 (cm^3/g)	0.63	0.65	0.52	0.53
D_{ave} (nm)	2.39	2.41	2.13	2.11

Comparing the specific surface area and pore volume of acid treated adsorbents with fresh samples indicates that pre-treatment of adsorbents with nitric acid has not affected the specific surface area and pore volume of adsorbents. The change in D_{ave} of acid treated samples compared with fresh ones is small indicating that the shift in average pore width has been very small or change in pore volume has been evenly distributed.

Calculation of Micropore and External Surface Area by the t-method

The EPs have bulky molecules [88] and adsorption of bulky molecules is affected by size exclusion effect [47] therefore; it is helpful to estimate the amount of micropores present in an adsorbent. For this purpose the t-method was employed, to distinguish the external surface area of adsorbents from the surface area attributed to the micropores. This method assumes that the monolayer of N_2 being adsorbed on the surface of adsorbent fills the micropores and any further adsorption occurs on the external surface area [89]. The Harkins-Jura equation (Equation 4-4) relates the partial pressure of the isotherm adsorption of N_2 to the thickness of the adsorption layer [89].

$$t(\text{Å}) = \left[\frac{13.99}{0.034 - \log\left(p/p_0\right)}\right]^{0.5} \qquad (4\text{-}4)$$

Using equation 4-4, the thickness of the adsorbed layer can be calculated. The ratio of increase in adsorption capacity of N_2 on adsorbent is proportional to the external surface area of the adsorbent, when the thickness of the N_2 layer is equal to the monolayer thickness (3.54 Å). To

find this ratio, it is required to find the slope of the trend-line in the plot of the volume of gas adsorbed against thickness of adsorbed layer.

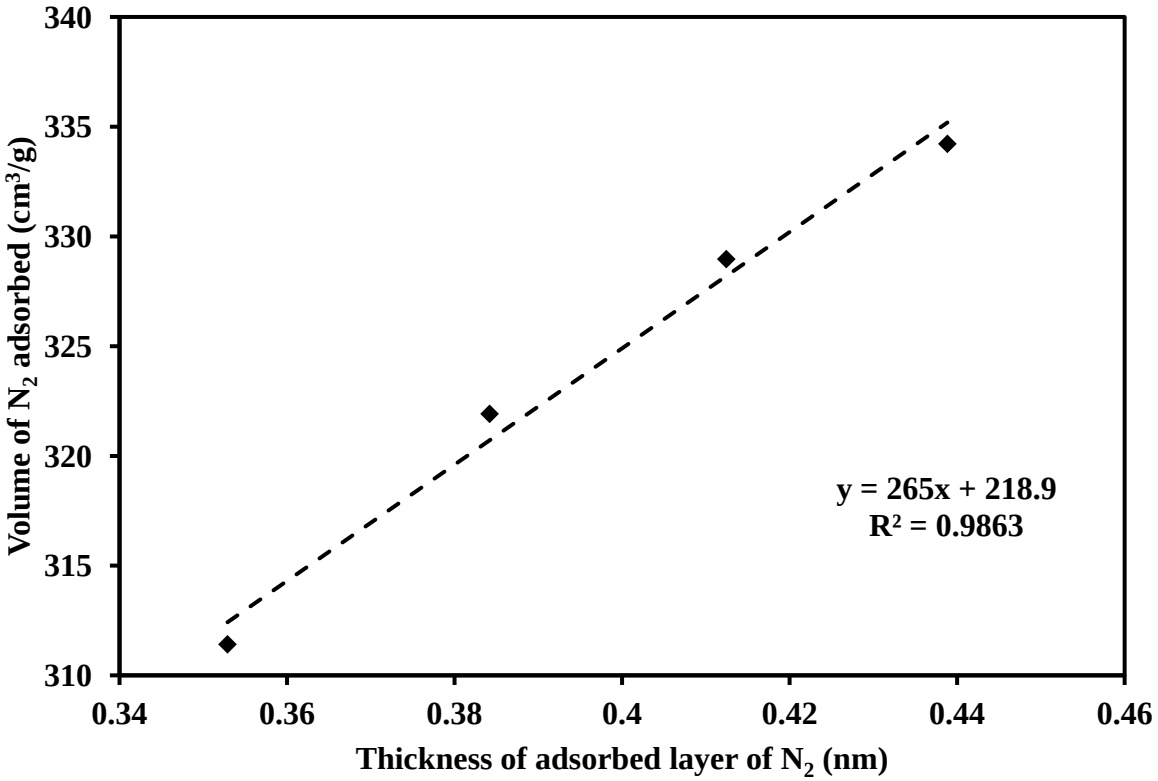

Figure 4-3. Linear trend-line fit to the thickness plot of adsorption of N_2 on BC (find the trend-line for N-BC, CS, and N-CS in Appendix B)

The external surface area is calculated using the following equation:

$$S_{External}(m^2/g) = 1000 \times Slope\ (cm^3/g.nm) \times \frac{1}{22{,}400} \times 28.02 \times \frac{1}{0.809} \qquad (4\text{-}5)$$

In equation 4-5 , 22,400 (cm^3/mole) is the volume of one mole of ideal gas at standard temperature and pressure, 28.02 (g/mole) is the molecular weight of N_2, and 0.809 (g/cm^3) is the density of N_2 at 77 K [85]. Using equation 4-5, the external surface area of each adsorbent was calculated. Subtracting the external surface area from the specific surface area, the micropore surface area is calculated.

Table 4-2. External surface area ($S_{External}$) and micropore surface area (S_{Micro}) calculated using t-method

Adsorbent	**BC**	**N-BC**	**CS**	**N-CS**
$\mathbf{S_{External}\ (m^2/g)}$	410	455	166	159
$\mathbf{S_{Micro}\ (m^2/g) = S_{BET} - S_{External}}$	643	630	816	842

The results of the t-method shows that 80-85% of CS and N-CS surface area were micropores, while approximately 60% for BC and N-BC. This observation indicates that the CS and N-CS have more micropores in their structure than BC and N-BC, and that this is in agreement with the literature that coconut shell based carbons have more microporous structure than bituminous based carbons [47]. The results indicate that acid pre-treatment decreased the external surface area of the CS and increased the microporosity. This occurred due to micropore opening through the removal of impurities [20, 75]. The acid pre-treatment increased the external surface area of BC and decreased the microporosity. This is explained due to the formation of oxygen-containing functional groups stretching to the walls of slit-shaped pores [10, 20].

Pore Size Distribution of the Adsorbents in Mesopore range

According to the literature, mesoporosity of an adsorbent affects the uptake of bulky molecules [47]. In order to characterize the size distribution of mesopore of the adsorbents, the Barrett-Joyner-Halenda (BJH) method of isotherm analysis is suitable for mesopore size distribution analysis [90]. In the method, the shape of pores is assumed to be cylindrical. The desorption isotherm data was used for analysis [91]. The results of incremental pore volume and surface area distribution of mesopore range (2 to 50 nm) were plotted in Figures 4-4 and 4-5 respectively.

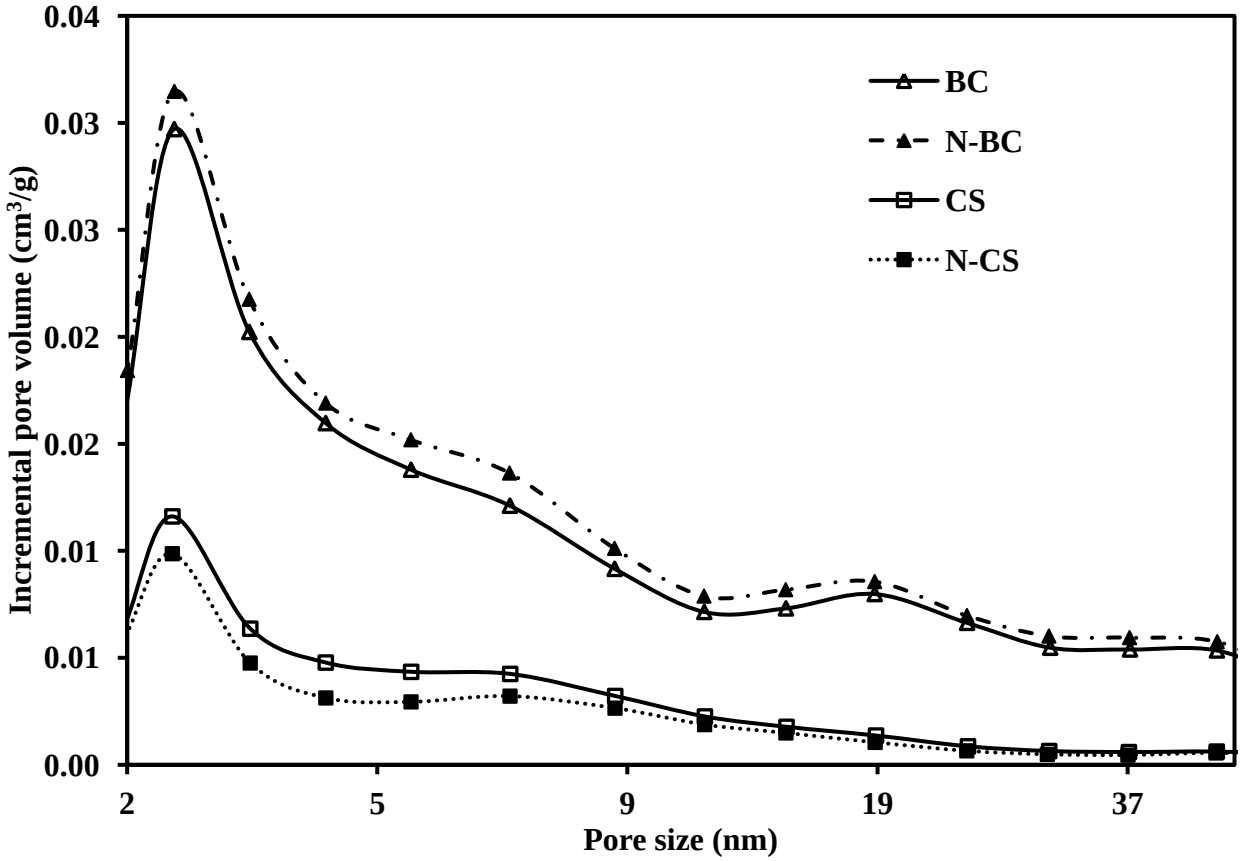

Figure 4-4. Incremental BJH pore volume versus pore size in mesopore range (2-50 nm)

According to the BJH pore volume analysis, the CS exhibited most of its meso-pore volume in the range of 2 to 8 nm. Whereas BC has a wider range of distribution of pore volume, up to 50 nm, which is in agreement with literature describing the bituminous based activated carbons to be have a wide range of mesoporosity [92]. The BJH meso-pore volume results indicate that the 73% of CS meso-pore volume is in range of 2 to 8 nm, while about 56% of the BC meso-pore volume is in the 2 to 8 nm range, which represents a narrow pore size distribution of CS. However the BJH surface area and pore size volume ranged 2 to 8 nm ($S_{BJH,\ 2\ to\ 8\ nm}$ and $V_{BJH,\ 2\ to\ 8\ nm}$) for BC, representing 2.80 and 2.79 times the same parameters for CS, respectively. This means that the BC exhibits a high porosity compared to the CS.

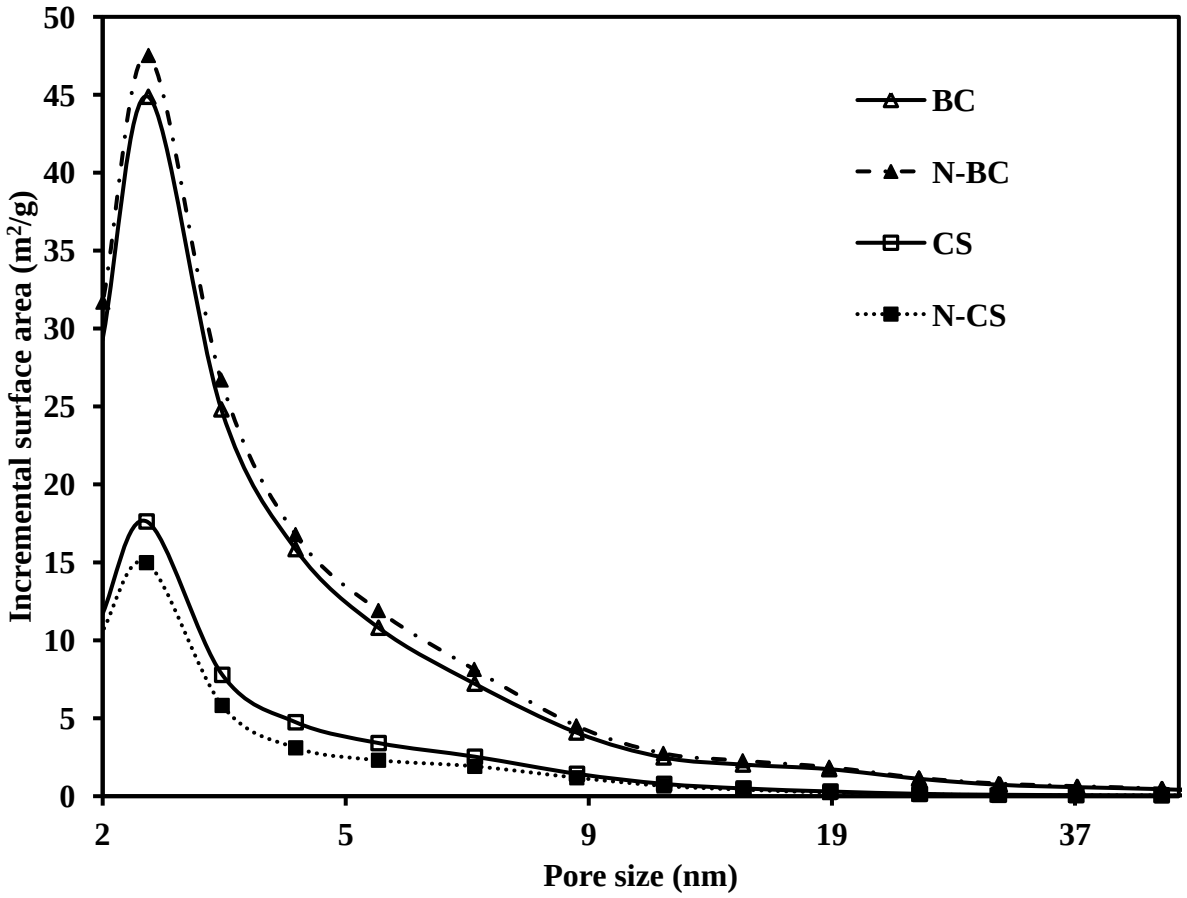

Figure 4-5. Incremental BJH surface area versus pore size in mesopore range (2-50 nm)

The BC and CS surface area and pore volume (BET results represent micro-, mess- and macro-pore surface area, S_{BET} and V_{BET} of BC) are 1.07 and 1.21 times the same parameters for CS, respectively. However, the BJH analysis representing the meso-pore range, S_{BJH} and V_{BJH} of BC are 2.88 and 3.41 times S_{BJH} and V_{BJH} of CS, respectively. Considering S_{BET} and V_{BET} values of BC and CS it can be concluded that both have increased after acid treatment, while the S_{BJH} and V_{BJH} have increased for N-BC and decreased for N-CS. This indicates that the BET analysis does not give reliable parameters to evaluate the change in the meso-pore surface area and pore volume. From this point of the document S_{BET} and V_{BET} represent the specific surface area and pore volume of the micro-, meso-, and macro-pore (Covering pore size 0f 0.4 to 50< nm) and S_{BJH} and V_{BJH} represent meso-pore (covering pore size of 2 to 50 nm).

4.2. Measurement of Point of Zero Charge

The point of zero charge (PZC) of BC, CS, and their acid treated samples (N-BC and N-CS) were determined using mass titration method, which is explained in chapter three. In case the pH diagrams did not converge, experiments were repeated to achieve the convergence of the pH diagram plateaus. The PZC diagrams were plotted (Figure 4-6) and the corresponding values were estimated (Table 4-3).

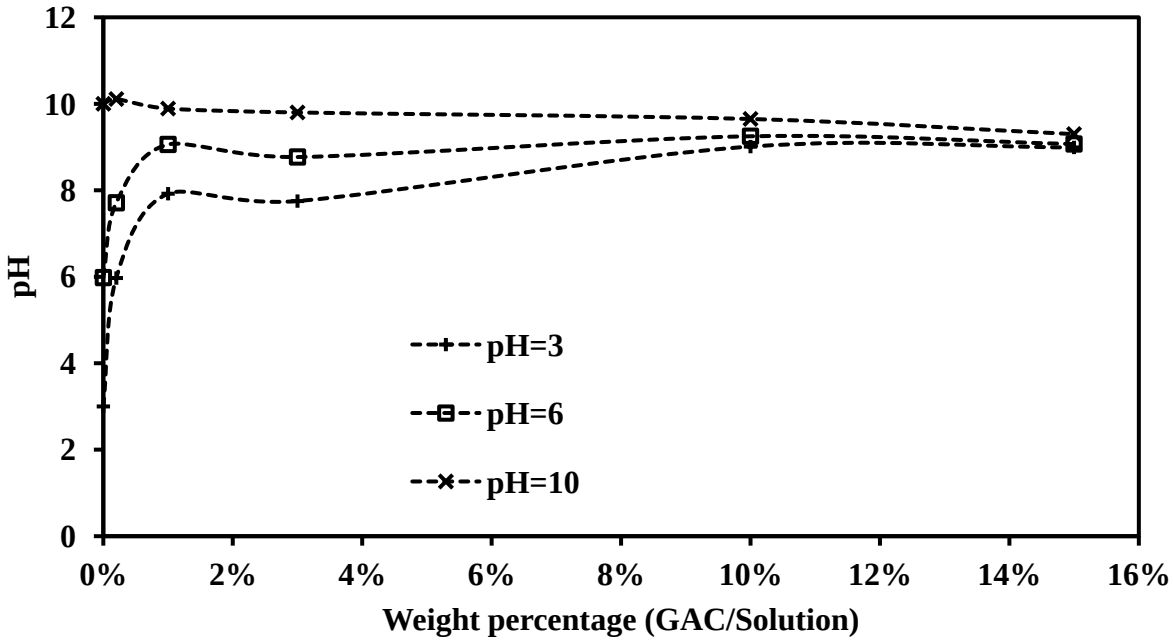

Figure 4-6. Determination of point of zero charge of BC (find diagrams for CS, N-CS, and N-BC in Appendix B)

The point of zero charge of BC was lower than the value that the company catalogue states. This could be due to surface oxidation of carbon in contact with air, or "aging" [65] which has made the surface of carbon more acidic than the fresh adsorbent. The PZC of CS is close to one unit higher than BC. This difference is also observed in PZC of acid-treated samples where PZC of N-BC is close to one unit less than N-CS (Table 4-3). The surface of adsorbents is more positively charged at pH values lower than the PZC and more negatively charged at pH values

higher than the PZC. This surface charge can induce repulsive and attractive electrostatic forces to the charged solute molecules and reduce or increase the adsorption.

Table 4-3. Point of zero charge values measured for adsorbents

Adsorbent	**BC**	**N-BC**	**CS**	**N-CS**
Point of zero charge	9.0	3.1	9.6	4.0

CHAPTER FIVE

ADSORPTION OF MODEL COMPOUNDS ON FRESH ADSORBENTS

This chapter presents results of adsorption of the model compounds on fresh adsorbents. Results of isotherm adsorption of model compounds in Milli-Q water at 280, 288, and 296 K are presented, the isotherm models are fit to the data and the best fit model parameters are found. Results of analysis are discussed. Thermodynamics of adsorption of model compounds on fresh adsorbents in Milli-Q water is studied using the results of isotherm experiments at 280, 288, and 296 K. The results of adsorption of model compounds on fresh adsorbents in tap water matrix are presented, model parameters are found and results are discussed.

5.1. Adsorption of Model Compounds on Fresh Adsorbents in Milli-Q Water

Adsorption experiments of IBP, 2,4-D, and BPA on BC and CS in Milli-Q Water were conducted following the experimental procedure explained in chapter three. Absorbance of isotherm samples containing model compounds was measured at equilibrium with a spectrophotometer at the wavelengths for each EP stated in chapter three. Absorbance of samples was converted to the concentration of model compounds using the calibration curves prepared and presented in chapter three. Equilibrium concentration of model compounds on adsorbents was calculated using equation (2-10). Isotherm equilibrium data was fit to the linear form of

Langmuir and Freundlich models (Equations 2-11 and 2-12, respectively). The trend-line fitted to the linear Langmuir model for adsorption of 2,4-D on BC in Milli-Q Water at 296 K is presented in Figure 5-1, showing C_e/q_e versus C_e. The trend-line fit the linear Freundlich model for adsorption of 2,4-D on BC in Milli-Q Water at 296 K is presented in Figure 5-2, showing Ln q_e versus LnC_e. Trend-lines fit the linear Langmuir model for other adsorption isotherms are available in Appendix C.

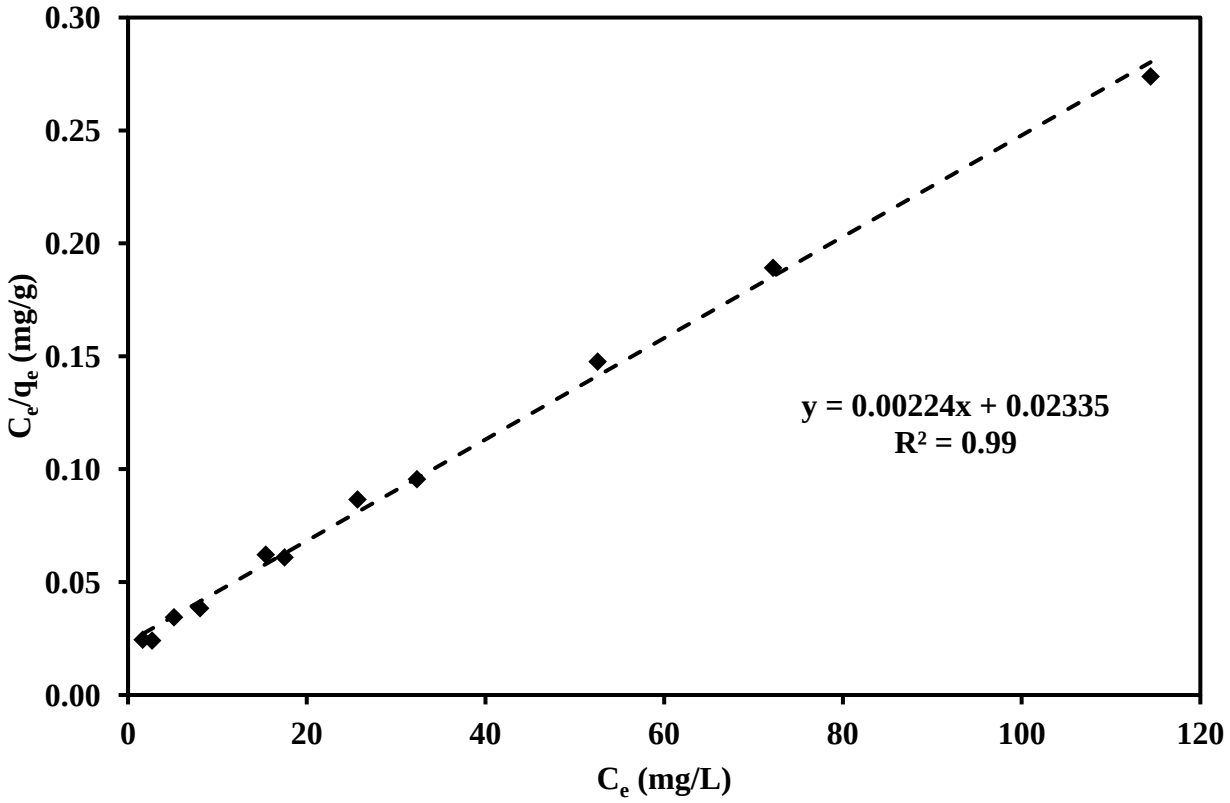

Figure 5-1. Linear Langmuir model fit to the equilibrium isotherm data of adsorption of 2,4-D on BC in Milli-Q Water at 296 K and pH=3.5-5.5

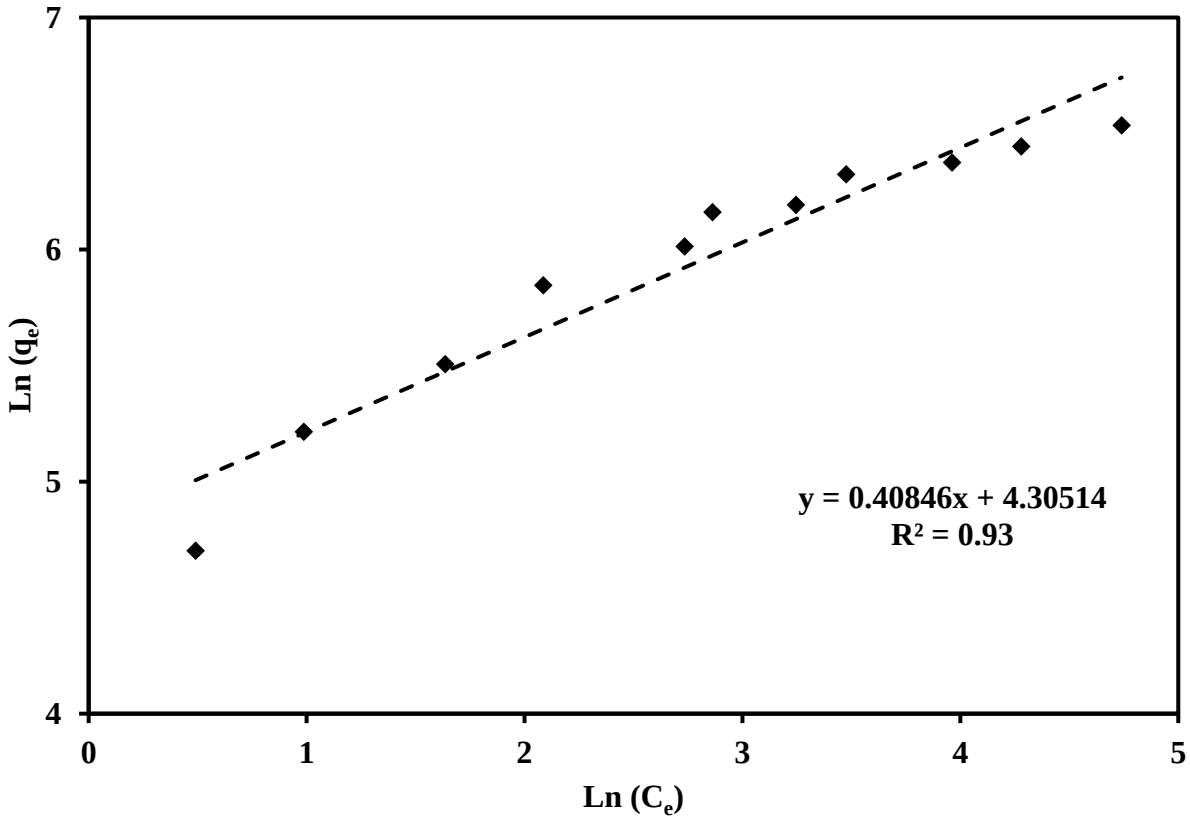

Figure 5-2. Linear Freundlich model fit to the equilibrium isotherm data of adsorption of 2,4-D on BC in Milli-Q water at 296 K and pH=3.5-5.5

Adsorption isotherm equilibrium data was collected for adsorption of IBP, 2,4-D, and BPA on BC and CS in Milli-Q water at 296, 288, and 280 K. For adsorption isotherm at 280 K higher concentration of 2,4-D and BPA than samples at 296 K were considered because of higher uptake at lower temperatures. For all three model compounds of this research isotherm equilibrium data was fitted to the linear form of Langmuir and Freundlich models. The trend-line with higher linear regression coefficient (R^2) showed the best fit model.

Maximum adsorption capacity and intensity of adsorption was calculated for both isotherm models of Langmuir and Freundlich. The calculated model parameters and the linear regression coefficients of the trend-lines for the experimental data are presented in Table 5-1. The model parameters obtained at 288 and 280 K are presented in Table 5-2 and Table 5-3, respectively.

Table 5-1. Langmuir and Freundlich isotherm model parameters for adsorption of model compounds on BC and CS in Milli-Q water at 296 K, Units: Q_{max} (mg/g), b (L/mg), and K_F ($mg^{(n-1)/n}.L^{1/n}.g^{-1}$)

		Langmuir			**Freundlich**		
	Adsorbent	Q_{max}	b	R^2	K_F	1/n	R^2
IBP	BC	249	1.322	0.99	114	0.29	0.76
2,4-D		446	0.094	0.99	91	0.35	0.94
BPA		238	0.049	0.98	31	0.41	0.93
IBP	CS	144	0.272	0.94	57	0.23	0.90
2,4-D		377	0.025	0.94	23	0.54	0.92
BPA		79	0.057	0.99	17	0.30	0.83

The Langmuir model was the best model, by comparing the regression coefficients of the trend-lines fit to the experimental data, listed in Table 5-1, for all three model compounds on BC and CS in the concentration range of the experiments. However, the Freundlich model parameters relatively followed the same trend as the Langmuir model parameters. Since the Langmuir model is the best fit for the isotherm adsorption data, Langmuir model parameters are used for the rest of the analysis. According to literature, a better fit of the Langmuir model to the adsorption isotherm data than Freundlich model is an indication of a monolayer adsorption of the solute on adsorbent and the uniform distribution of adsorption sites on the adsorbent [49]. The Langmuir model fitted to the experimental data together with the experimental data for adsorption of three model compounds on BC and CS is plotted in Figure 5-3 and Figure 5-4, respectively.

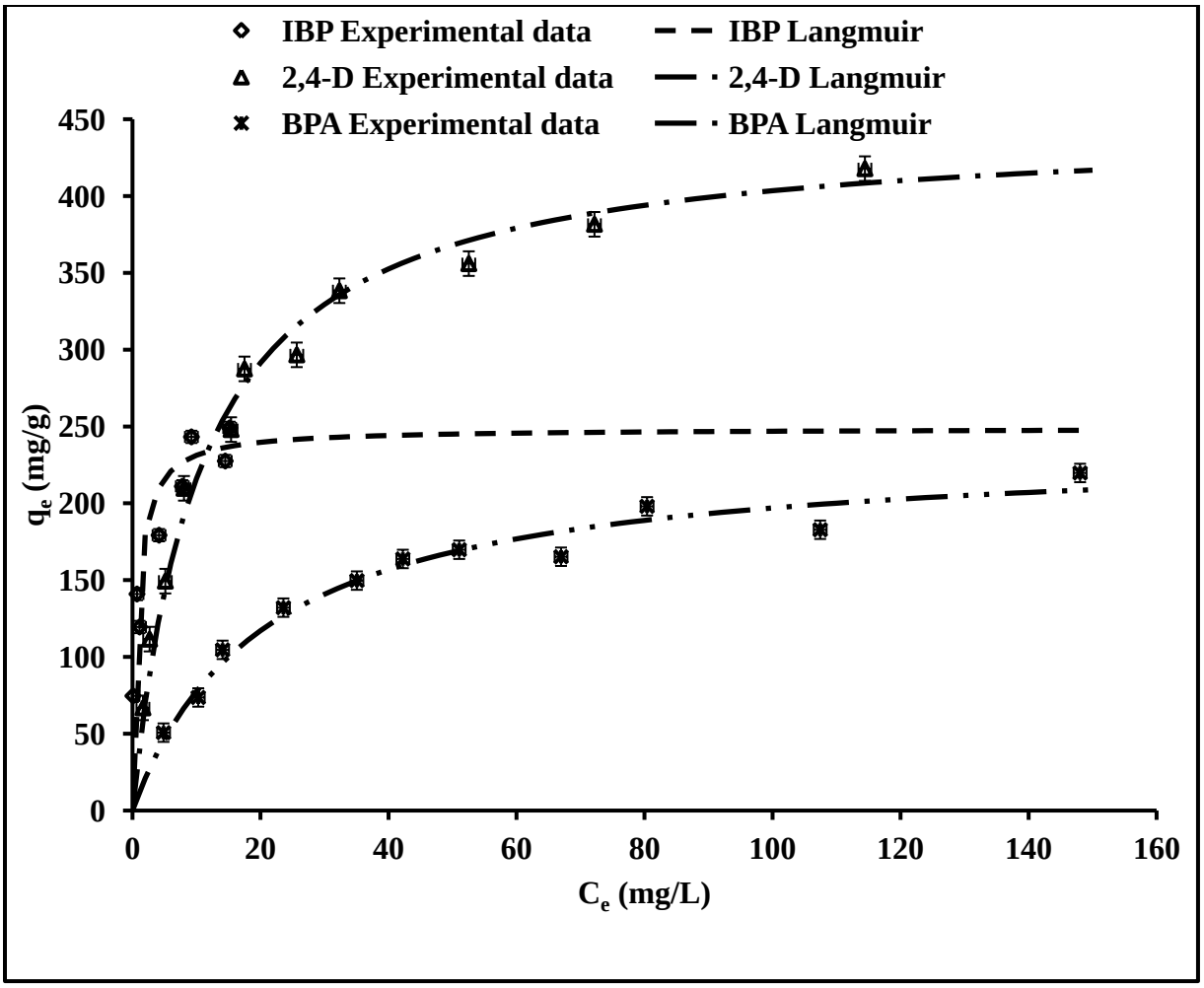

Figure 5-3. Isotherm experimental data and Langmuir model fit to the data for adsorption of model compounds in Milli-Q water on BC at 296 K (Please see pH of samples in Figure 5-5)

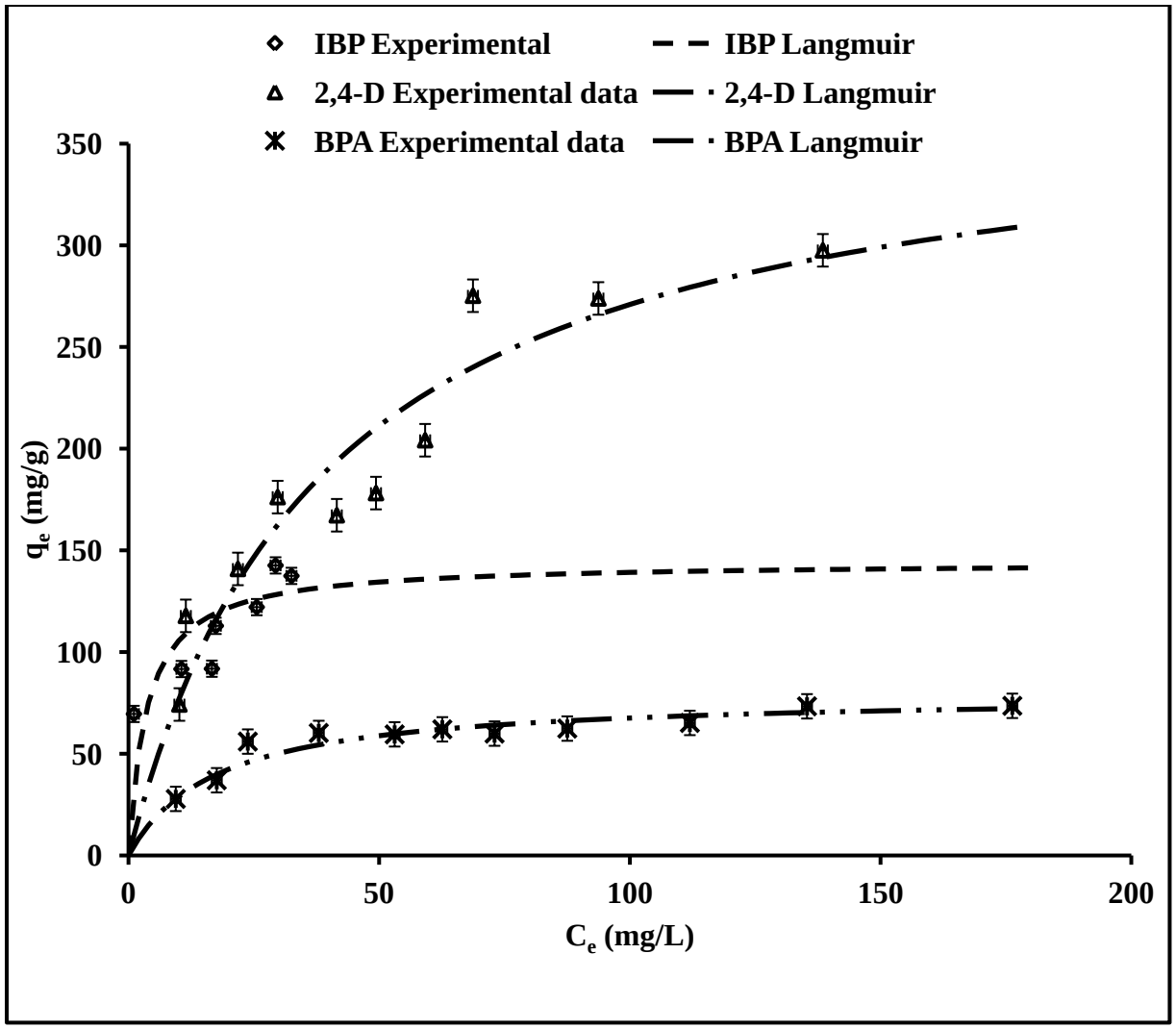

Figure 5-4. Isotherm experimental data and Langmuir model fit to the data for adsorption of model compounds in Milli-Q water on CS at 296 K (Please see pH of samples in Figure 5-5)

The pH of the isotherm samples was not adjusted to avoid introduction of an electrolyte into the solution as it affects the adsorption of model compounds [5, 82]. Variation in pH of the samples during the adsorption was less than 2 units and according to literature this variation does not affect significantly the maximum adsorption capacity (Q_{max}) of the IBP, 2,4-D, and BPA in this pH range [5, 6, 10]. Since the pH of solution impacts the electrostatic charge of the model compounds in solution, it is critical to know the pH of isotherm samples at equilibrium. For this purpose, equilibrium pH of isotherm samples was measured for a number of the samples.

Electrostatic charge of model compounds and adsorbents in equilibrium and pH range of adsorption samples in Milli-Q water is shown in Figure 5-5.

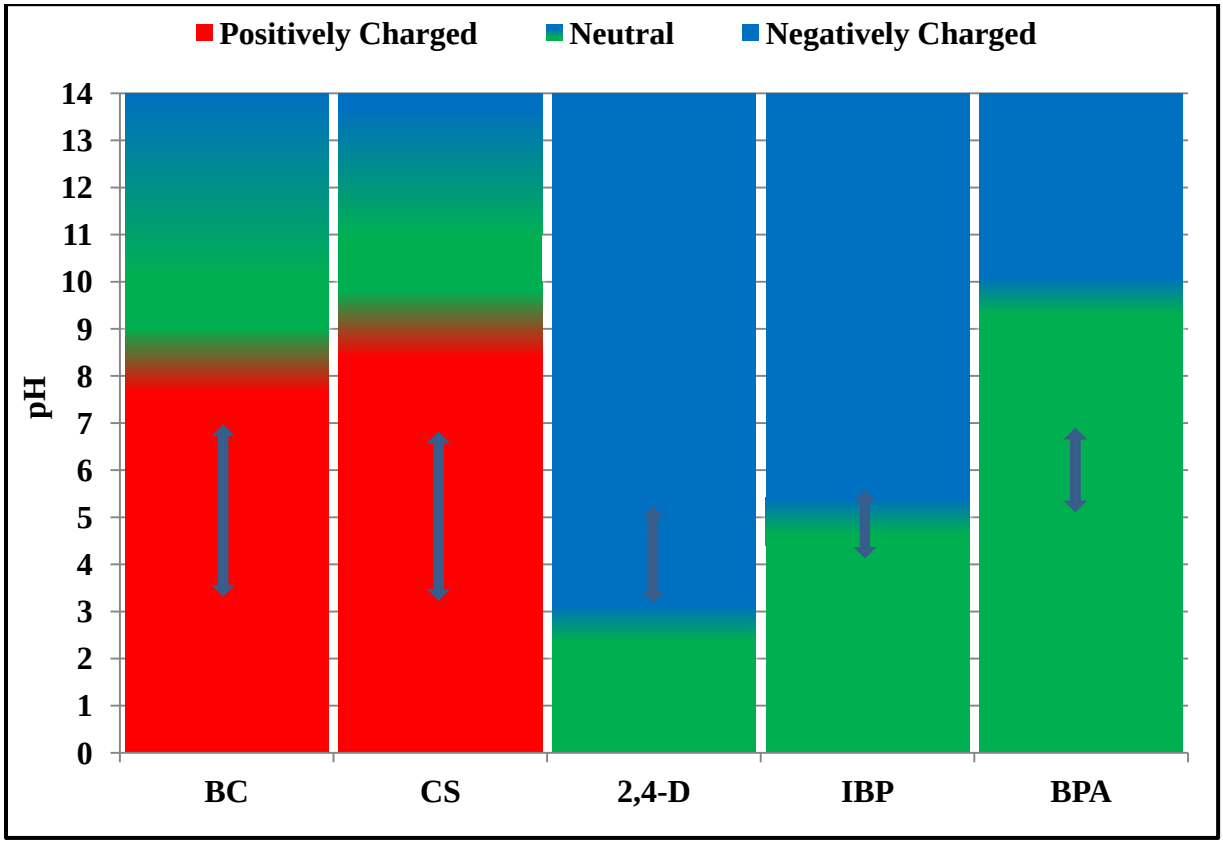

Figure 5-5. Electrostatic charge of BC, CS, and model compounds at equilibrium in adsorption on fresh adsorbents in Milli-Q water at 280, 288, and 296 K (pH range of samples are shown with up-down arrows)

Because of the stronger acidic characteristics of IBP and 2,4-D than BPA, a solution with higher concentration of IBP and 2,4-D had a lower pH than a solution with a lower concentrations of these two compounds. Accordingly isotherm samples with higher concentration levels of these two model compounds have lower pH than the isotherm samples with lower concentrations. According to the equilibrium pH of IBP isotherm samples, it can be observed that IBP molecules in samples with initial concentration levels of less than 30 mg/L are completely deprotonated at equilibrium and are in anionic form. On the other hand, IBP molecules in samples with initial

concentration levels of more than 30 mg/L are mostly not deprotonated and in neutral form. 2,4-D molecules were completely dissociated and in anionic form, and BPA molecules were not deprotonated and in neutral form.

The definition of London dispersion forces (chapter two) refers to the Van der Waals forces between the non-polar species [55]. Therefore, effect of these forces is dominant when the model compounds are in molecular form. Based on the pH of the solutions at equilibrium and pKa of the model compounds, most of the IBP molecules in isotherm samples with initial concentration levels higher than 30 mg/L are in molecular form. 2,4-D molecules in the pH range of isotherm experiments were in anionic form, and all of the BPA molecules were in molecular form.

IBP samples with initial concentration levels higher than 30 mg/L were located on the plateau of Langmuir curve and this part of curve indicates the Q_{max}. Therefore, IBP molecules in neutral form determine the Q_{max} of adsorption of IBP in Langmuir model more effectively than deprotonated IBP molecules. Q_{max} of IBP on BC was very close to Q_{max} of BPA on BC while Q_{max} of IBP on CS is about 2 times Q_{max} of BPA on CS. Since the only difference between adsorption experiments on BC and CS is the adsorbent and the rest of parameters are the same, it can be inferred that the higher ratio of Q_{max} of IBP to BPA on CS than on BC can be related to the characteristics of CS and BC. Because of dominance of London dispersion forces and donor-acceptor forces it can be speculated that specific surface functional groups on BC or CS caused this difference in Q_{max} ratios. According to the structure of IBP (Figure 2-1) and reports from literature [16] the higher Q_{max} of IBP for adsorption on BC than CS can be attributed to carboxylic group of IBP molecule interacting with carboxylic groups of BC surface.

According to the size of IBP, 2,4-D, and BPA molecules mentioned in chapter two, the longest dimension of the model compounds is about 1 nm and it does not exceed 1.1 nm. Therefore, it is reasonable to consider that IBP, 2,4-D, and BPA molecules have similar molecular sizes. The same molecular size will result in access to pores with the same diameter. Thus the size exclusion effect influencing any difference in maximum adsorption capacity of model compounds on the same adsorbent can be rejected.

Comparing the Q_{max} of the model compounds in Table 5-1, it can be observed that the Q_{max} of the model compounds for adsorption on BC is higher than for adsorption on CS. Comparing the order of magnitude of the Q_{max} for adsorption on each adsorbent, the same order of 2,4-D>IBP>BPA is observed for adsorption on both BC and CS. Since this order is the same on both BC and CS it can be inferred that this order is attributed to the characteristics of each model compound. Because each model compound has a different Q_{max} and contains different functional groups in their structure, it is more reasonable to compare adsorption of each of model compound on BC and CS.

Adsorption of IBP on both adsorbents at concentration levels higher than 30 mg/L is more dependent on the Van der Waals interactions between the IBP molecule and the GAC surface. It was observed that the presence of specific surface oxygen containing functional groups such as carboxylic groups [16] can be responsible for the adsorption of IBP on both adsorbents. The ratio of Q_{max} for adsorption of IBP on BC to CS is equal to 1.7, and this ratio is higher than the ratio of specific surface area of BC to CS which is equal to 1.1. This higher ratio can be attributed to the difference between the amount of the specific functional groups responsible for adsorption of IBP on BC and CS. Ratio of micro-pore surface area of BC to CS using the results of t-test is

0.79. This indicates that the assumption of adsorption of IBP through micro-pore trapping as the major mechanism of adsorption of IBP [28] is not valid.

The 2,4-D molecule is in anionic form in the pH range of adsorption on both BC and CS. The ratio of specific surface area of BC to CS was 1.1, and this ratio is close to the ratio of Q_{max} of adsorption of 2,4-D on BC to CS which is equal to 1.2. Based on the comparable ratios of specific surface area and Q_{max}, it can be speculated that the total surface area of the adsorbents are responsible for the adsorption of 2,4-D.

The BPA molecule was not deprotonated and was in neutral form. The ratio of Q_{max} for adsorption of BPA on BC to CS was equal to 3.0, and this ratio was considerably higher than the ratio of specific surface area of BC to CS equal to 1.1. This observation indicates that the adsorption of BPA should be dependent on the specific surface functional groups and it is not proportional to the surface area available for adsorption of BPA. Although BC exhibited a higher pore volume and specific surface area than CS, the intensity of adsorption of BPA on CS was higher than that on BC. This corroborates the idea that adsorption of BPA was more dependent on surface chemistry of adsorbents [5] than the porosity of adsorbents.

Electrostatic interactions were present between the charged molecules and the charged surface of the adsorbent. Surface of the BC and CS was more positively charged in the pH range of the experiments because the pH of solution was less than the point of zero charge of both BC and CS. Among IBP, 2,4-D, and BPA, the 2,4-D molecule was the only molecule that had an electrostatic charge in the pH range of adsorption experiments. The 2,4-D was completely deprotonated, thus in anionic form. The deprotonation as it was mentioned in chapter two is related to the hydrogen of the carboxylic group of 2,4-D [39]. IBP adsorption isotherm samples

with initial concentration levels of less than 30 mg/L have a pH higher than the pKa of IBP at equilibrium and consequently IBP molecules in samples with initial concentration levels less than 30 mg/L were in anionic from. The deprotonation of IBP was related to the dissociation of the hydrogen of carboxyl group [16].

The positively charged surface of BC and CS exerts attractive forces on the anionic 2,4-D molecules at all concentration levels and to the IBP molecules in samples with the IBP initial concentration levels of less than 30 mg/L. This attractive force is speculated to be the dominant force in adsorption of 2,4-D on both BC and CS. The surface charge of adsorbents was not exclusively attributed to the external surface area of the adsorbents or the internal surface area of the pores [65]. Therefore it can be assumed that the entire surface area of adsorbents was involved in adsorption of 2,4-D. The proportionality of ratio of Q_{max} of adsorption of 2,4-D on BC and CS with the ratio of specific surface area of BC and confirms this point.

5.2. Thermodynamics of Adsorption of Model Compounds in Milli-Q Water

The results of adsorption of IBP, 2,4-D, and BPA on BC and CS at 296, 288, and 280 K were used to calculate the thermodynamic parameters of adsorption. Experiments at 288 and 280 K were conducted under the same experimental conditions than those for 296 K, as explained in chapter three. The Langmuir and Freundlich models were fit to the data and the model parameters were calculated. The model parameters for 288 and 280 K are presented in Tables 5-2 and 5-3, respectively.

Table 5-2. Langmuir and Freundlich isotherm model parameters for adsorption of model compounds on BC and CS in Milli-Q water at 288 K, Units: Q_{max} (mg/g), b (L/mg), and K_F ($mg^{(n-1)/n}.L^{1/n}.g^{-1}$)

		Langmuir			Freundlich		
	Adsorbent	Q_{max}	b	R^2	K_F	1/n	R^2
IBP	BC	239	0.939	0.99	124	0.27	0.99
2,4-D		459	0.131	0.99	77	0.49	0.97
BPA		233	0.190	0.99	105	0.17	0.99
IBP	CS	173	0.212	0.99	40	0.43	0.99
2,4-D		407	0.044	0.99	33	0.57	0.98
BPA		74	0.093	0.99	28	0.19	0.97

Table 5-3. Langmuir and Freundlich isotherm model parameters for adsorption of model compounds on BC and CS in Milli-Q water at 280 K, Units: Q_{max} (mg/g), b (L/mg), and K_F ($mg^{(n-1)/n}.L^{1/n}.g^{-1}$)

		Langmuir			Freundlich		
	Adsorbent	Q_{max}	b	R^2	K_F	1/n	R^2
IBP	BC	234	0.909	0.95	100	0.39	0.98
2,4-D		472	0.318	0.99	156	0.31	0.94
BPA		243	1.19	0.99	147	0.13	0.87
IBP	CS	134	0.242	0.95	40	0.34	0.92
2,4-D		410	0.047	0.97	45	0.48	0.96
BPA		69	0.272	0.99	42	0.108	0.82

To estimate the standard Gibbs free energy of adsorption one needs to determine standard equilibrium constant (K°_c) which was found in chapter two to be equal to the product of Q_{max} and b from the Langmuir model [68]. Having the K°_c for each temperature, using Equation 2-15 it is possible to calculate the standard Gibbs free energy of adsorption at such temperature. The standard Gibbs free energy for 280 and 296 K were calculated and presented in Table 5-4.

To find the standard enthalpy and standard entropy of adsorption, $\ln(Q_{max}.b)$ at different temperatures was plotted against 1/T. This plot is called the "Van't Hoff Plot". A trend-line was fitted to the data. Slope and intercept of the trend-line were used according to Equation 2-16 to calculate the standard enthalpy and standard entropy of adsorption. The data and the Van't Hoff

Plot fitted to the data for adsorption of BPA on BC were used to calculate the standard enthalpy and standard entropy of adsorption of BPA as presented in Figure 5-6.

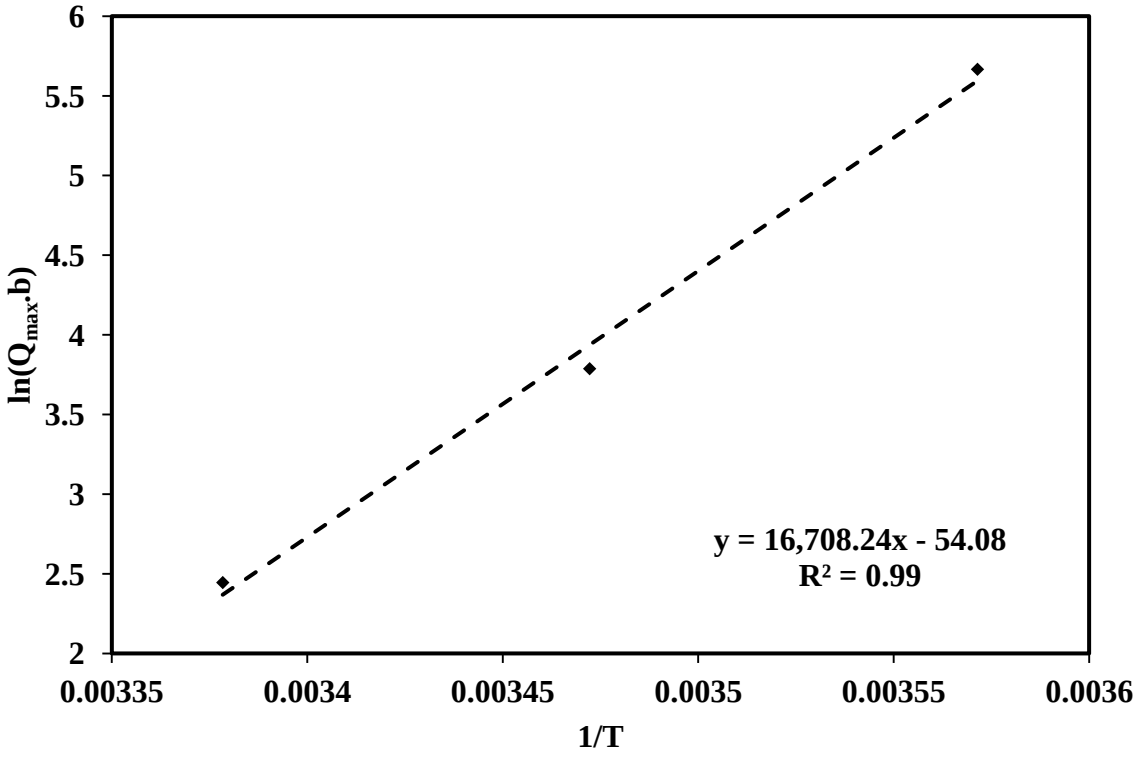

Figure 5-6. Van't Hoff Plot for thermodynamic analysis of adsorption of BPA on BC in temperature range of 280-296 K (please find rest of the Van't Hoff Plots in Appendix D)

Using the slope and intercept of Van't Hoff Plots, the standard enthalpy and standard entropy of adsorption of model compounds on BC and CS were calculated. The standard enthalpy and standard entropy of adsorption are present in Table 5-4.

Table 5-4. Thermodynamic parameters of adsorption of model compounds on BC and CS in temperature range of 280-296 K (ΔG° at 280 and 296 K, respectively)

Model compound	Adsorbent	ΔG° (kJ/mol)	ΔS° (J/mol.K)	ΔH° (kJ/mol)	R^2 of Van′t Hoff Plot
IBP	BC	-12.5 and -14.3	110	18.6	0.83
2,4-D		-11.7 and -9.2	-156	-55	0.95
BPA		-13.2 and -6	-450	-139	0.99
IBP	CS	-8 and -9	59	8.4	0.98
2,4-D		-6.9 and -5.6	-81.5	-30	0.82
BPA		-6.8 and -3.7	-195	-61	0.96

Negative values of ΔG° indicate the spontaneous nature of the adsorption process for all three model compounds on both BC and CS [6, 59, 62, 69, 71, 72]. Comparing the difference between the ΔG° at 280 K and 296 K shows that magnitude of change in spontaneity of adsorption of model compounds with the increase in temperature from 280 to 296 K is in order of BPA>2,4-D>IBP which is the same for adsorption on both BC and CS.

Paying closer attention to the Equation 2-15 used for calculation of ΔG° it can be observed that the magnitude of the Gibbs free energy is a function of Langmuir maximum capacity (Q_{max}) and the Langmuir intensity (b). Therefore it is apparent that an adsorbent with higher pore volume and surface area will yield in a higher value of ΔG°, which consequently affects the value of ΔH° and ΔS°. This is observed in the results of the thermodynamic parameters in Table 5-4, indicating that ΔG° and ΔH° of adsorption of all three model compounds on BC are about double the values for adsorption on CS. Therefore it can be inferred that, the magnitude of the enthalpy of adsorption of a compound are surface area dependent and not a key parameter to compare the chemical interaction and strength of bonds. However, it is useful in comparing the adsorption of different model compounds on one adsorbent.

The ΔH° and ΔS° of adsorption of IBP on both adsorbents have a positive value indicating an endothermic adsorption and increase in randomness on the surface of adsorbent. The positive

value of enthalpy is in agreement with the slight increase in adsorption of IBP with the increase in temperature in Mestre et al [10] experiments. It also confirms the endothermic adsorption of IBP on a novel mesoporous GAC in Dubey et al [16] experiments. Positive enthalpy yields less adsorption at low temperatures. The positive value of entropy compensates the negative effect of enthalpy on adsorption and maintains the spontaneity of adsorption of IBP on GAC by reduction in temperature. Low value of $\Delta H°$ describes the physical nature of adsorption. The positive value of entropy of adsorption of IBP on both adsorbents indicates an increase in randomness on surface of adsorbent. It is assumed to be due to desorption of water and methanol molecules from IBP molecule and competition in adsorption among IBP, methanol, and water molecules for adsorption on adsorbent surface [28].

The $\Delta H°$ of adsorption of both 2,4-D and BPA have negative values indicating the exothermic nature of adsorption and as a result increase in uptake with decrease in temperature for adsorption of 2,4-D. The exothermic nature of adsorption was in conformity with the results of Gupta et al. [66] analysis for adsorption of 2,4-D on a carbonaceous adsorbent. The negative value of enthalpy for adsorption of BPA on both GAC is in agreement with the decrease in adsorption with increase in temperature in Sui et al. [62] analysis. This shows that adsorption is an ideal process for removal of these compounds in regions with temperatures close to the freezing temperature of water. The largest negative value for entropy of adsorption of BPA on both BC and CS indicates the large decrease in randomness on the surface of the adsorbent which is not favorable for adsorption of BPA. Although BPA adsorption is exothermic and the tendency of adsorption is higher at 280 K than at 296 K, the Q_{max} of adsorption on CS decreases with decrease in temperature. This could be due to the large entropy of adsorption of BPA.

Gibbs free energy of adsorption of three model compounds at 296 K for both BC and CS is in the order of IBP>2,4-D>BPA. Whereas this order changes at 280 to BPA>IBP>2,4-D for BC while remaining the same for CS. This indicates that results of thermodynamic analysis for adsorption of a solute on two adsorbents with very similar characteristics cannot be generalized. That also indicates that the order of tendency of adsorption of compounds may change at a different temperature.

5.3. Adsorption of Model Compounds on BC and CS in Tap Water Matrix at 296 K

Adsorption of IBP, 2,4-D, and BPA on BC and CS in tap water matrix was studied with all experimental conditions the same as the adsorption in Milli-Q water. The results of adsorption of model compounds in tap water at equilibrium were fit to the linear form of Langmuir and Freundlich models. Langmuir model performed better in fitting most of experimental data except the adsorption of BPA on BC and adsorption of 2,4-D on CS. The model parameters were calculated and are present in Table 5-5.

Table 5-5. Langmuir and Freundlich isotherm model parameters for adsorption of model compounds on BC and CS in tap water at 296 K, Units: Q_{max} (mg/g), b (L/mg), and K_F ($mg^{(n-1)/n}.L^{1/n}.g^{-1}$)

		Langmuir			**Freundlich**		
	Adsorbent	Q_{max}	b	R^2	K_F	1/n	R^2
IBP	BC	174	0.696	0.99	69	0.32	0.97
2,4-D		262	0.366	0.996	115	0.25	0.99
BPA		260	0.046	0.83	39	0.39	0.89
IBP	CS	110	0.056	0.97	10	0.58	0.96
2,4-D		178	0.043	0.96	26	0.39	0.98
BPA		68	0.139	0.98	29	0.18	0.67

Comparing the regression coefficients of the Freundlich models for adsorption in tap water and in Milli-Q water, it can be observed that Freundlich model fits the data in tap water better than the data for Milli-Q water except the case of adsorption of BPA on CS. The better fit of

Freundlich model in tap water matrix than in Milli-Q water in the first place indicates that adsorption of model compounds is happening in competition with other species present in tap water. Secondly it shows that adsorption is happening in more than monolayer and adsorption of species present in tap water has caused the heterogeneity of the adsorbent surface [51].

The pH of the samples was not adjusted in experiments to avoid the introduction of ions [10] and change in the ionic strength of the tap water as it is one of the characteristic of tap water that influences the adsorption of model compounds on the adsorbents in real condition [5]. The pH of the samples for these set of experiments were very close to the pH of tap water (See Table 3-1).

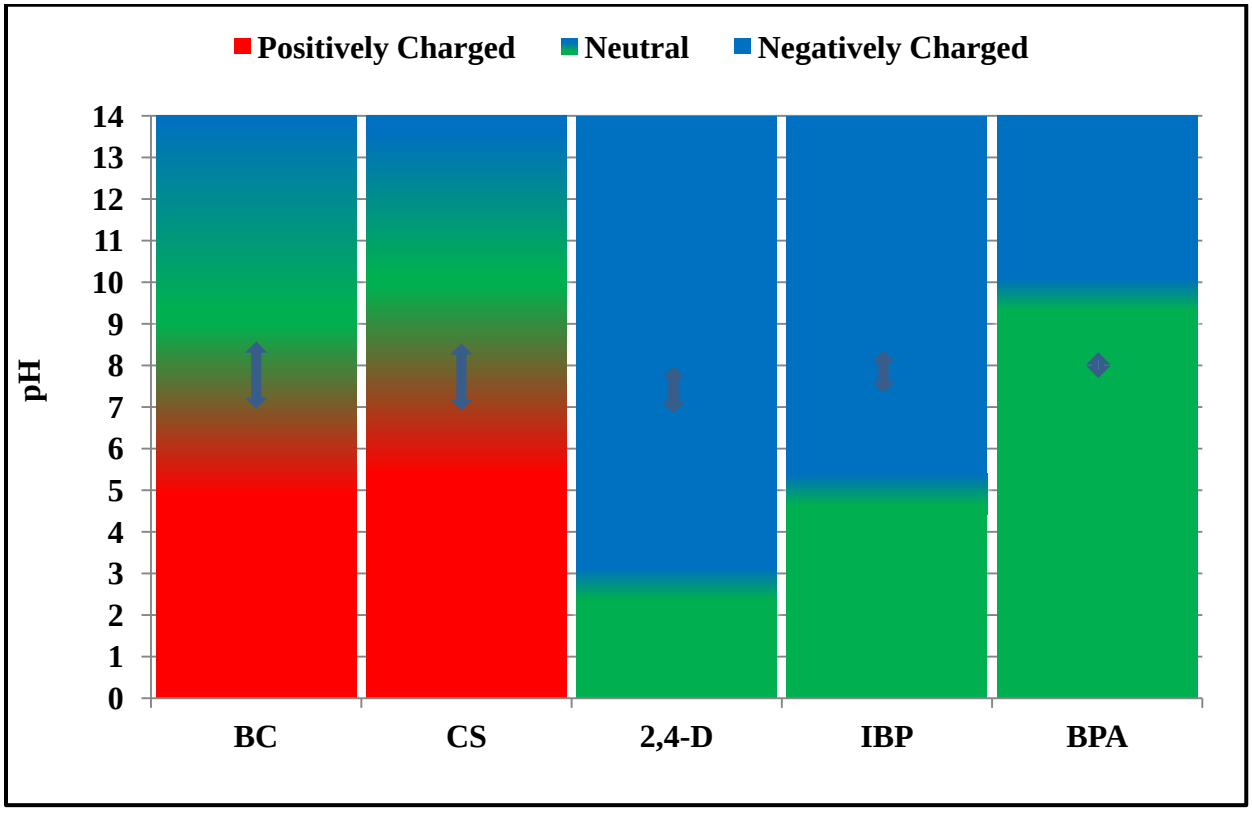

Figure 5-7. Electrostatic charge of BC, CS, and model compounds at equilibrium in adsorption on fresh adsorbents in tap water at 296 K (pH range of samples are shown with up-down arrows)

According to the pH of samples and pKa of model compounds (Table 2-1); IBP molecules were deprotonated and were in anionic form and, 2,4-D molecules were also deprotonated and were in

anionic form. BPA molecules were in molecular form and neutral. Surface of BC and CS were positively charged however, were less positively charged than in experiments with Milli-Q water.

Because of the dominance of London dispersion forces in adsorption of solute molecules in neutral condition, adsorption of BPA molecules was mainly controlled by this force in the adsorption experiments with tap water matrix. According to previous reports in literature, highest uptake of BPA occurs when BPA is in neutral condition and net charge of GAC surface is zero [5]. Q_{max} of adsorption of BPA on BC increased in comparison with adsorption in Milli-Q water while Q_{max} of adsorption of BPA on CS in tap water decreased insignificantly in comparison with Q_{max} of adsorption of BPA in Milli-Q water. This can be due to the lower PZC of BC than CS and more neutral surface of BC than CS. The adsorption of ions on adsorption sites with electrostatic charge also increased the neutrality of the surface of adsorbents and consequently has increased the Q_{max} of adsorption of BPA on BC and did not allow the significant decrease of Q_{max} of adsorption of BPA on CS [67] in comparison with the Milli-Q water.

Competition in adsorption between the species present in tap water matrix and the model compounds in adsorption on the surface of adsorbents can reduce the uptake of model compounds by filling the pores and reducing the surface area and pore volume available for adsorption of model compounds [93]. By comparing the Q_{max} of adsorption of model compounds on BC with CS presented in Table 5-5, it can be observed that all three model compounds exhibited a higher Q_{max} in adsorption on BC than CS. This indicates that adsorbent with higher porosity will maintain its higher capacity in presence of species present in tap water. Although CS exhibited lower porosity than BC it is still effective in adsorption of model compounds in tap water matrix.

Electrostatic forces between the model compounds and surface of adsorbents can influence adsorption of model compounds by attractive or repulsive forces. In the pH range of adsorption of model compounds in tap water matrix, IBP and 2,4-D were deprotonated and were in anionic form while BPA molecule were in neutral form. Therefore, IBP and 2,4-D will be interacting with the charged surface of BC and CS. Surface of BC and CS were more positively charged and attractive forces were present between anionic form of IBP and 2,4-D and the surface of BC and CS. The Q_{max} of adsorption of IBP in Milli-Q water was larger than Q_{max} of adsorption in tap water matrix. This is when IBP molecules were in anionic form in adsorption in Milli-Q water and in anionic form in adsorption in tap water. This indicates that dispersive and donor-acceptor forces were more effective forces in adsorption of IBP than electrostatic forces.

CHAPTER SIX

ADSORPTION OF MODEL COMPOUNDS ON PRE-TREATED ADSORBENTS

This chapter presents results of adsorption of IBP, 2,4-D, and BPA on acid pre-treated BC (N-BC) and acid pre-treated CS (N-CS) at 296 K. Results of isotherm adsorption experiments were fit to the Langmuir and Freundlich models and model parameters were calculated. Best fit model to equilibrium data was used to discuss the effect of point of zero charge (PZC) of acid pre-treated adsorbents on removal of micro-pollutants.

6.1. Acid Pre-treatment of BC and CS for Reduction of Point of Zero Charge

Acid pre-treatment of BC and CS was carried out with the purpose of reduction of PZC, using 2 N nitric acid performed at 296 K through the experimental procedure explained in chapter three. During the acid treatment variation of pH of the distilled water, tap water, and Milli-Q water was plotted (Figure 6-1).

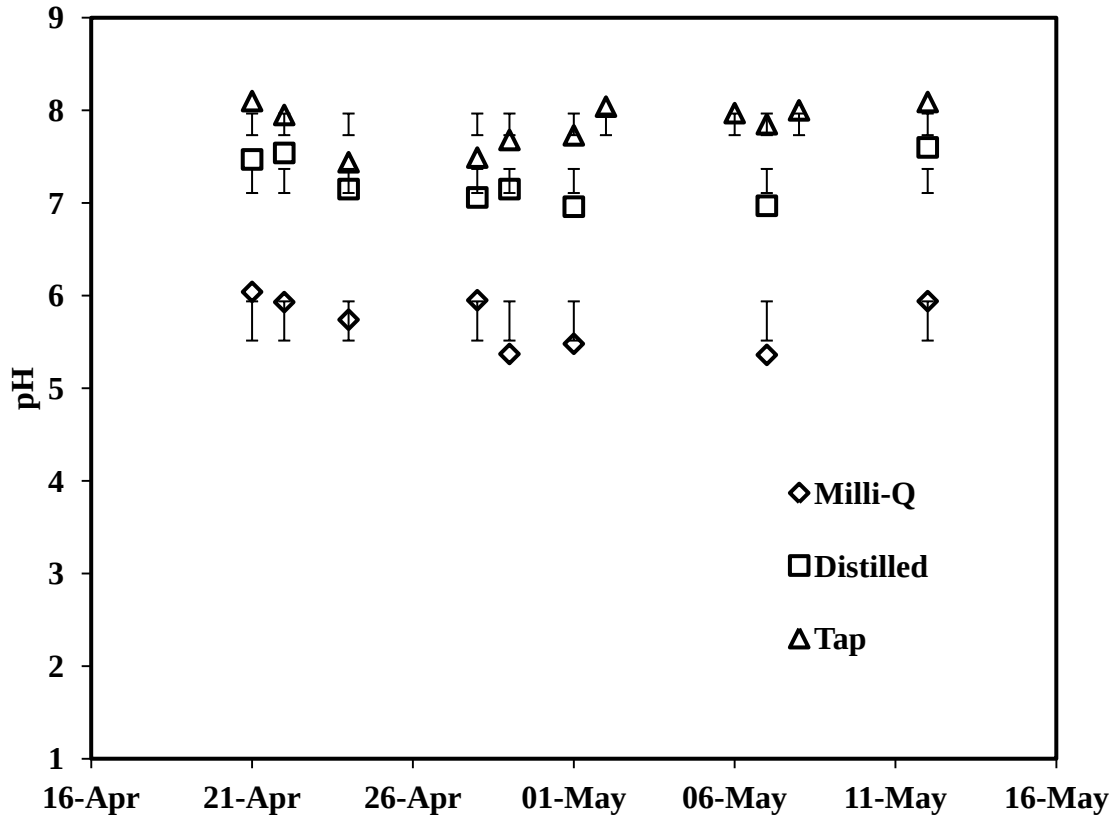

Figure 6-1. Variation of pH of Tap, Distilled, and Milli-Q water

Samples were washed with distilled water every day until the pH of the solutions became stable [76]. The pH of the solution was measured after the samples were washed with distilled water. The pH of distilled water was also measured, so that the average pH of the distilled water during the experiments was recorded. Figure 6-2 indicates the variation of pH of acid washed solution versus the volume of distilled water consumed.

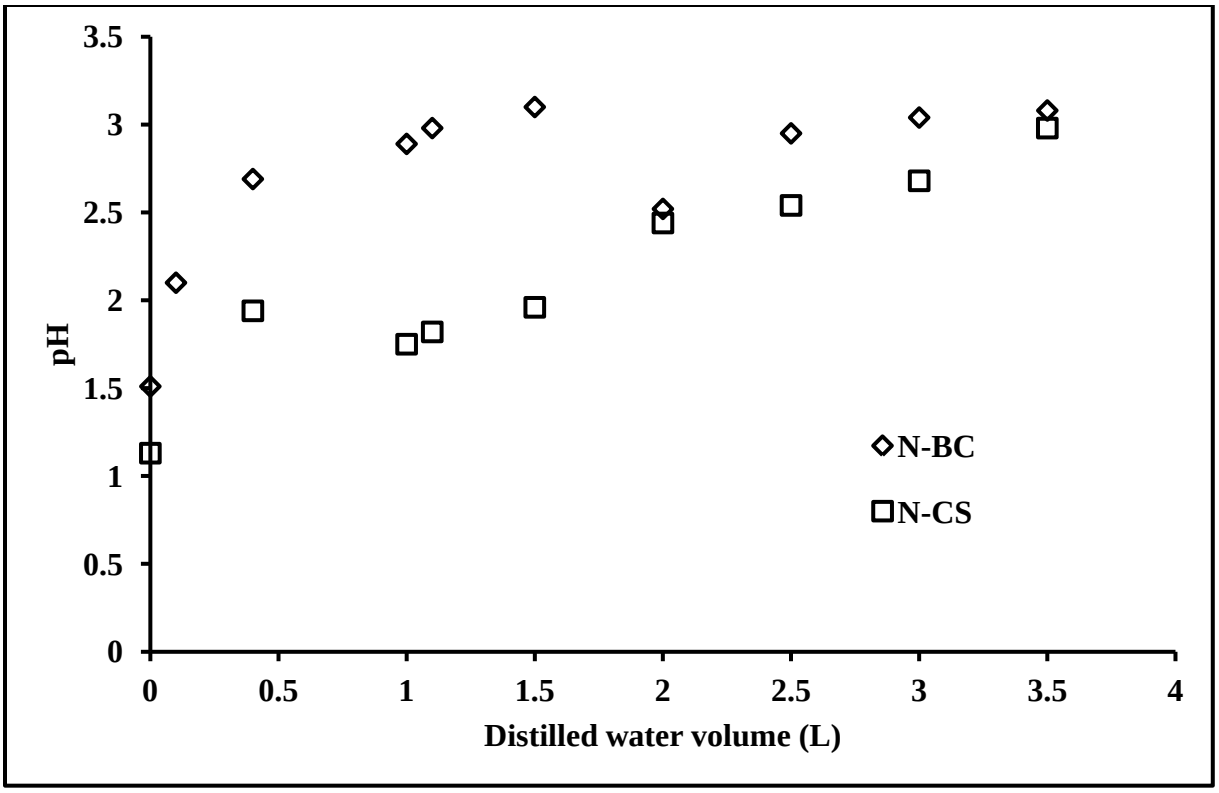

Figure 6-2. Variation of pH of solution of acid washed carbons, using distilled water

The acid pre-treated BC and CS were named N-BC and N-CS, respectively. Change in porosity of the adsorbents was not the purpose of the acid pre-treatment, therefore acid treatment was carried out with 2 N nitric acid and at room temperature [74] to be able to control the oxidation level of acid pre-treatment [65] and not to modify the porosity of adsorbents [74]. Results of porosity characterization of adsorbents presented in chapter four confirmed that porosity of adsorbents has not changed significantly and porosity characteristics of acid pre-treated adsorbents were identical to the porosity characteristics of fresh adsorbents. Results of PZC measurements presented in chapter four also indicated that the PZC of fresh adsorbent decreased with nitric acid pre-treatment at 296 K and the desirable acidic PZC was achieved.

According to literature nitric acid pre-treatment of GAC with low concentration of nitric acid of about 2 N, generates acidic surface oxygen-containing functional groups [74-76] particularly

carbonyl groups [75] and carboxyl groups [20, 74, 76]. Chen et al. [75] treated a GAC with different concentrations of nitric acid in range of 0.1 to 16 N at 363 K. They observed that the highest concentration of carbonyl groups occurred when the concentration of nitric acid used for acid treatment was 2 N. Based on literature reports it is assumed that the acidic surface functional groups formed on surface of N-BC and N-CS causing the reduction in PZC of BC and CS to be mainly carbonyl and carboxyl groups.

6.2. Adsorption of Model Compounds on N-BC and N-CS in Milli-Q Water

Isotherm adsorption experiments with the same experimental condition as adsorption in Milli-Q water were carried out while N-BC and N-CS as adsorbents at 296 K. The data from the isotherm experiments was fitted to the Langmuir and Freundlich models. The isotherm model parameters were calculated and are present in Table 6-1. The best fitted model based on the higher regression coefficient was chosen. The regression coefficients are presented in Table 6-1.

Table 6-1. Langmuir and Freundlich isotherm model parameters for adsorption of model compounds on N-BC and N-CS in Milli-Q water at 296 K, Units: Q_{max} (mg/g), b (L/mg), and K_F ($mg^{(n-1)/n}.L^{1/n}.g^{-1}$)

		Langmuir			**Freundlich**		
	Adsorbent	Q_{max}	b	R^2	K_F	1/n	R^2
IBP	N-BC	310	1.238	0.98	156	0.57	0.89
2,4-D		368	0.089	0.99	58	0.45	0.99
BPA		274	0.050	0.98	28	0.51	0.90
IBP	N-CS	213	0.225	0.98	44	0.52	0.88
2,4-D		347	0.052	0.99	38	0.49	0.99
BPA		115	0.067	0.96	26	0.31	0.86

Comparing the regression coefficients of the Langmuir and Freundlich models, it can be observed that the Langmuir model fitted the data better because of higher or equal coefficients of determination in comparison with Freundlich model for all cases. The better fit of adsorption data to Langmuir model indicates that adsorption is occurring in monolayer [49].

The pH of isotherm adsorption samples was not adjusted to avoid introduction of electrolytes to the solution [5, 82]. In order to determine the range of pH of the samples, pH of some of the samples with different concentrations of model compounds was recorded at equilibrium condition. The equilibrium pH of samples of adsorption of model compounds on N-BC and N-CS is presented in Figure 6-3.

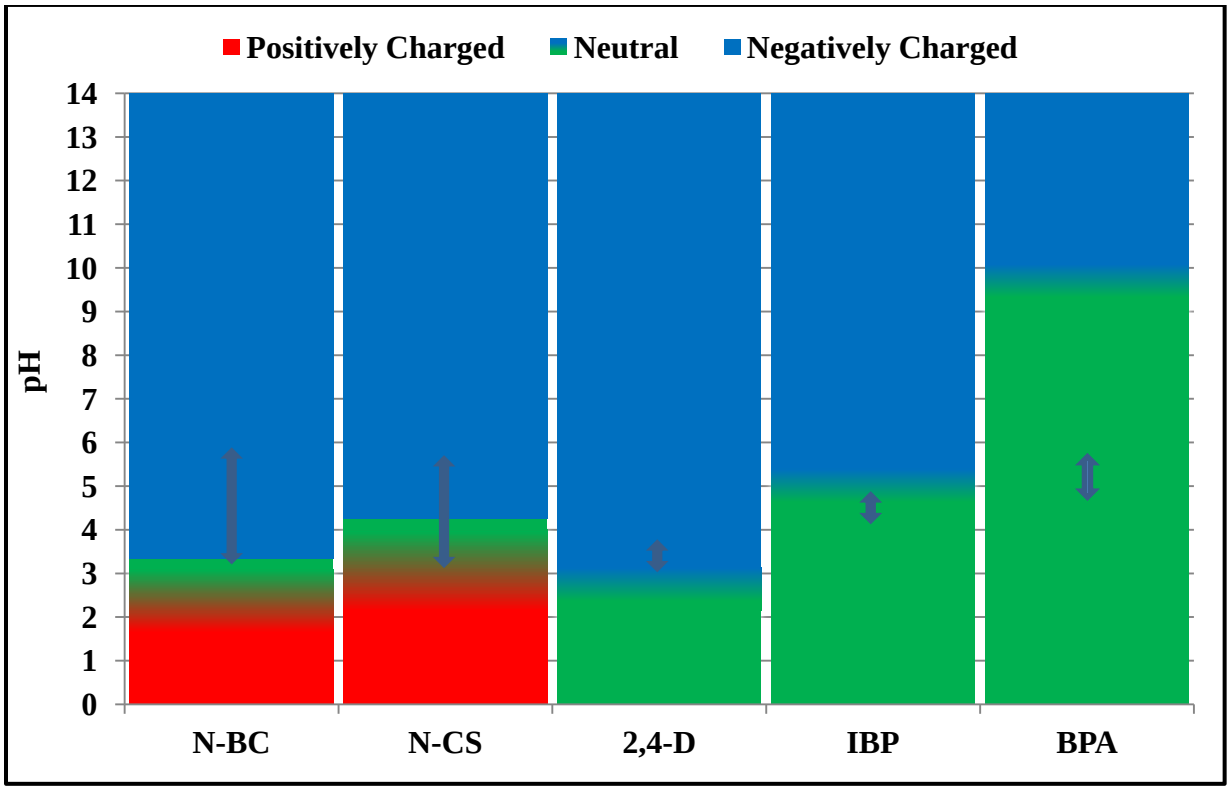

Figure 6-3. Electrostatic charge of N-BC, N-CS, and model compounds at equilibrium in adsorption on pretreated adsorbents in Milli-Q water at 296 K (pH range of samples are shown with up-down arrows)

According to the measured pH of samples, the pH of isotherm samples with N-BC and N-CS were slightly lower than the same samples with BC and CS which is due to acidic nature of N-BC and N-CS reducing the pH of samples. However this reduction of pH is not significant. Based on the pH of samples, the IBP molecules were mostly in molecular form, 2,4-D molecules were in anionic form, and BPA molecules were in molecular form. The surface of N-BC in

adsorption of IBP molecules were more negatively charged while surface of N-CS exhibited a net zero charge. The surface of N-BC in adsorption of 2,4-D was more negatively charged and the surface of N-CS was more positively charged. Surface of N-BC for adsorption of BPA was more negatively charged while surface of N-CS exhibited a net zero charge.

In the pH range of experiments IBP and BPA were in molecular form therefore, London dispersion forces were the dominant forces in adsorption for these two compounds [55]. The Q_{max} of adsorption of IBP on N-BC was 1.2 times Q_{max} of adsorption of IBP on BC and Q_{max} of adsorption of IBP on N-CS was 1.5 time Q_{max} of adsorption of IBP on the CS. This shows that nitric acid pre-treatment increased adsorption of IBP on CS more than BC. The higher maximum adsorption capacity of IBP on nitric acid treated samples indicates that the presence of acidic functional groups on the surface of nitric acid pre-treated adsorbents most probably carbonyl [28] and carboxyl groups favored adsorption of IBP. Q_{max} of adsorption of BPA on N-BC was 1.2 times Q_{max} of adsorption of BPA on BC and Q_{max} of adsorption of BPA on N-CS was 1.5 times Q_{max} of adsorption of BPA on CS. The higher maximum adsorption capacity on nitric acid pre-treated BC and CS shows that nitric acid pre-treatment favored adsorption BPA. This can be due to introduction of acidic functional groups on the surface of adsorbents. The higher increase of Q_{max} of adsorption of IBP and BPA on N-CS than on N-BC supports the idea of existence of more acidic functional groups on BC than on CS. The lower PZC of BC than CS corroborates this speculation.

The modification of porosity of adsorbents was not the purpose of the nitric acid pre-treatment and results of characterization of porosity of adsorbents presented in chapter four confirms that the porosity of adsorbents did not change significantly. The ratio of Q_{max} of adsorption of model compounds on N-BC to N-CS was close to the ratio of Q_{max} of adsorption of model compounds

on BC to CS. This is in conformity with the same porosity of fresh adsorbents and nitric pre-treated adsorbents. Intensity of adsorption of model compounds on nitric acid pre-treated samples present in Table 6-1 was very close to the intensity of adsorption of model compounds on fresh adsorbents presented in Table 5-1. Because of the same porosity of fresh and nitric acid pre-treated adsorbents, it can be inferred that the intensity of adsorption was mainly related to the porosity of adsorbents.

The 2,4-D was the only model compound that was not in molecular form in the adsorption experiments with nitric acid pre-treated adsorbents. The pH of 2,4-D adsorption isotherm samples were higher than the pKa of 2,4-D which is equal to 2.6. Therefore, 2,4-D was present in solution in anionic form. Q_{max} of adsorption of 2,4-D on nitric acid pre-treated adsorbents was lower than the Q_{max} of adsorption of 2,4-D on fresh adsorbents. This can be explained by the more negatively charged surface of nitric acid pre-treated adsorbents than fresh adsorbents, creating more repulsive forces. The ratio of Q_{max} of adsorption of 2,4-D on BC to N-BC was 1.2 and the ratio of Q_{max} of adsorption of 2,4-D on CS to N-CS was 1.1. This indicates that nitric acid pre-treatment reduced the adsorption capacity of BC for adsorption of 2,4-D more than CS. This can be because of lower PZC of N-BC than N-CS and more negatively charged surface of N-BC than N-CS.

CHAPTER SEVEN

SEMI-BATCH REGENERATION OF ADSORBETS WITH OZONE

This chapter presents the procedure and results of regeneration of BC and CS saturated with IBP, 2,4-D, and BPA with ozone. The effectiveness of regeneration of saturated BC and CS was studied. The results of assessment of effectiveness of regeneration is presented and discussed.

7.1. Saturation of BC and CS with The Mixture of IBP, 2,4-D, and BPA

The operation of an adsorption system will eventually result in saturated adsorbent that do not have more capacity. Saturated adsorbents can be regenerated to restore their adsorption capacity. To study the regeneration of BC and CS with ozone, it is required to saturate the BC and CS with model compounds and then study the regeneration of saturated BC and CS. In order to saturate the BC and CS as it was explained in chapter three; 1 g of each of BC and CS was placed in contact with a mixture of model compounds containing 200 mg/L of each model compound. The mixture of model compounds contained 75 mL of ethanol to increase the solubility of model compounds. The mixture was stirred and concentration of model compounds in solution was measured until the change in concentration of model compounds became less than 5 % of the initial concentration. At this point adsorbents were considered saturated. Saturated adsorbents

were filtered, washed, and dried with the experimental procedure explained in chapter three. Saturated BC and CS were named S-BC and S-CS, respectively.

7.2. Regeneration of S-BC and S-CS with Ozone

In order to evaluate the effectiveness of the regeneration time with ozone, three times of 15, 30, and 60 minutes were selected, and identical to the regeneration times experiments with ozone reported in the literature [80, 94]. The saturated adsorbents were divided into three equal aliquots, each aliquot weighting approximately 0.3 g. Each aliquot was ozonated for a period of time. Concentration of ozone used for ozonation regeneration experiments was selected to be 18 g/m^3 in gas phase, close to the concentration of ozone reported to be effective in removal of EPs in literature [78, 80, 95]. Ozone was produced from pure oxygen using ozone generator. The dissolved ozone in solution reacted with organic matter in solution. Concentration of ozone dissolved in solution was measured to be in range of 3.5-4.5 mg/L. Unreacted ozone left the reactor, passed through ozone destruction unit and then it was vented to the environment. Ozonated S-BC and S-CS were collected and dried at 383 K. The schematic of the regeneration setup [78] is shown in Figure 7-1.

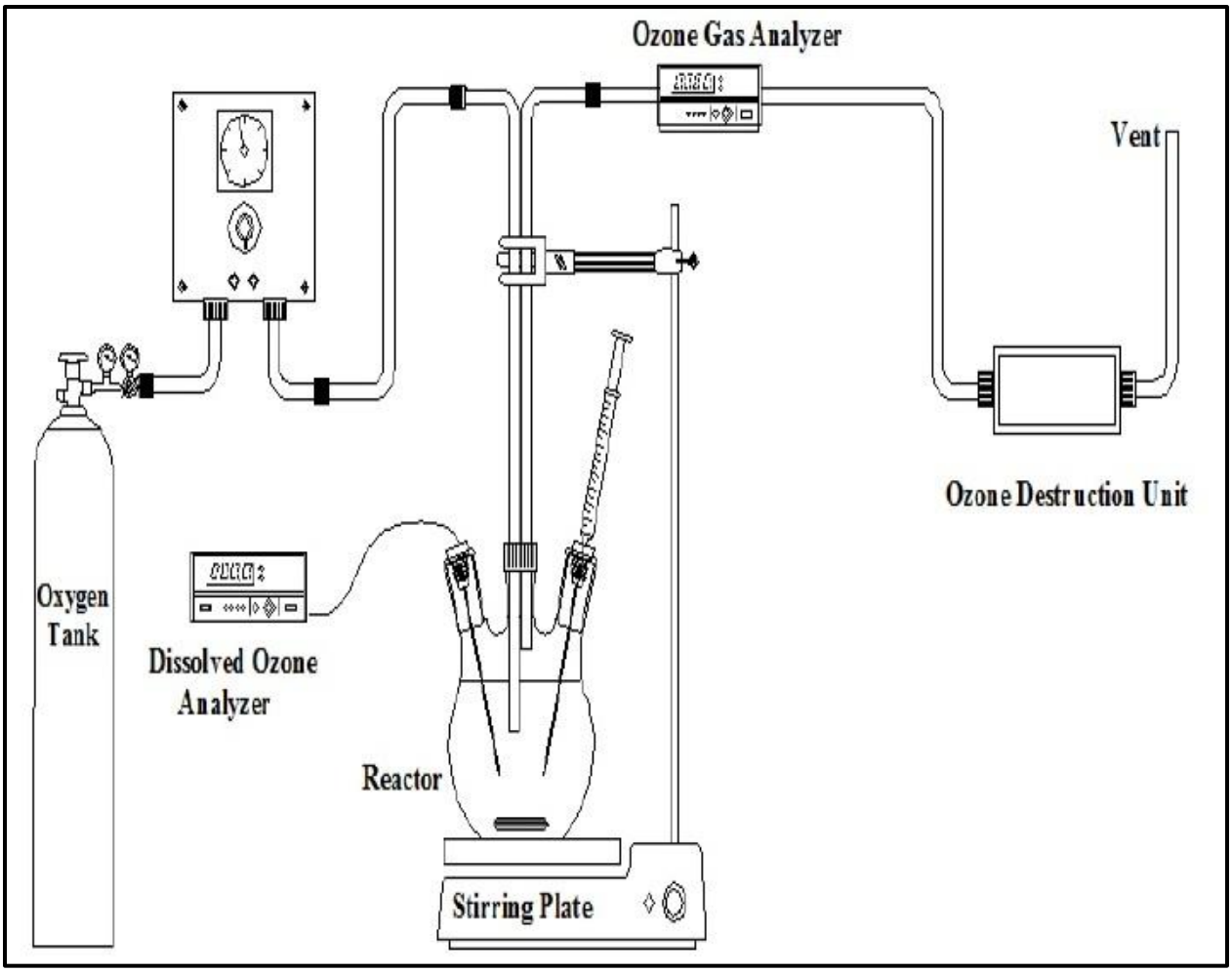

Figure 7-1. Semi-batch regeneration setup [78] used for regeneration of saturated adsorbents

7.3. Assessment of Effectiveness of Regeneration of Ozone Treated S-BC and S-CS

In order to determine the effectiveness of regeneration with ozone, adsorption capacity of ozone regenerated adsorbents for each model compound was determined. 40 mg of each adsorbent was contacted with 200 mL of solution containing the model compound. To have an identical initial concentration for IBP, 2,4-D, and BPA, maximum achievable concentration of IBP for isotherm experiments in Milli-Q water (50 mg/L) were chosen for all three model compounds. Samples were shaken until the change in concentration of model compounds in solution became less than 5 % of initial concentration. Concentration of model compounds at equilibrium conditions in

solution and on adsorbent was measured. Concentration of model compound on each adsorbent at equilibrium was calculated and presented in Figure 7-2 and 7-3.

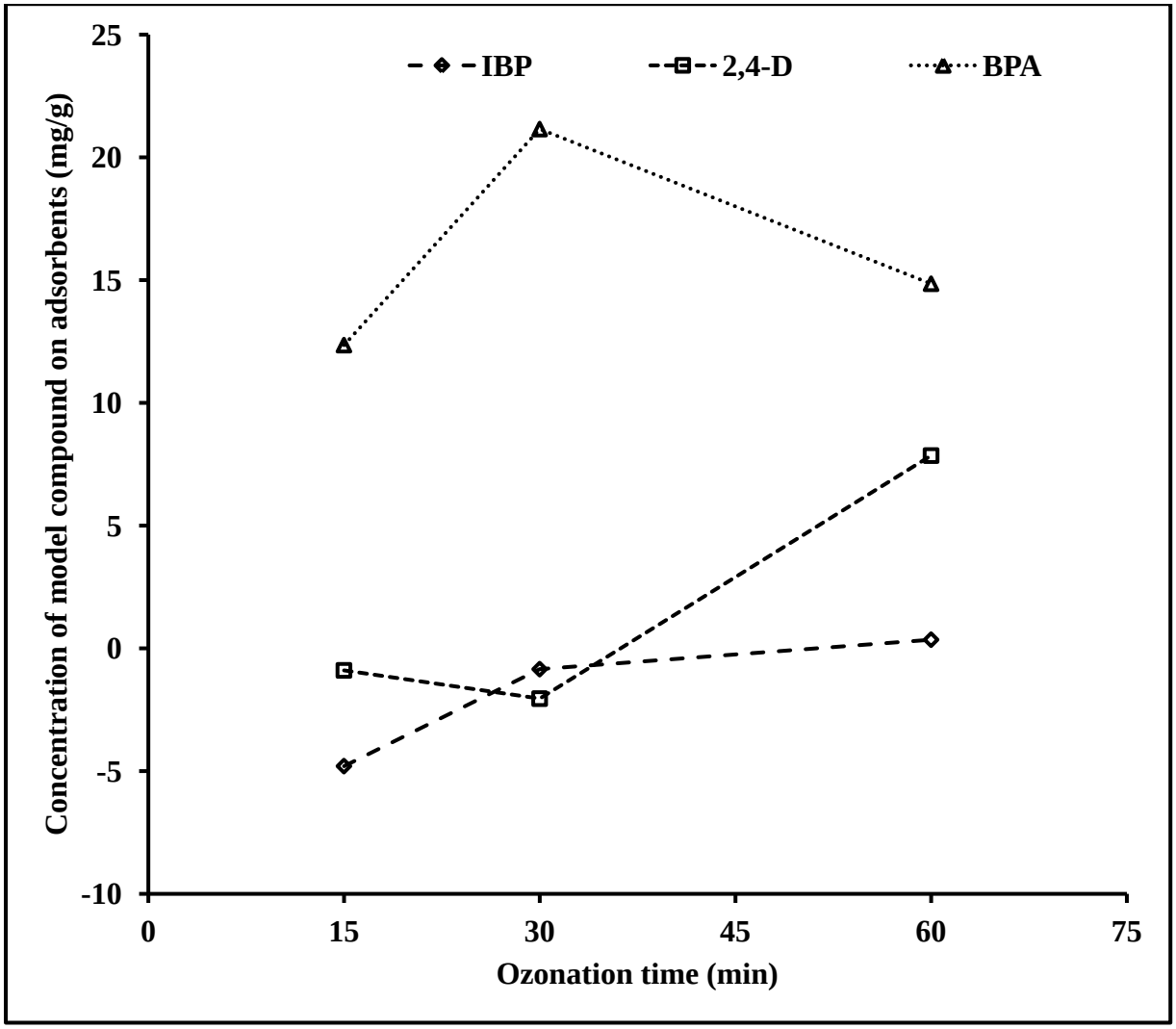

Figure 7-2. Concentration of IBP, 2,4-D, and BPA on ozone treated S-BC regenerated for 15, 30 and 60 minutes (Trend-lines are added for better illustration of results)

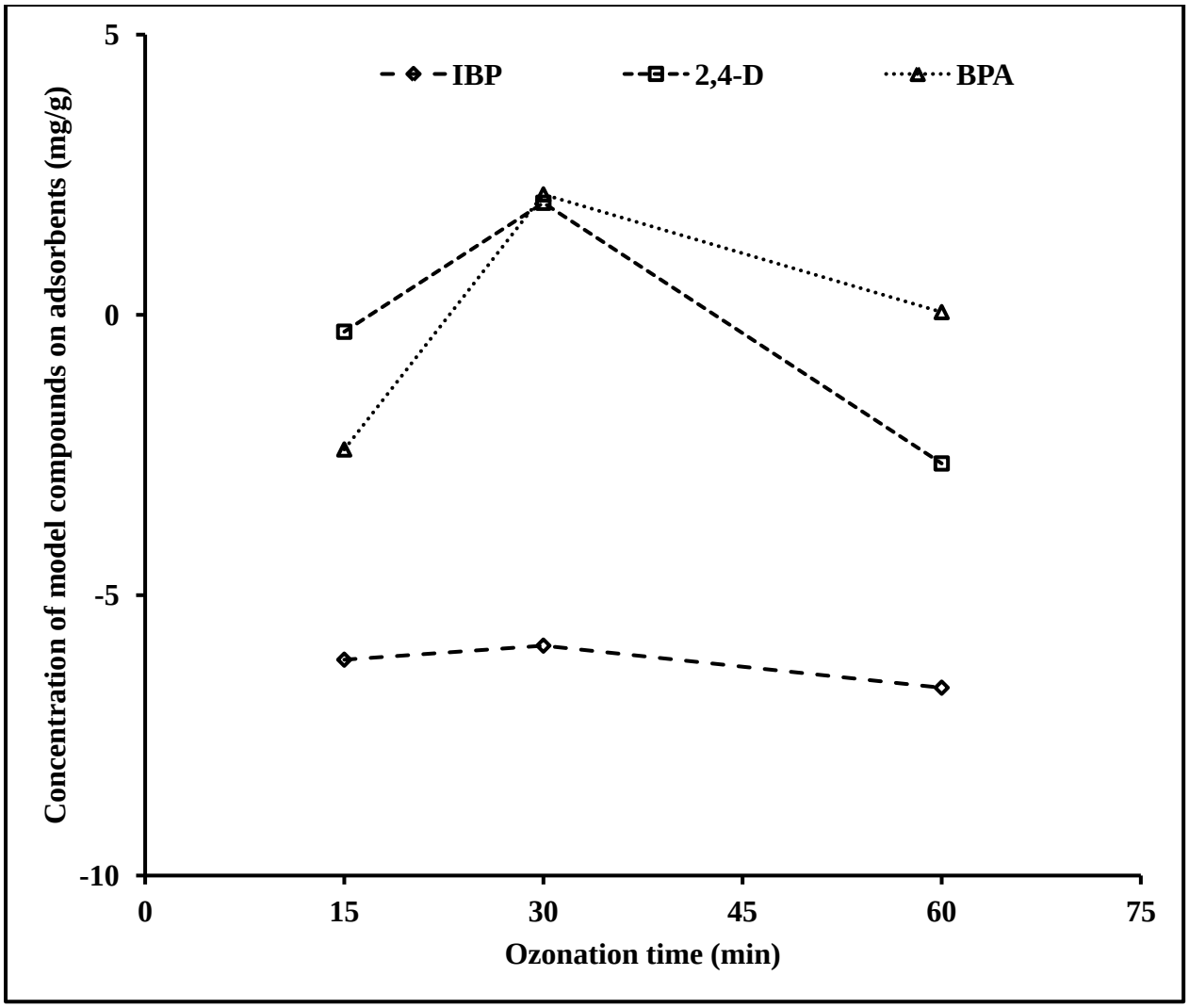

Figure 7-3. Concentration of IBP, 2,4-D, and BPA on ozone treated S-CS regenerated for 15, 30 and 60 minutes (Trend-lines are added for better illustration of results)

The negative values of uptake of model compounds indicate release of adsorbed model compounds from saturated adsorbents into the solution. Uptake of model compounds with ozone regenerated samples was not significant. The highest uptake occurred in adsorption of BPA on ozone treated S-BC equal to 21 mg/g which is 15% of uptake of BPA on the fresh BC with the same initial concentration of 50 mg/L. According to the results of adsorption of model compounds on ozone regenerated S-BC and S-CS, it is concluded that regeneration with ozone did not recover the adsorption capacity and did not open the plugged pores of S-BC and S-CS

[79]. Although ozone treatment could not restore the adsorption capacity of adsorbents, conventional regeneration methods such as acid back wash as an in-situ regeneration method or thermal regeneration can be used to regenerate the saturated adsorbents [96].

Adsorption uptake of S-BC and S-CS adsorbents regenerated after 30 minutes of ozonation shows a slight improvement in restoration of the adsorption capacity of adsorbents [27] while, results of uptake of S-BC and S-CS regenerated with 60 minutes of ozonation indicates that more oxidation of the saturated adsorbents has a detrimental effect on restoration of capacity of adsorbents. Reports in the literature attribute this phenomenon to destruction of the porosity of adsorbents as a result of excessive oxidation [79]. Results show that ozone does not restore the adsorption capacity of saturated adsorbents and excessive ozone treatment destroys the porosity of adsorbents through oxidation of adsorbent.

CHAPTER EIGHT

GENERAL CONCLUSIONS AND RECOMMENDATIONS FOR FUTURE WORKS

The effectiveness of adsorption for removal of emerging pollutants with granular activated carbon for drinking water treatment was studied. For this purpose adsorption of IBP, 2,4-D, and BPA as model compounds on bituminous and coconut shell based GACs was studied. Thermodynamic of adsorption in temperature ranges lower than room temperature was calculated and discussed. Effect of PZC of adsorbent and tap water matrix on adsorption of model compounds was investigated. The effectiveness of regeneration of saturated adsorbents with ozone was studied.

General Conclusions

Based on the findings of experiments and discussions, the following aspects are concluded:

- Isotherm adsorption experiments were employed to study the adsorption of three model compounds on BC and CS at 296, 288, and 280 K in Milli-Q water. Freundlich and Langmuir models were used to fit to the isotherm adsorption data and the model parameters were calculated. Langmuir model provided a better fit for the data in all experimental conditions in Milli-Q water indicating monolayer adsorption of model compounds on BC and CS. It was concluded that Q_{max} of adsorption of emerging

pollutants in anionic form in the pH range of adsorption was proportional to the total surface area of adsorbents. Higher porosity of bituminous based adsorbent together with its more acidic surface most probably due to the aging resulted in higher Q_{max} for adsorption of all three model compounds than adsorption on CS.

- The Gibbs free energy, entropy, and enthalpy of adsorption of model compounds in temperature range of 280 to 296 K were determined using Langmuir model parameters of isotherm experiments at 296, 288, and 280 K. The negative value of Gibbs free energy for adsorption of all three model compounds indicated the spontaneous adsorption of model compounds on BC and CS. This suggests that adsorption is an ideal candidate for removal of model compounds from drinking water in regions with the temperature range of 280 to 296 K such as Canada. Insignificant decrease in spontaneity of adsorption of IBP with reduction of temperature from 296 K to 280 K was observed. This indicated the significant effect of entropy of adsorption on spontaneity of adsorption. Although adsorption of 2,4-D and BPA were found to be exothermic, the increase of Q_{max} with the reduction of temperature from 296 K to 280 K was not significant. The insignificant change in Q_{max} of adsorption of model compounds on both adsorbents with reduction of temperature from 296 K to 280 K indicates that adsorption is an effective method for removal of emerging pollutants even at temperatures as low as 280 K. The change in Q_{max} of model compounds with the reduction of temperature from 296 K to 280 K was in range of 2 to 13% of the Q_{max} at 296 K. This small change in Q_{max} indicates the insignificant effect of temperature on removal of EPs with GAC.
- Nitric acid pre-treatment of BC and CS for the purpose of reduction of PZC was carried out. Nitric acid pre-treatment increased the amount of acidic functional groups on the

surface of both BC and CS and reduced the PZC of both BC and CS. Nitric acid pre-treatment of bituminous coal based carbon at room temperature removed the high ash content and slightly increased the pore volume and surface area. Whereas nitric acid pre-treatment of coconut shell based carbon at room temperature reduced the surface area and pore volume which is assumed to be due to the formation of oxygen containing functional groups at the entrance of slit shaped pores. 46 and 48% increase in Q_{max} of adsorption of BPA and IBP on N-CS in comparison to CS corroborated the idea that presence of specific acidic surface functional groups most probably carbonyl and carboxylic groups are responsible for adsorption of solute molecules present in molecular form. The identical ratio of Q_{max} of adsorption of 2,4-D on N-BC to N-CS with the ratio of total surface area of N-BC to N-CS supports the possibility that Q_{max} of adsorption of solutes present in anionic form in pH range of adsorption is proportional to the total surface area of adsorbent. Comparing the Q_{max} of adsorption of model compounds on adsorbents with acidic PZC with adsorbents with basic PZC, it is concluded that adsorbent with acidic PZC was a better adsorbent for removal of emerging pollutants in drinking water.

- Isotherm adsorption of model compounds on BC and CS in tap water at 296 K was conducted. It was observed that presence of species as components of tap water in general reduced the capacity of adsorbents for adsorption of model compounds. It was inferred that interaction of ions present in tap water matrix with the charged adsorption sites of adsorbent could increase the neutrality of the surface of adsorbent. It was concluded that adsorption in tap water favored adsorption of emerging pollutants, that neutral surface of adsorbent is a desirable condition for their adsorption.

- Regeneration of activated carbon saturated with model compounds was conducted using a semi-batch reactor with continuous flow of gaseous ozone. Regenerated adsorbents had a weak uptake of the model compounds after regeneration. The results showed a poor regeneration with ozone in restoration of adsorption capacity of saturated activated carbon. Excessive ozone treatment was observed to damage the porosity of adsorbent as a result of oxidation of adsorbent.

According to the results, it is concluded that adsorption with granular activated carbon is a feasible and effective method for removal of emerging pollutants from drinking water.

Recommendations for Future Works

The effectiveness of removal of organics from drinking water together with the promising results of this research for removal of emerging pollutants from drinking water opens the possibility of additional research on removal of emerging pollutants using granular activated carbons. For more research on removal of emerging pollutants with GAC following recommendations are suggested:

- Granular activated carbon used for filtration in treatment of drinking water is used in continuous mode and kinetics of adsorption plays an important role in adsorption process in continuous mode therefore, it is necessary to measure the kinetics of adsorption
- Reduction of PZC of adsorbents with nitric acid pre-treatment results in introduction of acidic surface functional groups. Presence of these acidic functional groups affects adsorption of compounds in molecular form with reactive functional groups in their structure thus, it is recommended to characterize the type and amount of those functional groups created on surface of adsorbent and study the effect of those functional groups on adsorption of emerging pollutants in specific

- Promising results of removal of emerging pollutants in tap water matrix as the water matrix in real condition warrants more research with a synthetic tap water matrix containing major components of tap water matrix and investigation of effect of those major components of tap water matrix on adsorption of emerging pollutants
- Since the costs of a treatment process is an important factor in choosing a process, it is recommended to run a pilot adsorption tests and plot breakthrough curves for adsorption of emerging pollutants in tap water matrix. The results will contribute to determining the adsorption behaviour of model compounds in real conditions and conducting accurate cost evaluations

REFERENCES

1. P. Verlicchi, A. Galletti, M. Petrovic, D. Barcelo, **Hospital effluents as a source of emerging pollutants: an overview of micropollutants and sustainable treatment options**, Journal of Hydrology 389 (2010) 416-28.

2. R. Rosal, A. Rodriguez, J.A. Perdigon-Melon, A. Petre, E. Garcia-Calvo, M.J. Gomez, A. Aguera, A.R. Fernandez-Alba, **Occurrence of emerging pollutants in urban wastewater and their removal through biological treatment followed by ozonation**, Water Res. 44 (2010) 578-88.

3. D.J. Lapworth, N. Baran, M.E. Stuart, R.S. Ward, **Emerging organic contaminants in groundwater: A review of sources, fate and occurrence**, Environmental Pollution 163 (2012) 287-303.

4. S. Kumar, M. Zafar, J.K. Prajapati, S. Kumar, S. Kannepalli, **Modeling studies on simultaneous adsorption of phenol and resorcinol onto granular activated carbon from simulated aqueous solution**, J. Hazard. Mater. 185 (2011) 287-94.

5. I. Bautista-toledo, I. Bautista-Toledo, Ferro-García M.A., J. Rivera-Utrilla, C. Moreno-Castilla, Vegas Fernández F.J., **Bisphenol A removal from water by activated carbon. Effects of carbon characteristics and solution chemistry**, Environ. Sci. Technol. 39 (2005) 6246.

6. Z. Aksu, K., Z. Aksu, E. Kabasakal, **Batch adsorption of 2,4-dichlorophenoxy-acetic acid (2,4-D) from aqueous solution by granular activated carbon**, Separation and Purification Technology 35 (2004) 223-240.

7. A. Sosiak, P. Biol, **A preliminary survey of pharmaceuticals and endocrine disrupting compounds in treated municipal wastewaters and receiving rivers of Alberta** (2005).

8. A.J. Cessna, J.A. Elliott, L. Tollefsonc, W. Nicholaichuk, **Herbicide and nutrient transport from an irrigation district into the south Saskatchewan river**, Journal of Environmental Quality 30 (2001) 1796-1807.

9. S.D. Faust, S.D.(.D. Faust 1929-1997, **Chemistry of drinking water treatment**, 2nd edition ed., Chelsea, MI : Ann Arbor Press, Chelsea, MI, 1998.

10. A.S. Mestre, P., A.S. Mestre, J. Pires, J.M.F. Nogueira, A.P. Carvalho, **Activated carbons for the adsorption of ibuprofen**, Carbon 45 (2007) 1979-1988.

11. K.K. Kolasinski, **Surface science: Foundation of catalysis and nanosecience**, 3rd ed., John Wiley & Sons Ltd., West Sussex England, 2012.

12. K.E. Noll, K.E. Noll, **Adsorption technology for air and water pollution control**, Chelsea, Mich. : Lewis Publishers, Chelsea, Mich., 1992.

13. Z.K. Chowdhury, L.B. Passantino, **Activated carbon : solutions for improving water quality**, Denver : American Water Works Association, Denver, 2013.

14. Calgon Carbon Corporation, **FILTRASORB 400 cataloge** 2014 (2012).

15. Jacobi Company, **AquaSorb CS cataloge** 2014 (2011).

16. S.P. Dubey, A.D. Dwivedi, M. Sillanpää, K. Gopal, **Artemisia vulgaris-derived mesoporous honeycomb-shaped activated carbon for ibuprofen adsorption**, Chem. Eng. J. 165 (2010) 537-544.

17. K.M. Jeffries, L.J. Jackson, M.G. Iknomou, H.R. Habibi, **Presence of natural and anthropogenic organic contaminants and potential fish health impacts along two river gradients in Alberta, Canada**, Environmental Toxicity and Chemistry 29 (2010) 2379-87.

18. V. Gun'ko, S. Mikhalovskii, M. Melillo, E. Voronin, L. Nosach, E. Pakhlov, V. Gun'ko, S. Mikhalovskii, M. Melillo, E. Voronin, L. Nosach, E. Pakhlov, **The effect of the nature and structure of adsorbents on interaction with ibuprofen**, Theoretical and Experimental Chemistry 40 (2004) 137-143.

19. D.J. de Ridder, A.R.D. Verliefde, S.G.J. Heijman, J.Q.J.C. Verberk, L.C. Rietveld, d.A. van, G.L. Amy, J.C. van Dijk, **Influence of natural organic matter on equilibrium adsorption of neutral and charged pharmaceuticals onto activated carbon**, Water Science & Technology 63 (2011) 416-423.

20. H. Shamsi Jazeyi, T. Kaghazchi, **Investigation of nitric acid treatment of activated carbon for enhanced aqueous mercury remova**l, Journal of Industrial and Engineering Chemistry 16 (2010) 852-858.

21. R. Nedunuri, C.A. Guzman-Perez, J. Soltan, V. Himabindu, **Adsorption characteristics of atrazine on granular activated carbon and carbon nanotubes**, Chemical Engineering Technology 35 (2012) 272-280.

22. O. Hamdaoui, E. Naffrechoux, **Modeling of adsorption isotherms of phenol and chlorophenols onto granular activated carbon part I. two-parameter models and equations allowing determination of thermodynamic parameters**, J. Hazard. Mater. 147 (2007) 381-94.

23. D.B. Mawhinney, B.J. Vanderford, S.A. Snyder, **Transformation of 1H-Benzotriazole by ozone in aqueous solution**, Environ. Sci. Technol. 46 (2012) 7102-11.

24. J. Xiaohui, S. Peldszus, P.M. Huck, **Reaction kinetics of selected micropollutants in ozonation and advanced oxidation processes**, Water Res. 46 (2012) 6519-30.

25. X. Yang, R.C. Flowers, H.S. Weinberg, P.C. Singer, **Occurrence and removal of pharmaceuticals and personal care products (PPCPs) in an advanced wastewater reclamation plant**, Water Res. 45 (2011) 5218-5228.

26. J.F. Beltrán, **Ozone reaction kinetics for water and wastewater systems**, Lewis Publishers, New York, 2004.

27. P.M. Álvarez, F.J. Beltrán, V. Gómez-Serrano, J. Jaramillo, E.M. Rodríguez, **Comparison between thermal and ozone regenerations of spent activated carbon exhausted with phenol**, Water Res. 38 (2004) 2155-2165.

28. H. Guedidi, L. Reinert, J.-.M. Leveque, Y. Soneda, N. Bellakhal, L. Duclaux, H. Guedidi, L. Reinert, J. Leveque, Y. Soneda, N. Bellakhal, L. Duclaux, **The effects of the surface oxidation of activated carbon, the solution pH and the temperature on adsorption of ibuprofen.(Report)**, Carbon 54 (2013) 432.

29. K.Y. Bell, M.M. Wells, K.A. Traexler, M. Pellegrin, A. Morse, J. Bandy, **Emerging pollutants**, Water environment research 83 (2011) 1906-84.

30. N. Ratola, A. Cincinelli, A. Alves, A. Katsoyiannis, **Occurrence of organic microcontaminants in the wastewater treatment process. A mini review**, Journal of Hazadous Materials 239-40 (2012) 1-18.

31. P. Verlicchi, M. Al Aukidy, E. Zambello, **Occurrence of pharmaceutical compounds in urban wastewater- removal, mass load, and environmental risk after a secondary treatment- A review**, Science of the Total Environement 429 (2012) 123-55.

32. B.H. Hameed, J.M. Salman, A.L. Ahmad, **Adsorption isotherm and kinetic modeling of 2,4-D pesticide on activated carbon derived from date stones**, J. Hazard. Mater. 163 (2009) 121-126.

33. W. Tsai, H. Hsu, T. Su, K. Lin, C. Lin, **Adsorption characteristics of bisphenol-A in aqueous solutions onto hydrophobic zeolite**, J. Colloid Interface Sci. 299 (2006) 513-519.

34. M.C. Hermosin, C., M.C. Hermosin, J. Cornejo, **Removing 2,4-D from water by organo-clays**, Chemosphere 24 (1992) 1493-1503.

35. K.J. Choi, S.G. Kim, C.W. Kim, S.H. Kim, K.J. Choi, S.G. Kim, C.W. Kim, S.H. Kim, **Effects of activated carbon types and service life on removal of endocrine disrupting chemicals: amitrol, nonylphenol, and bisphenol-A**, Chemosphere 58 (2005) 1535-1545.

36. J. Saab, G. Bassil, R. Abou Naccoul, J. Stephan, I. Mokbel, J. Jose, **Salting-out phenomenon and 1-octanol/water partition coefficient of metalaxyl pesticid**e, Chemosphere 82 (2011) 929-934.

37. D.S. Hart, L.C. Davis, L.E. Erickson, T.M. Callender, **Sorption and partitioning parameters of benzotriazole compounds**, Microchemical Journal 77 (2004) 9-17.

38. B. Hilger, H. Fromme, W. Volkel, M. Coelhan, **Effects of chain length, chlorination degree, and structure on the octanol-water partition coefficients of polychlorinated n-alkanes**, Environmental science & technology 45 (2011) 2842-2849.

39. P. Benoit, E. Barriuso, R. Calvet, **Biosorption characterization of herbicides, 2,4-D and atrazine, and two chlorophenols on fungal mycelium**, Chemosphere 37 (1998) 1271-1282.

40. S. Bakhtiary, M. Shirvani, H. Shariatmadari, **Characterization and 2,4-D adsorption of sepiolite nanofibers modified by N-cetylpyridinium cations**, Microporous and Mesoporous Materials 168 (2013) 30-36.

41. R.S.S. V.L. Snoeyink, **Water quality and treatment**, Fifth edition ed., McGRAW-HILL, INC., New York, 1999.

42. L.F. Delgado, P. Charles, K. Glucina, C. Morlay, **The removal of endocrine disrupting compounds, pharmaceutically activated compounds and cyanobacterial toxins during drinking water preparation using activated carbon—A review**, Sci. Total Environ. 435–436 (2012) 509-525.

43. J. Wilcox, **Carbon capture**, SpringerLink, Online, 2012.

44. O.S. Amuda, A.A. Giwa, I.A. Bello, **Removal of heavy metal from industrial wastewater using modified activated coconut shell carbon**, Biochem. Eng. J. 36 (2007) 174-181.

45. R.R. Bansode, J.N. Losso, W.E. Marshall, R.M. Rao, R.J. Portier, **Pecan shell-based granular activated carbon for treatment of chemical oxygen demand in municipal wastewater**, Bioresour. Technol. 94 (2004) 129-35.

46. F. Rodríguez-reinoso, **The role of carbon materials in heterogeneous catalysis**, Carbon 36 (1998) 159-175.

47. L. Ji, F. Liu, Z. Xu, S. Zheng, D. Zhu, **Adsorption of pharmaceutical antibiotics on template-synthesized ordered micro- and mesoporous carbons**, Environmental science & technology 44 (2010) 3116-3122.

48. W. Tsai, C. Lai, T. Su, **Adsorption of bisphenol-A from aqueous solution onto minerals and carbon adsorbents**, J. Hazard. Mater. 134 (2006) 169-175.

49. M. Melillo, P., M. Melillo, G.J. Phillips, J.G. Davies, A.W. Lloyd, S.R. Tennison, O.P. Kozynchenko, S.V. Mikhalovsky, **The effect of protein binding on ibuprofen adsorption to activated carbons**, Carbon 42 (2004) 565-571.

50. J.M. Salman, H., J.M. Salman, B.H. Hameed, **Adsorption of 2,4-dichlorophenoxyacetic acid and carbofuran pesticides onto granular activated carbon**, Desalination 256 (2010) 129-135.

51. A.O. Dada, A.P. Olalekan, A.M. Olatunya, O. Dada,
Langmuir, Freundlich, Temkin and Dubinin–Radushkevich isotherms studies of equilibrium sorption of Zn^{2+} unto phosphoric acid modified rice husk, IOSR Journal of applied chemistry 3 (2012) 38-45.

52. P. Mourão, P. Carrott , Ribeiro Carrott, P.A.M. Mourão, P.J.M. Carrott, M.M.L. Ribeiro Carrott, **Application of different equations to adsorption isotherms of phenolic compounds on activated carbons prepared from cork**, Carbon 44 (2006) 2422-2429.

53. J. Rivera-Utrilla, J. Rivera-Utrilla, M. Sánchez-Polo, **The role of dispersive and electrostatic interactions in the aqueous phase adsorption of naphthalenesulphonic acids on ozone-treated activated carbons**, Carbon 40 (2002) 2685-2691.

54. C. Jung, J. Park, K.H. Lim, S. Park, J. Heo, N. Her, J. Oh, S. Yun, Y. Yoon, C. Jung, J. Park, K.H. Lim, S. Park, J. Heo, N. Her, J. Oh, S. Yun, Y. Yoon, **Adsorption of selected endocrine disrupting compounds and pharmaceuticals on activated biochars**, J. Hazard. Mater. 263 Pt 2 (2013) 702.

55. K.M. Smith, **Characterization of activated carbon for taste and odour control** (2011).

56. A. Fokin, D. Gerbig, P. Schreiner, **σ/σ- and π/π-Interactions are equally important: Multilayered graphanes**
, Journal of The American Chemical Society 133 (2011) 20036-20039.

57. J. Margot, C. Kienle, A. Magnet, M. Weil, L. Rossi, L.F. de Alencastro, C. Abegglen, D. Thonney, N. Chèvre, M. Schärer, D.A. Barry, **Treatment of micropollutants in municipal wastewater: Ozone or powdered activated carbon?**, Sci. Total Environ. 461–62 (2013) 480-98.

58. Y. Al-Degs, Y. Al-Degs, M.A.M. Khraisheh, S.J. Allen, M.N. Ahmad, **Effect of carbon surface chemistry on the removal of reactive dyes from textile effluent**, Water Res. 34 (2000) 927-935.

59. G. Liu, J. Ma, X. Li, Q. Qin, G. Liu, J. Ma, X. Li, Q. Qin, **Adsorption of bisphenol A from aqueous solution onto activated carbons with different modification treatments**, J. Hazard. Mater. 164 (2009) 1275-1280.

60. R.W. Coughlin, F.S. Ezra, **Role of surface acidity in the adsorption of organic pollutants on the surface of carbon**, Environmental science & technology 2 (1968) 291-297.

61. F. Zhu, K. Choo, H. Chang, B. Lee, F. Zhu, K. Choo, H. Chang, B. Lee, **Interaction of bisphenol A with dissolved organic matter in extractive and adsorptive removal processes**, Chemosphere 87 (2012) 857-864.

62. Q. Sui, J. Huang, Y. Liu, X. Chang, G. Ji, S. Deng, T. Xie, G. Yu, Q. Sui, J. Huang, Y. Liu, X. Chang, G. Ji, S. Deng, T. Xie, G. Yu, **Rapid removal of bisphenol A on highly ordered mesoporous carbon**, Journal of Environmental Sciences 23 (2011) 177-182.

63. S. Kodama, H. Sekiguchi, **Estimation of point of zero charge for activated carbon treated with atmospheric pressure non-thermal oxygen plasmas**, Thin Solid Films 506–507 (2006) 327-330.

64. J.P. Reymond, F. Kolenda, **Estimation of the point of zero charge of simple and mixed oxides by mass titration**, Powder Technol 103 (1999) 30-36.

65. H.P. Boehm, **Surface oxides on carbon and their analysis: a critical assessment**, Carbon 40 (2002) 145-149.

66. V.K. Gupta, I. Ali, V.K. Suhas, V.K. Saini, V.K. Gupta, I. Ali, V.K. Suhas, V.K. Saini, **Adsorption of 2,4-D and carbofuran pesticides using fertilizer and steel industry wastes**, J. Colloid Interface Sci. 299 (2006) 556-563.

67. L.M. Pastrana-Martínez, M.V. López-Ramón, M.A. Fontecha-Cámara, C. Moreno-Castilla, **Batch and column adsorption of herbicide fluroxypyr on different types of activated carbons from water with varied degrees of hardness and alkalinity**, Water Res. 44 (2010) 879-885.

68. Y. Tu, C. You, C. Chang, **Kinetics and thermodynamics of adsorption for Cd on green manufactured nano-particles**, J. Hazard. Mater. 235–236 (2012) 116-122.

69. Z. Aksu, K., Z. Aksu, E. Kabasakal, **Adsorption characteristics of 2,4-dichlorophenoxyacetic acid (2,4-D) from aqueous solution on powdered activated carbon**, Journal of environmental science and health.Part.B, Pesticides, food contaminants, and agricultural wastes 40 (2005) 545.

70. J. Ma, Y. Jia, Y. Jing, Y. Yao, J. Sun, J. Ma, Y. Jia, Y. Jing, Y. Yao, J. Sun, **Kinetics and thermodynamics of methylene blue adsorption by cobalt-hectorite composite**, Dyes and Pigments 93 (2012) 1441-1446.

71. J. Pedro Silva, S. Sousa, J. Rodrigues, H. Antunes, J.J. Porter, I. Gonçalves, S. Ferreira-Dias, **Adsorption of acid orange 7 dye in aqueous solutions by spent brewery grains**, Separation and Purification Technology 40 (2004) 309-315.

72. K. Nejati, S. Davary, M. Saati, **Study of 2,4-dichlorophenoxyacetic acid (2,4-D) removal by Cu-Fe-layered double hydroxide from aqueous solution**, Appl. Surf. Sci. 280 (2013) 67-73.

73. J. Choi, T. Kim, K. Choo, J. Sung, M.B. Saidutta, S. Ryu, S. Song, B. Ramachandra, Y. Rhee, **Direct synthesis of phenol from benzene on iron-impregnated activated carbon catalysts**, Applied Catalysis A: General 290 (2005) 1-8.

74. C. Yu, X. Fan, L. Yu, T.J. Bandosz, Z. Zhao, J. Qiu, C. Yu, X. Fan, L. Yu, T.J. Bandosz, Z. Zhao, J. Qiu, **Adsorptive removal of thiophenic compounds from oils by activated carbon modified with concentrated nitric acid**, Energy Fuels 27 (2013) 1499-1505.

75. C. Chen, J. Xu, M. Jin, G. Li, C. Hu, C. Chen, J. Xu, M. Jin, G. Li, C. Hu, **Direct synthesis of phenol from benzene on an activated carbon catalyst treated with nitric acid**, Chinese Journal of Chemical Physics 24 (2011) 358-364.

76. A. Houshmand, W. Daud, **Study of changes in a palm-shell-based activated carbon characteristics by nitric acid**, Journal of Applied Sciences 10 (2010) 1116.

77. S.X. Liu, X. Chen, X.Y. Chen, Z.F. Liu, H.L. Wang, **Activated carbon with excellent chromium(VI) adsorption performance prepared by acid–base surface modification**, J. Hazard. Mater. 141 (2007) 315-319.

78. C.A. Guzman-Perez, J. Soltan, J. Robertson, **Kinetics of catalytic ozonation of atrazine in the presence of activated carbon**, Separation and Purification Technology 79 (2011) 8-14.

79. P.M. Alvárez', F.J. Beltrán, F.J. Masa, J.P. Pocostales, P.M. Alvárez', F.J. Beltrán, F.J. Masa, J.P. Pocostales, **A comparison between catalytic ozonation and activated carbon adsorption/ ozone- regeneration processes for wastewater treatment**, Applied Catalysis B, Environmental 92 (2009) 393-400.

80. H. Valdés, C.A. Zaror, **Ozonation of benzothiazole saturated-activated carbons: Influence of carbon chemical surface properties**, J. Hazard. Mater. 137 (2006) 1042-1048.

81. K. Yaghmaeian, G. Moussavi, A. Alahabadi, K. Yaghmaeian, G. Moussavi, A. Alahabadi, **Removal of amoxicillin from contaminated water using NH.sub.4Cl- activated carbon: Continuous flow fixed-bed adsorption and catalytic ozonation regeneration**, Chem. Eng. J. 236 (2014) 538.

82. M.A. Ferro-garcía, J. Rivera-utrilla, I. Bautista-toledo, C. Moreno-castilla, M.A. Ferro-garcía, J. Rivera-utrilla, I. Bautista-toledo, C. Moreno-castilla, **Adsorption of humic substances on activated carbon from aqueous solutions and their effect on the removal of Cr(III) ions**, Langmuir 14 (1998) 1880-1886.

83. T. LaFreniere, **Drinking water quality and comliance City of Saskatoon- for year 2013 annual notice to consumers** 2014 (2013).

84. A.D. Eaton, L.S. Clesceri, E.W. Rice, A.E. Greenberg, **Standard methods for the examination of water and wastewater**, American public health association, American water works association, Water environment federation, Washington DC, 2005.

85. M. Che, J. Védrine, **Chapter 19: Surface area/porosity, adsorption, diffusion**, in: **Characterization of solid materials and heterogenous catalysts: from structure to surface reacticvity, volume 1&2**, Wiley Online Library, 2012, pp. 853-879.

86. L. Gelb, K. Gubbins, **Characterization of porous glasses: simulation models, adsorption isotherms, and the Branauer-Emmett-Teller analysis method**, Langmuir 14 (1998) 2097-2111.

87. I. Ismail, **Cross-sectional areas of adsorbed N2, Ar, Kr, and O2 on carbons and fumed silicas at liquid nitrogen temperature**, Langmuir 8 (1991) 360-365.

88. B.S. Girgis, S.S. Yunis, A.M. Soliman, **Characteristics of activated carbon from peanut hulls in relation to conditions of preparation**, Mater Lett 57 (2002) 164-172.

89. S. Lowell, E. Shields, M. Thomas, M. Thommes, **Micropore Analysis**, in: **Characterization of porous solids and powders: surface area, pore size, and density**, Springer Netherlands, 2004, pp. 129-156.

90. M. Ojeda, J. Esparza, A. Campero, S. Cordero, I. Kornhauser, F. Rojas, **On comparing BJH and NLDFT pore-size distributions determined from N_2 sorption on SBA-15 substrata**, Phys. Chem. Chem. Phys. 5 (2003) 1859-1866.

91. D. Kim, S. Han, S. Kwak, **Synthesis and photocatalytic activity of mesoporous TiO_2 with the surface area, crystallite size, and pore size**, Journal of colloid and interface science 316 (2007) 85-91.

92. L. Qiuli, G.A. Sorial, **A comparative study of multicomponent adsorption of phenolic compounds on GAC and ACFs**, Journal of Hazardeous Materials 167 (2009) 89-96.

93. C. Pelekani, V.L. Snoeyink, **Competitive adsorption in natural water: Role of activated carbon pore size**, Water research 33 (1999) 1209-19.

94. P.M. Alvarez, J. Pablo Pocostales, F.J. Beltran, **Granular activated carbon promoted ozonation of food-processing secondary effluent**, Journal of Hazardeous Materials 185 (2011) 776-83.

95. J. Reungoat, M. Macova, B.I. Escher, S. Carswell, J.F. Mueller, J. Keller, **Removal of micropollutants and reduction of biological activity in a full scale reclamation plant using ozonation and activated carbon filtration**, Water Res. 44 (2010) 625-37.

96. E. Sabio, E. González, J.F. González, C.M. González-García, A. Ramiro, J. Gañan, **Thermal regeneration of activated carbon saturated with p-nitrophenol**, Carbon 42 (2004) 2285-2293.

APPENDIX A. Absorbance and Calibration Curves of Model Compounds

Absorbance curves were plotted to find the maximum absorbance of a model compound at different concentration levels of compound. Absorbance is the difference between absorbance of the sample containing the model compound with the absorbance of the water matrix with no model compound present in it considered as blank. Absorbance curve of different dilutions of IBP stock solution containing 7% of methanol in Milli-Q water was presented in chapter three, Figure 3-6. Absorbance curves for IBP in tap water matrix, 2,4-D, and BPA is presented below:

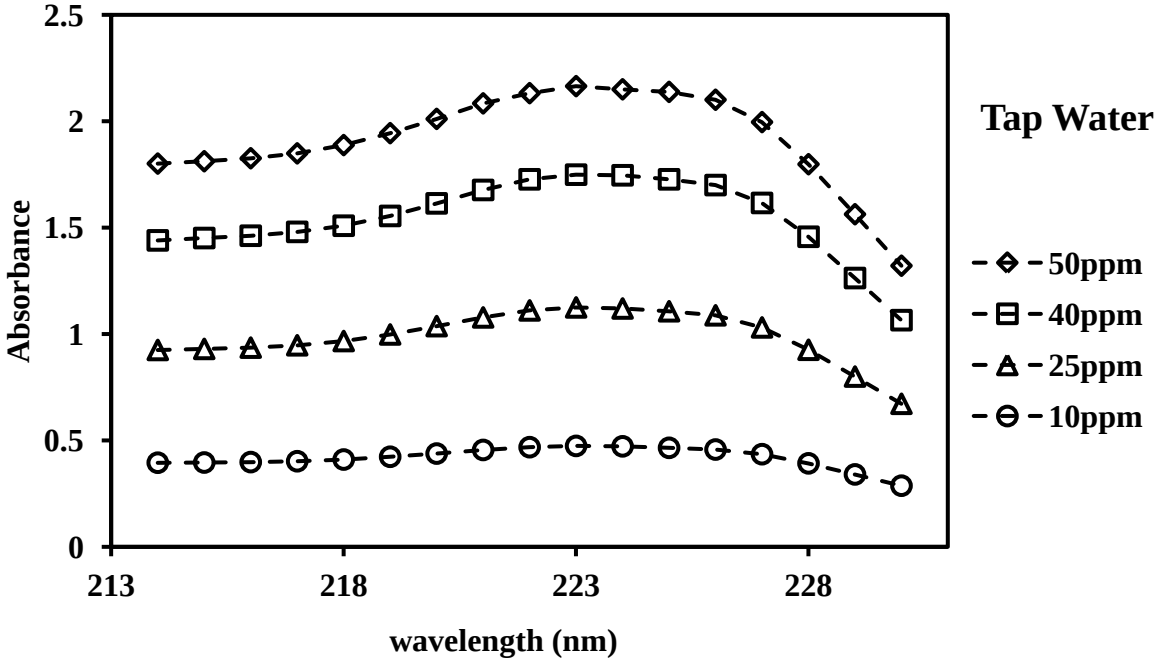

Figure A-1. Absorbance Curve of IBP (7%, w/w; Methanol/Tap water), maximum absorbance occurring at 223 nm

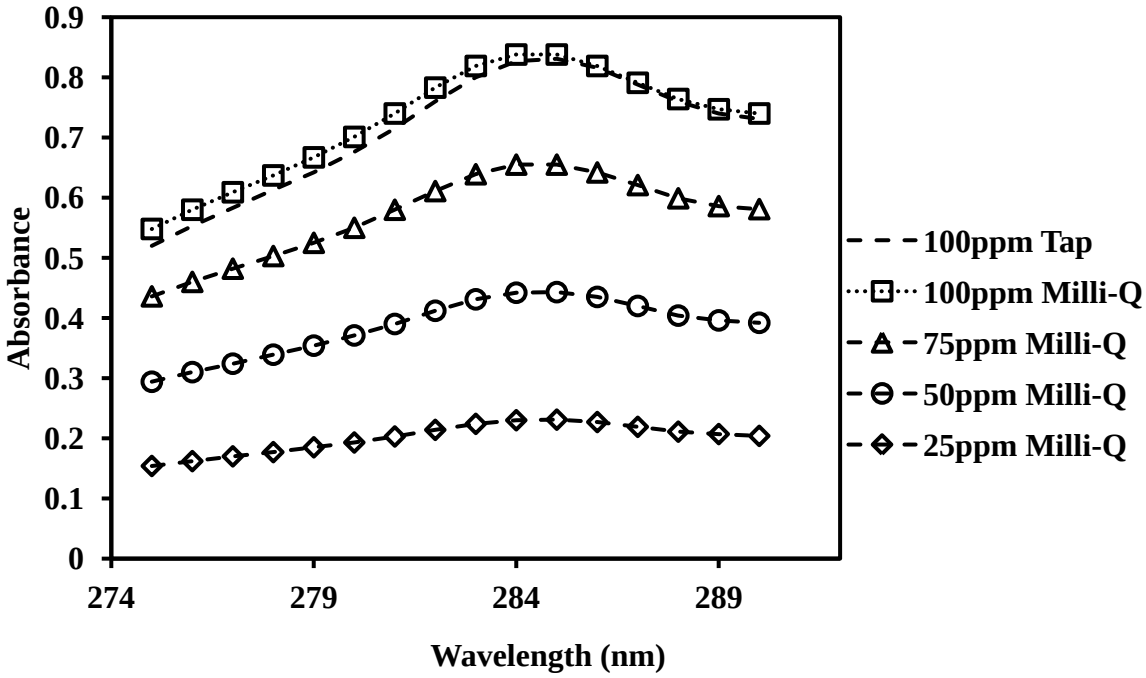

Figure A-2. Absorbance Curve of 2,4-D, maximum absorbance occurring at 284 nm

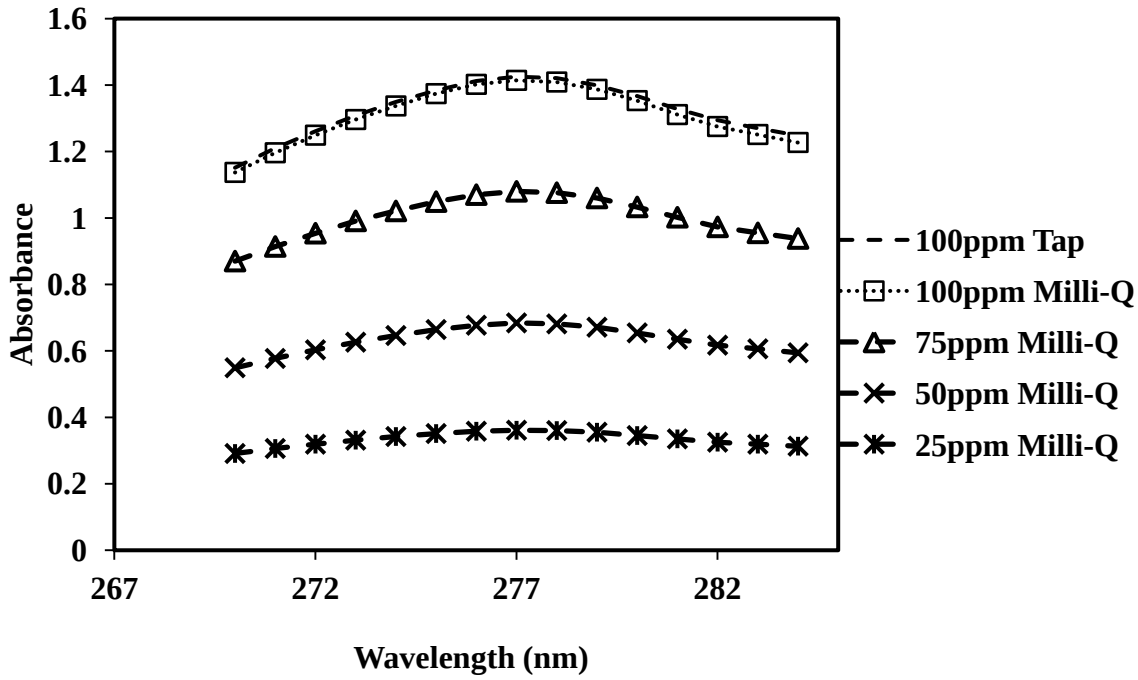

Figure A-3. Absorbance Curve of BPA, maximum absorbance occurring at 277 nm

Maximum absorbance of model compounds found for each concentration level in Appendix A-1 was plotted against the concentrations. Trend-lines fitting to the data were used to convert the absorbance to concentrations. A calibration line to convert the concentration of IBP in Milli-Q water was presented in chapter three, Figure 3-7. Calibration lines for the conversion of absorbance to concentration for IBP in tap water matrix, 2,4-D, and BPA are presented below:

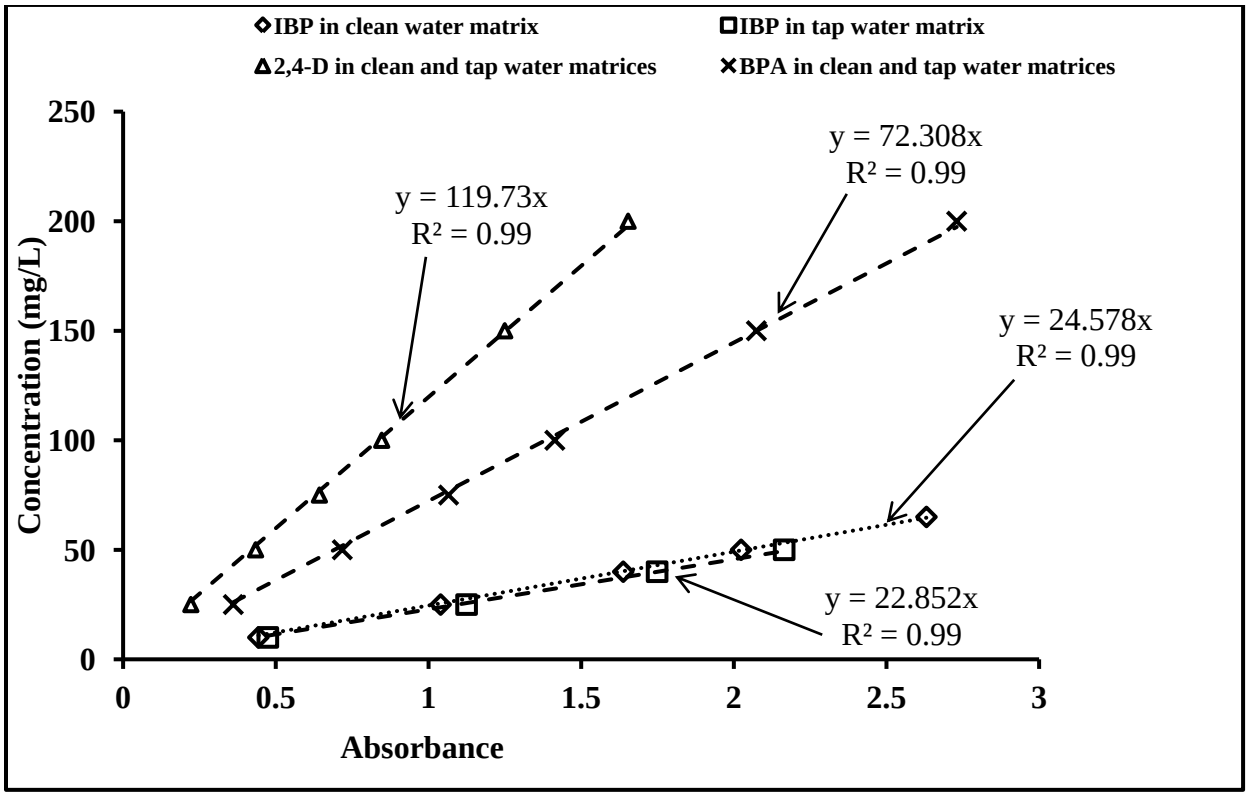

Figure A-4. IBP, 2,4-D, and BPA concentration measurement calibration lines

In order to calculate the concentration of a model compound in solution, the difference between absorbance of a sample with Milli-Q water and the sample containing the model compound should be measured and recorded. The recorded difference in absorbance is the X value in trend-lines of Figure A-4. Multiplying the absorbance by the slope of the trend-line attributed to the model compound equals to the concentration of model compound in solution in mg/L.

APPENDIX B. Characterization of Adsorbents

Adsorption and desorption of N_2 on adsorbents at 77 K was carried out. Isotherm data for adsorption and desorption of N_2 on CS was presented in Figure 4-1. Adsorption and desorption isotherm data for BC, N-CS and N-BC are presented below:

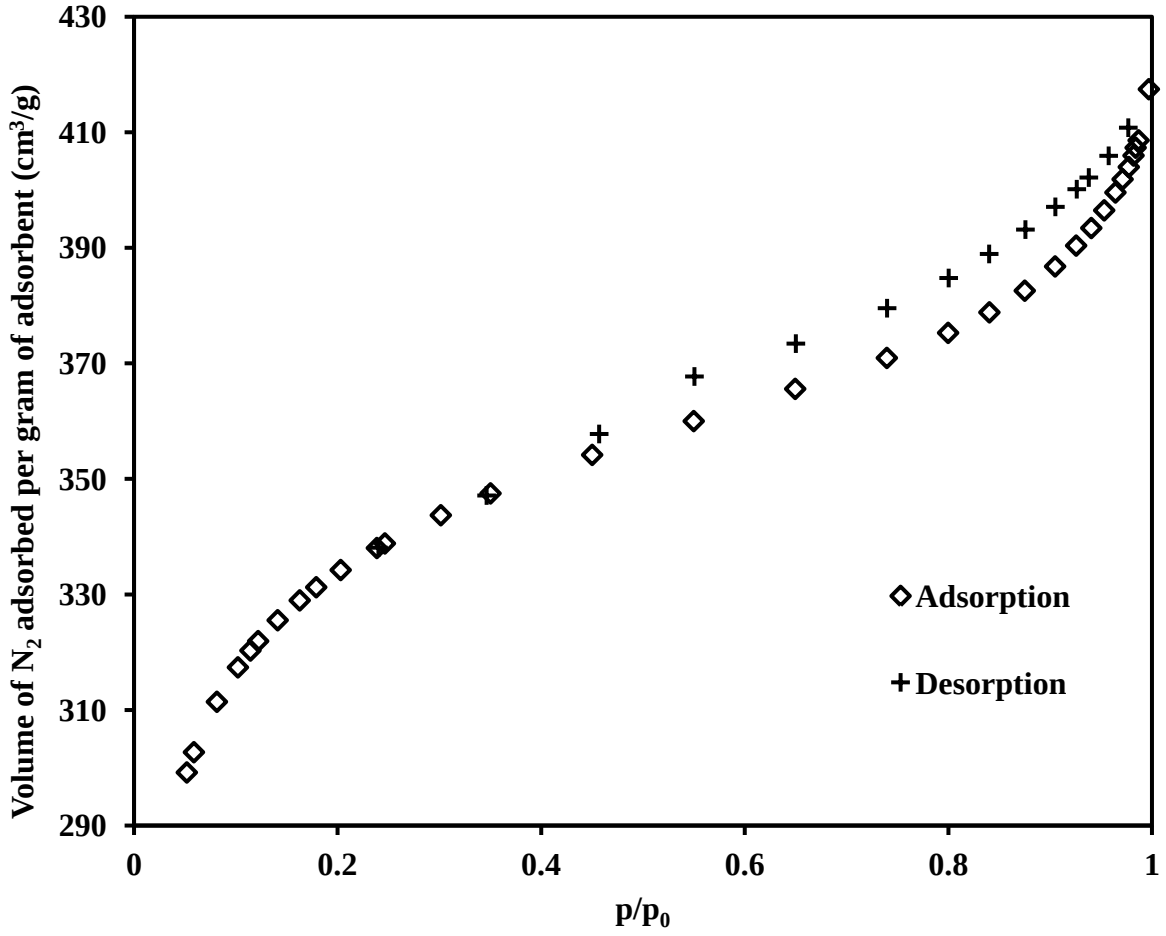

Figure B-1. Isotherm data of adsorption and desorption of N_2 on BC at 77 K

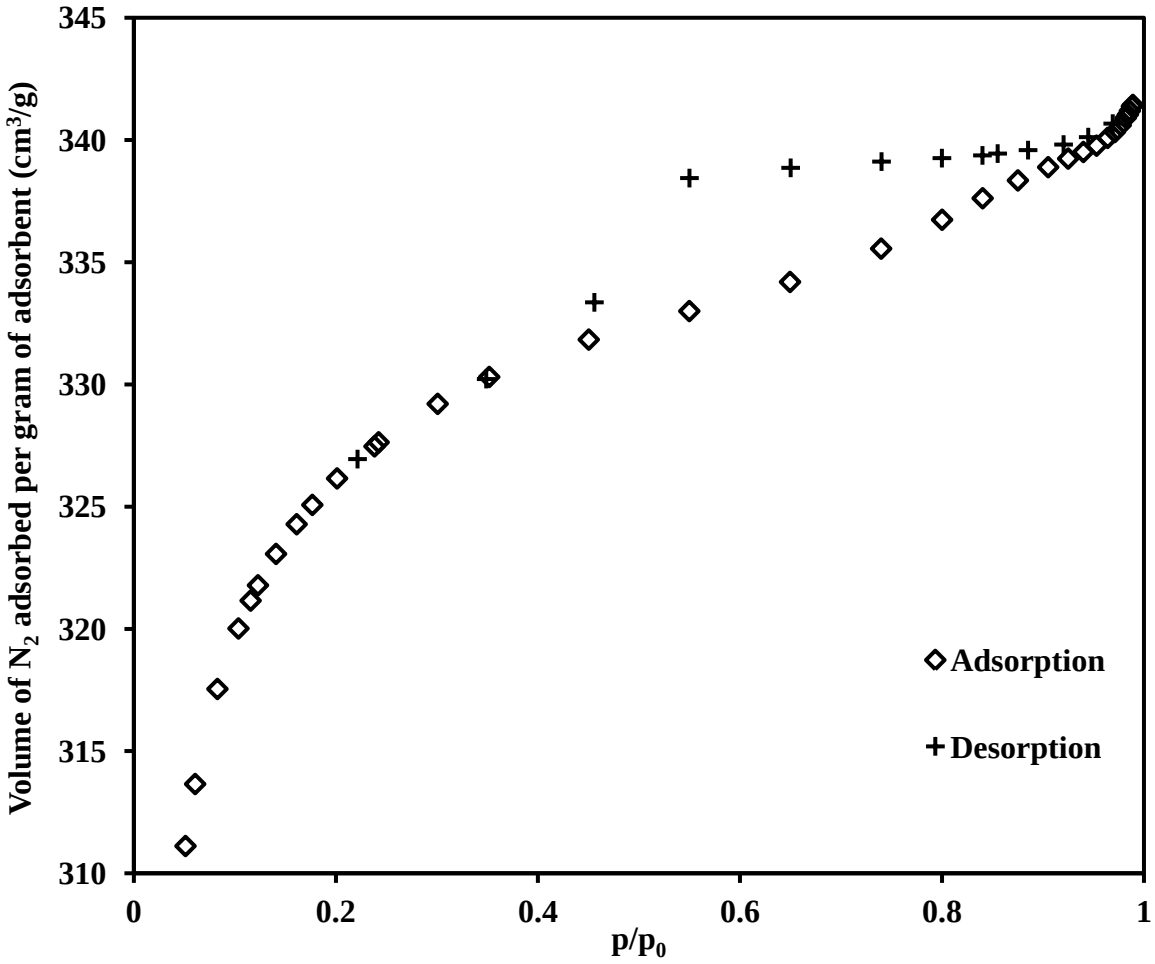

Figure B-2. Isotherm data of adsorption and desorption of N_2 on N-CS at 77 K

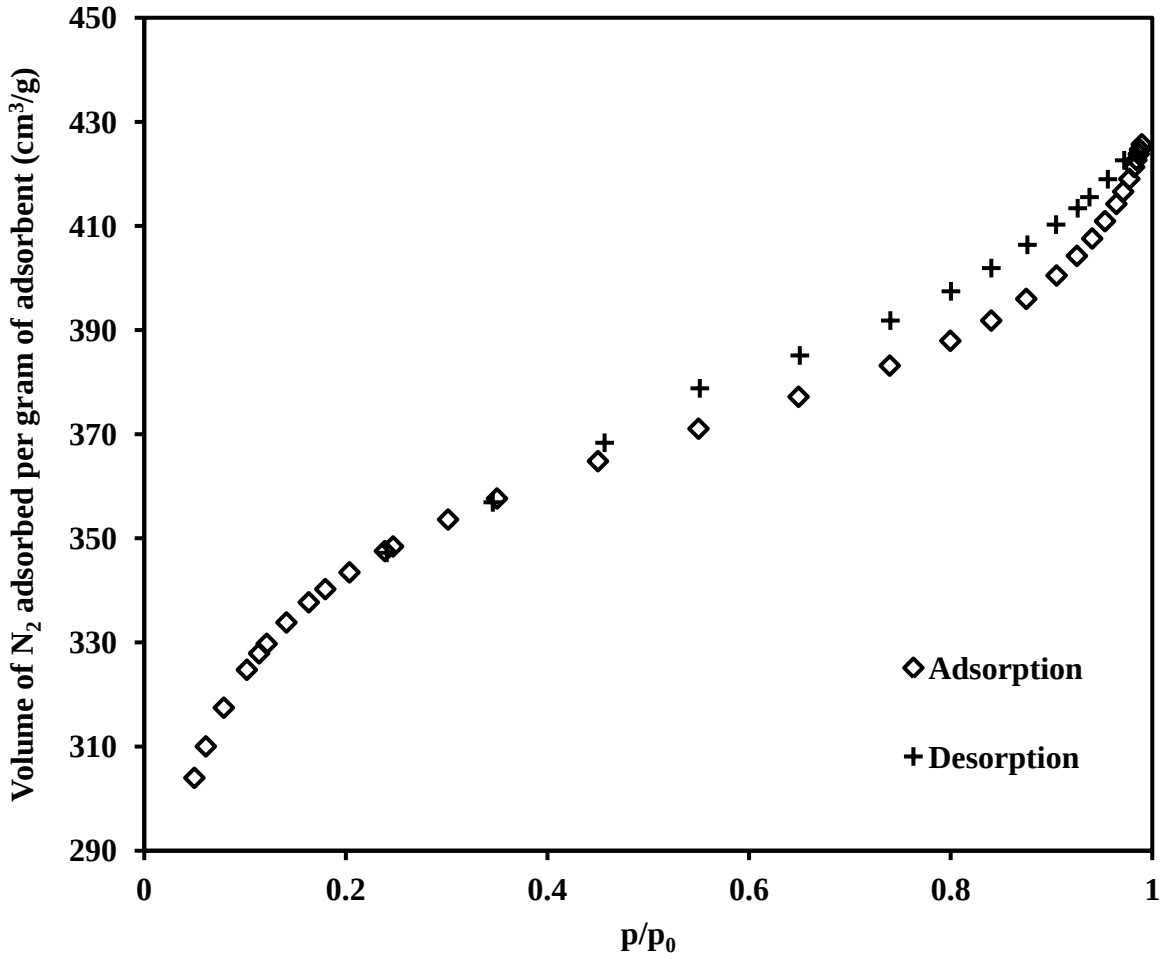

Figure B-3. Isotherm data of adsorption and desorption of N_2 on N-BC at 77 K

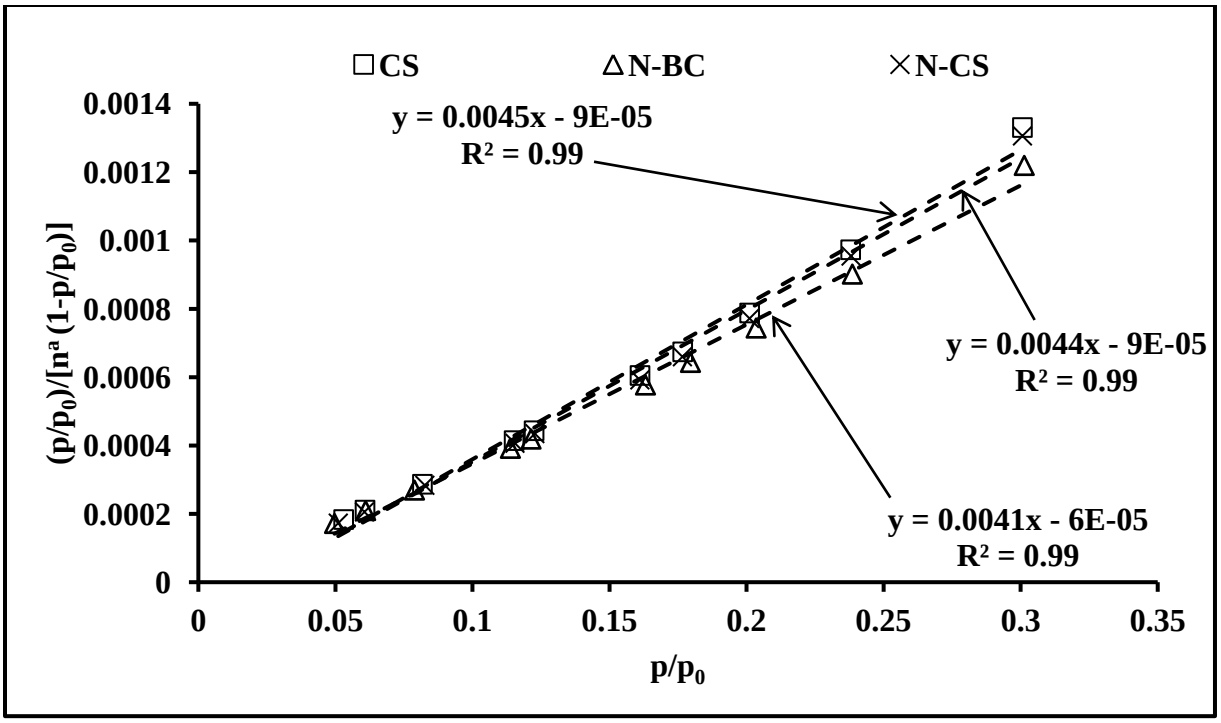

Figure B-4. Linear trend-line fitted to the isotherm data from adsorption of N_2 on CS, N-BC, and N-CS using BET equation

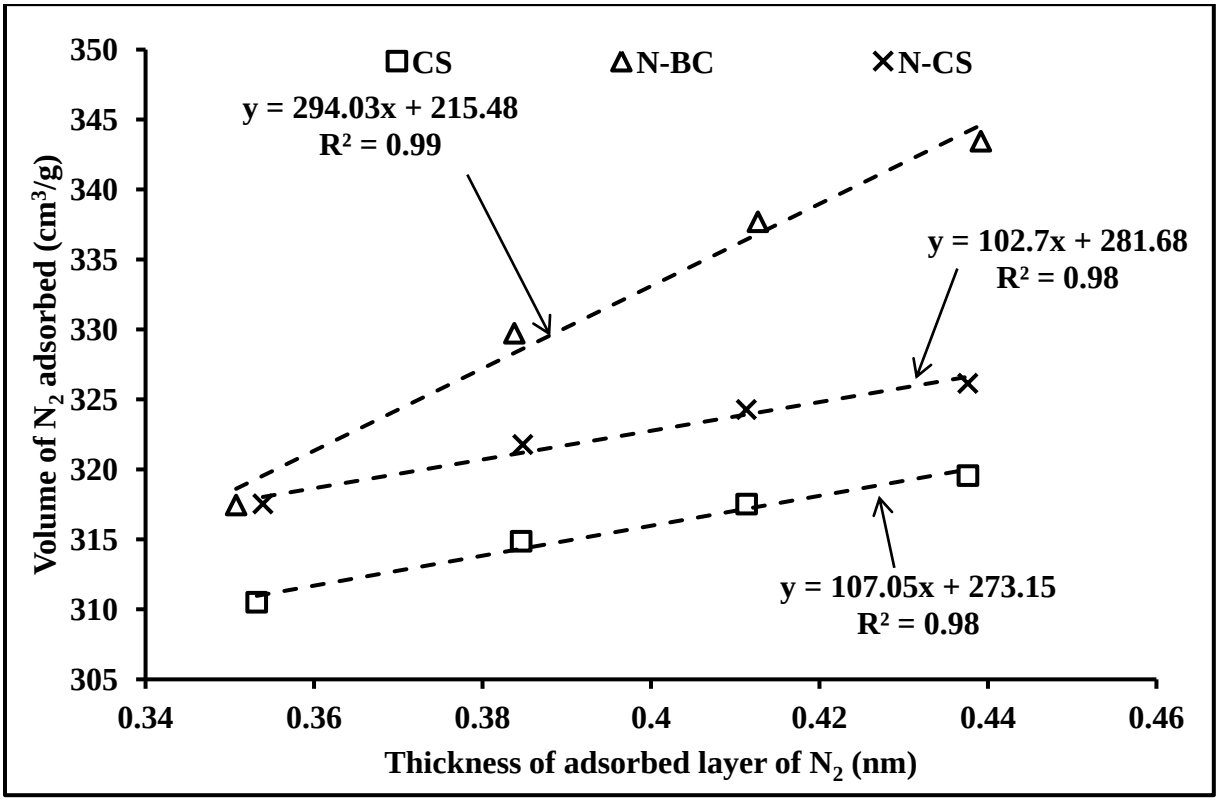

Figure B-5. Linear trend-line fitted to the thickness plot of adsorption of N_2 on N-BC, CS, N-CS

Point of zero charge measurement curves for BC was presented in chapter four Figure 4-6. The convergence of the plateau of the curves indicates the point of zero charge of the adsorbent. Point of zero charge measurement curves for N-BC, CS, and N-CS are presented below:

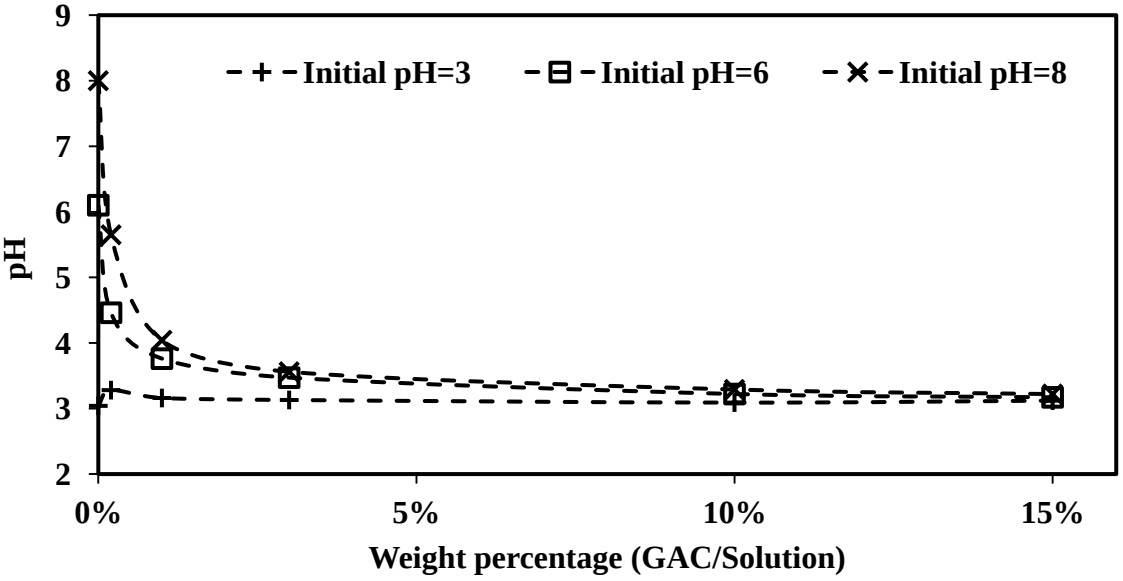

Figure B-6. Determination of point of zero charge of N-BC

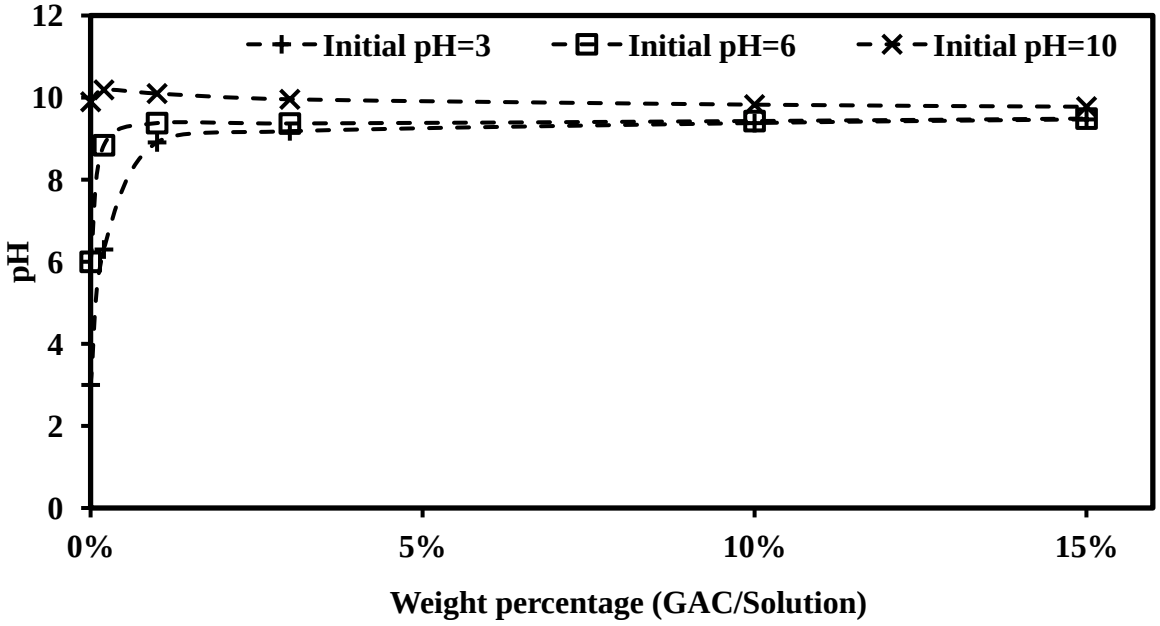

Figure B-7. Determination of point of zero charge of CS

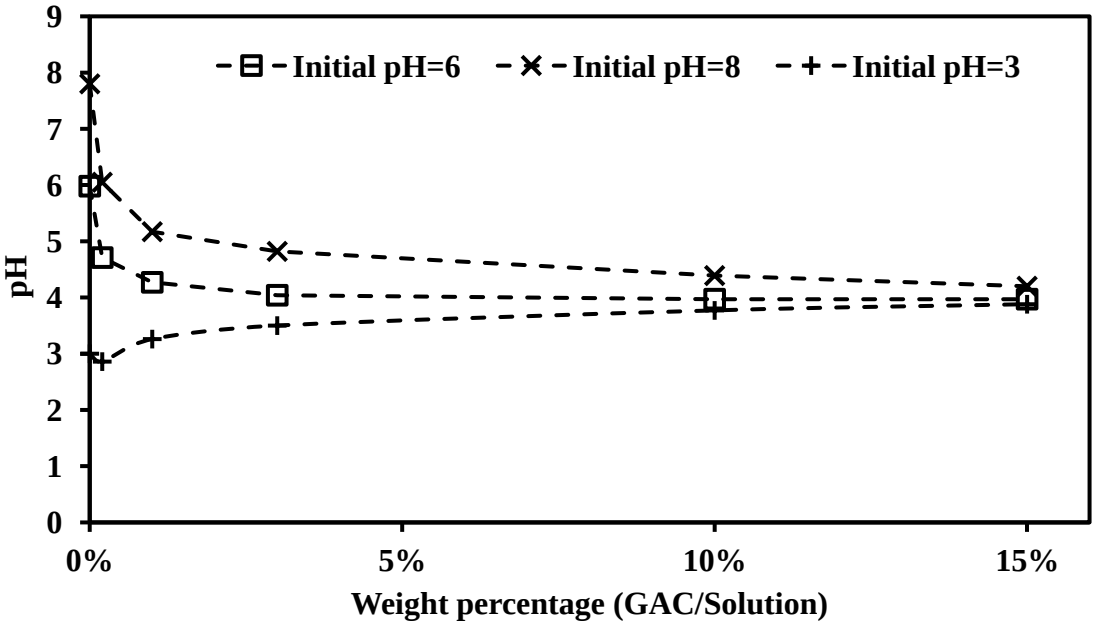

Figure B-8. Determination of point of zero charge of N-CS

APPENDIX C. Linear Langmuir Model Fit to the Experimental Adsorption Isotherm Data

The experimental adsorption isotherm data for adsorption of model compounds was collected. The Langmuir model fitted the data better than the Freundlich model therefore, the Langmuir model parameters were used for analysis. Calculation of model parameters using the linear Langmuir trend-line equation is explained in detail in chapter two. The linear Langmuir model fit to the experimental adsorption isotherm data for adsorption of model compounds is presented below:

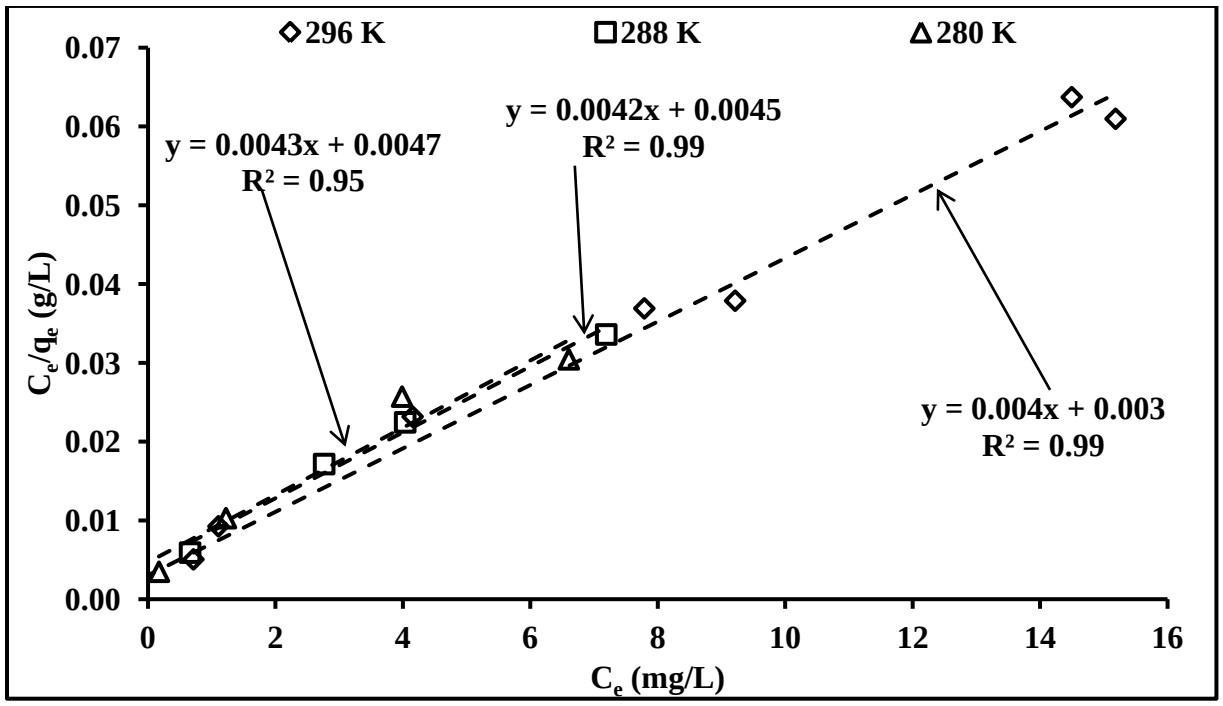

Figure C-1. Isotherm experimental data and linear Langmuir model fit to the data for adsorption of IBP on BC in Milli-Q water at 280, 288, and 296 K

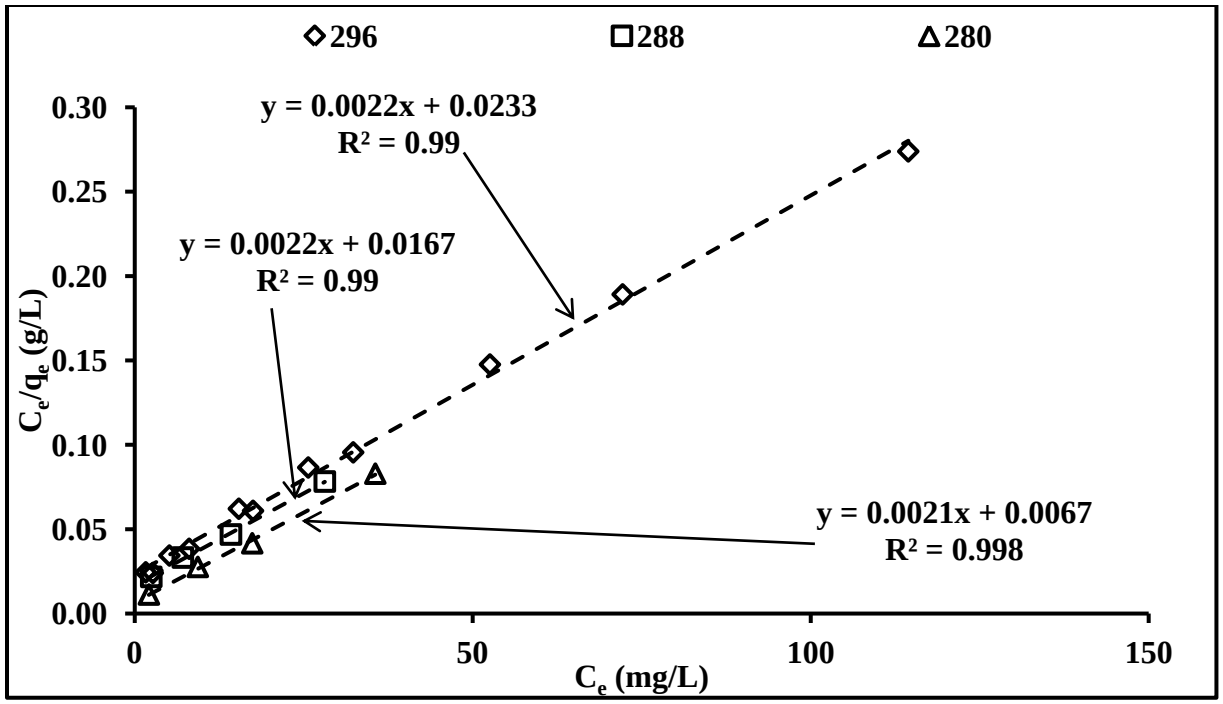

Figure C-2. Isotherm experimental data and linear Langmuir model fit to the data for adsorption of 2,4-D on BC in Milli-Q water at 280, 288, and 296 K

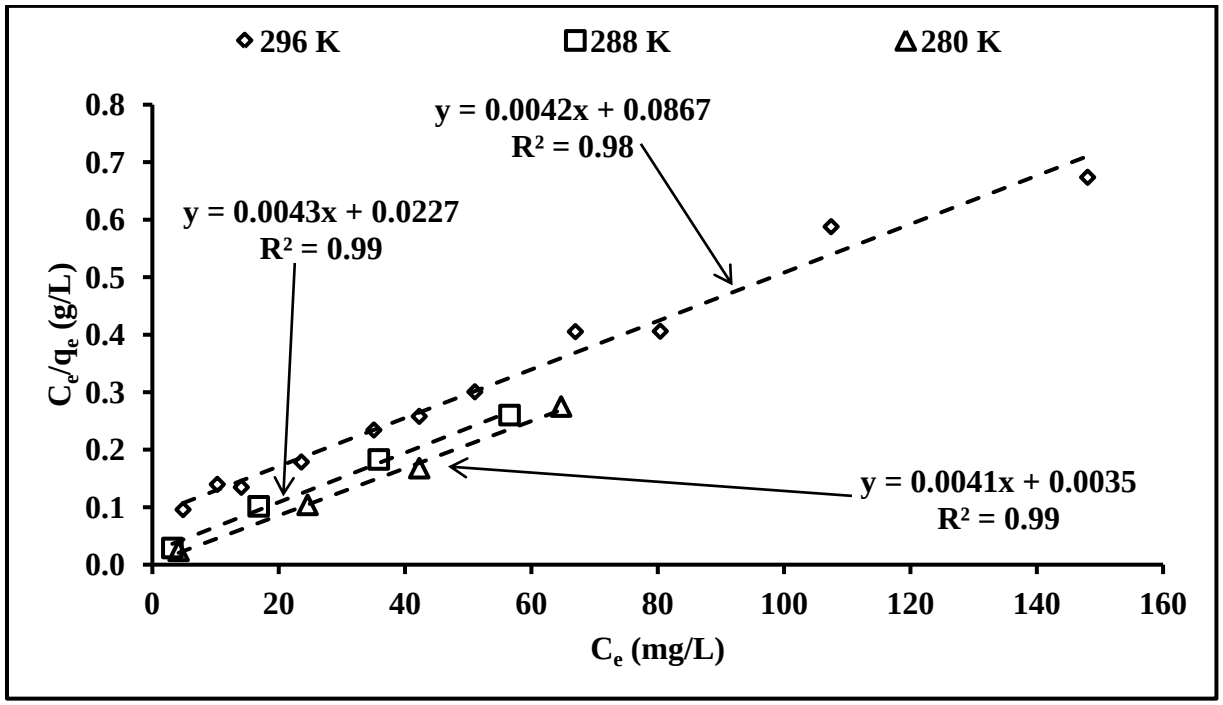

Figure C-3. Isotherm experimental data and linear Langmuir model fit to the data for adsorption of BPA on BC in Milli-Q water at 280, 288, and 296 K

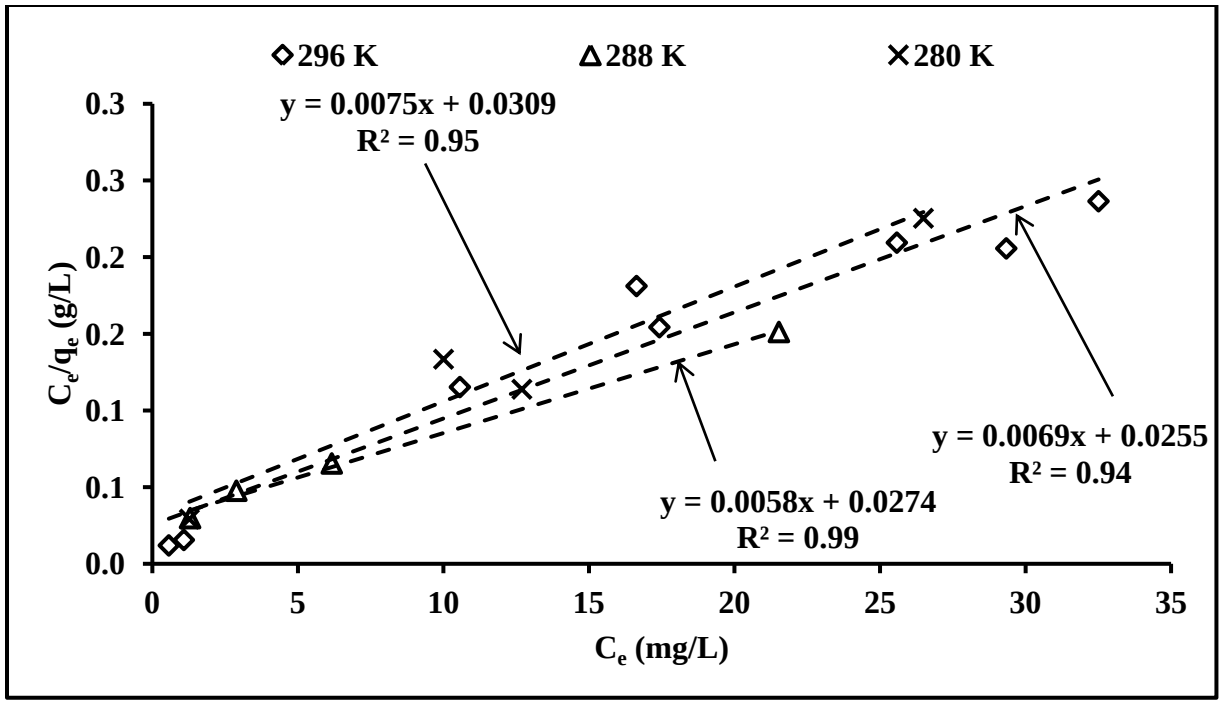

Figure C-4. Isotherm experimental data and linear Langmuir model fit to the data for adsorption of IBP on CS in Milli-Q water at 280, 288, and 296 K

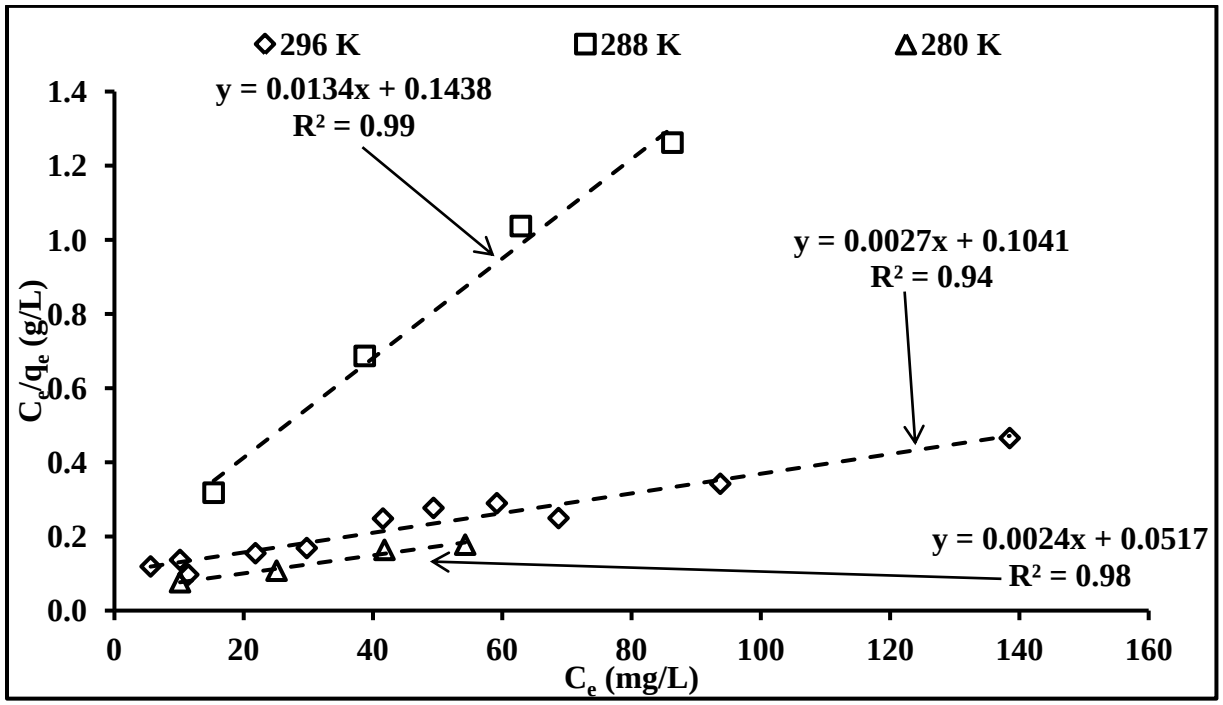

Figure C-5. Isotherm experimental data and linear Langmuir model fit to the data for adsorption of 2,4-D on CS in Milli-Q water at 280, 288, and 296 K

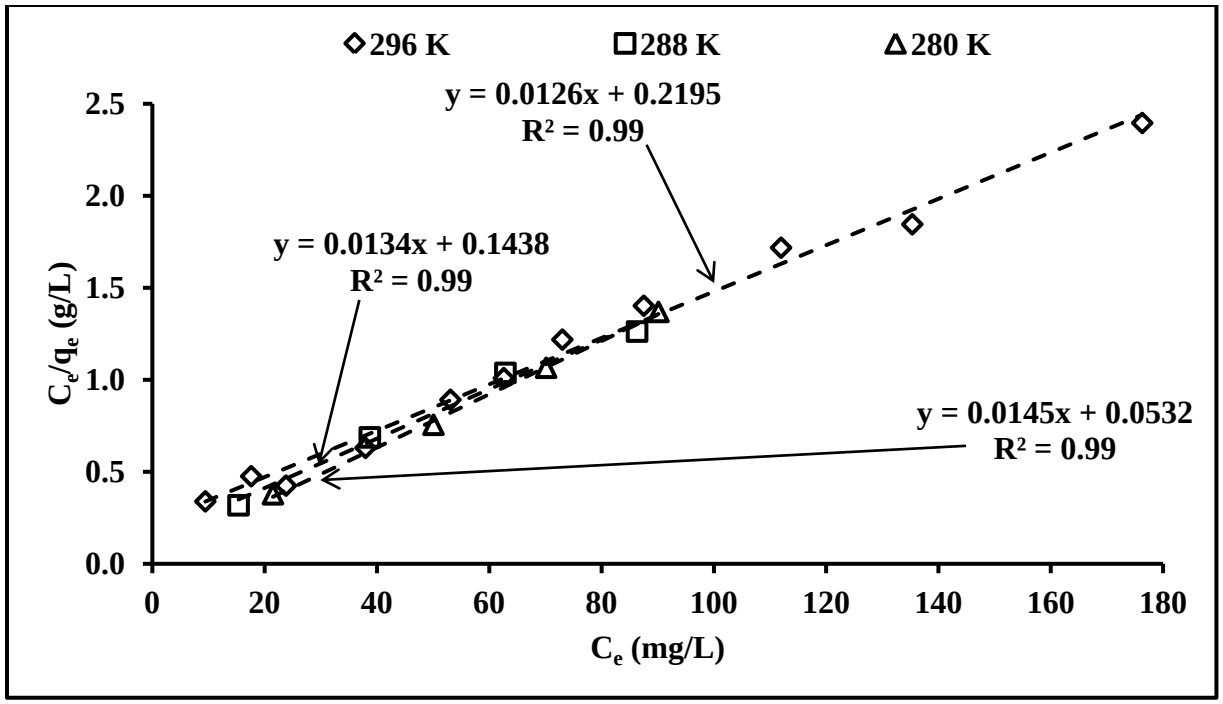

Figure C-6. Isotherm experimental data and linear Langmuir model fit to the data for adsorption of BPA on CS in Milli-Q water at 280, 288, and 296 K

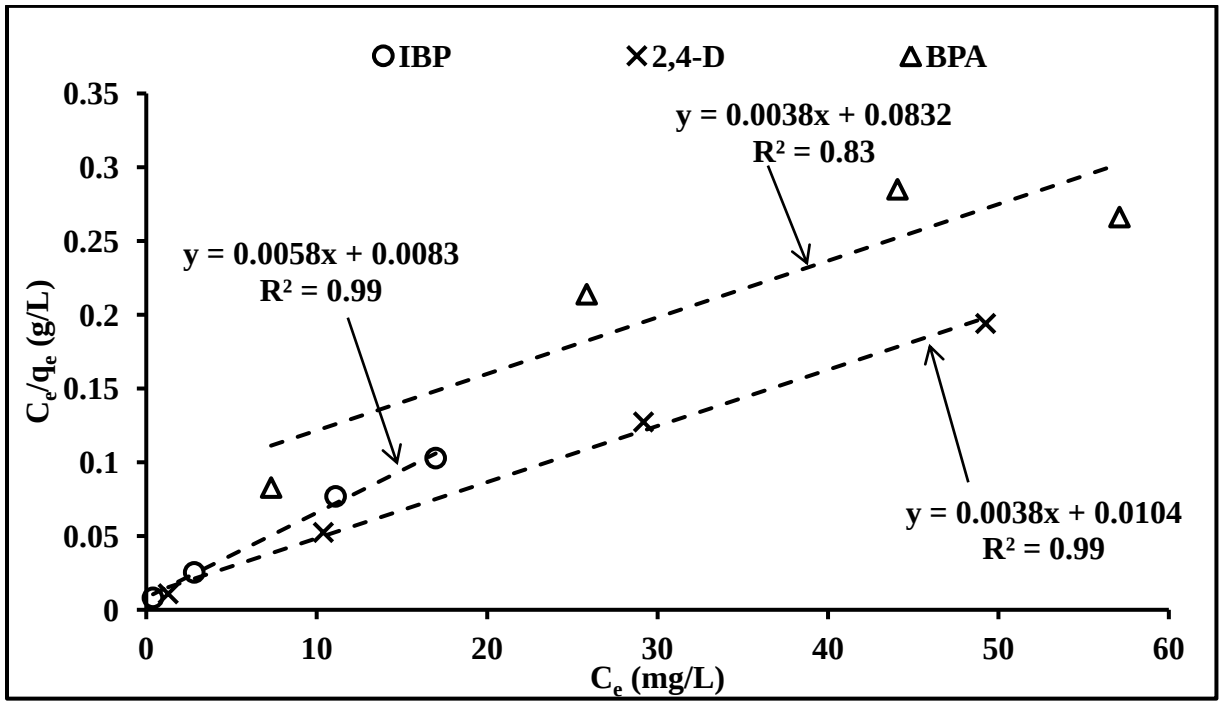

Figure C-7. Isotherm experimental data and linear Langmuir model fit to the data for adsorption of IBP, 2,4-D, and BPA on BC in tap water matrix at 296 K

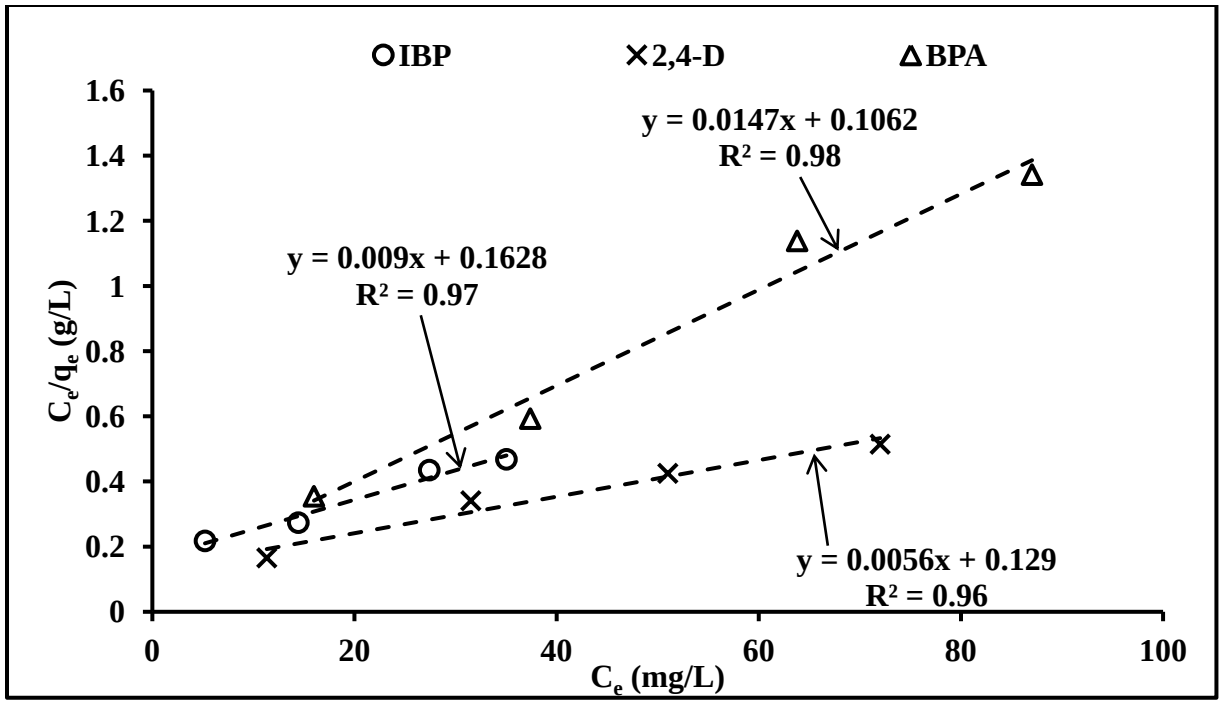

Figure C-8. Isotherm experimental data and linear Langmuir model fit to the data for adsorption of IBP, 2,4-D, and BPA on CS in tap water matrix at 296 K

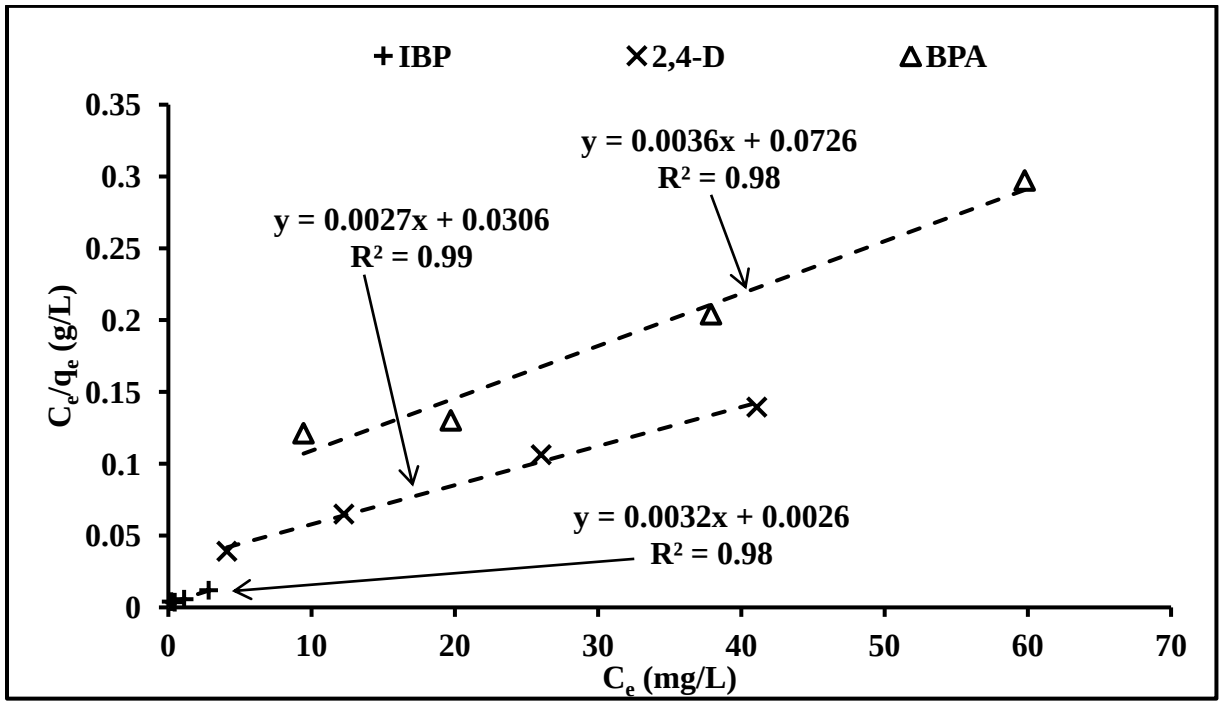

Figure C-9. Isotherm experimental data and linear Langmuir model fit to the data for adsorption of IBP, 2,4-D, and BPA on N-BC in Milli-Q water at 296 K

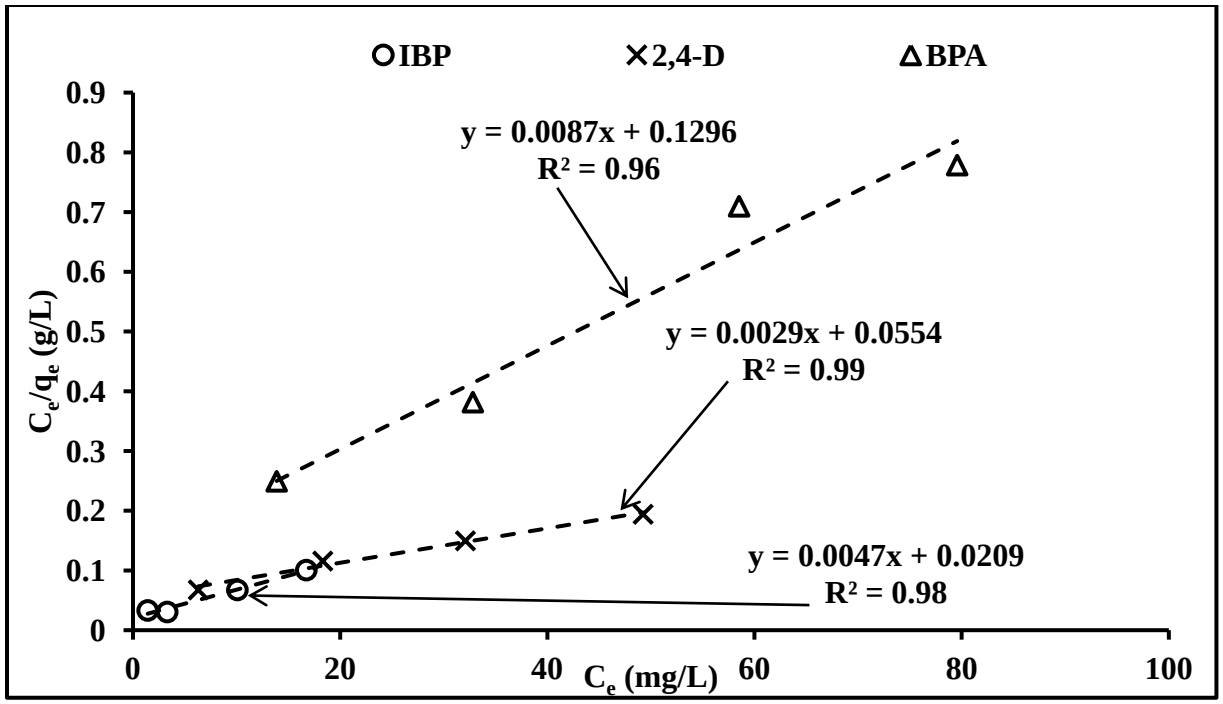

Figure C-10. Isotherm experimental data and linear Langmuir model fit to the data for adsorption of IBP, 2,4-D, and BPA on N-CS in Milli-Q water at 296 K

APPENDIX D. Van't Hoff Plot for Thermodynamic Analysis of Adsorption

In order to calculate the Gibbs free energy, enthalpy, and entropy of adsorption of model compounds on BC and CS in Milli-Q water, Langmuir model parameters for isotherm data of adsorption at 296, 288, and 296 K were used. Van't Hoff Plot for adsorption of BPA on BC using Langmuir model parameters for isotherm data of adsorption at 280, 288, and 296 K was presented in Figure 5-6. Van't Hoff Plot for adsorption of IBP, 2,4-D, and BPA on BC and CS in Milli-Q water using Langmuir model parameters for isotherm data of adsorption at 280, 288, and 296 K is presented below:

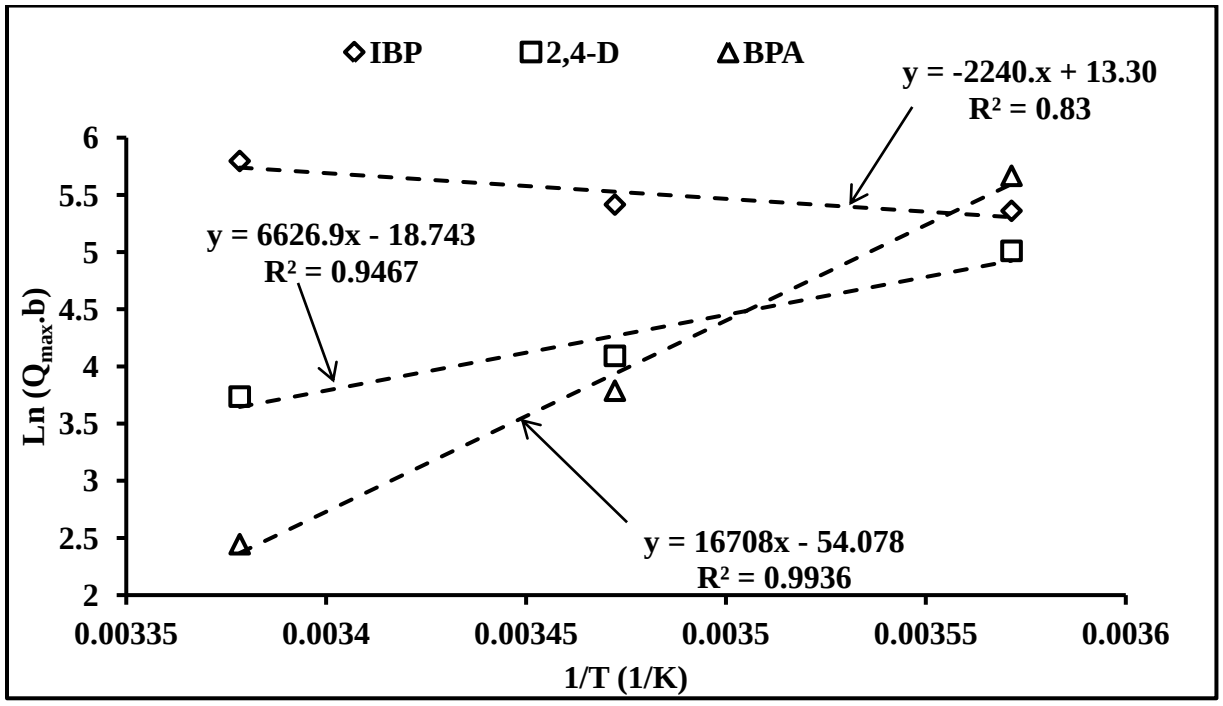

Figure D-1. Van't Hoff Plot for thermodynamic analysis of adsorption of IBP, 2,4-D, and BPA on BC in temperature range of 280-296 K

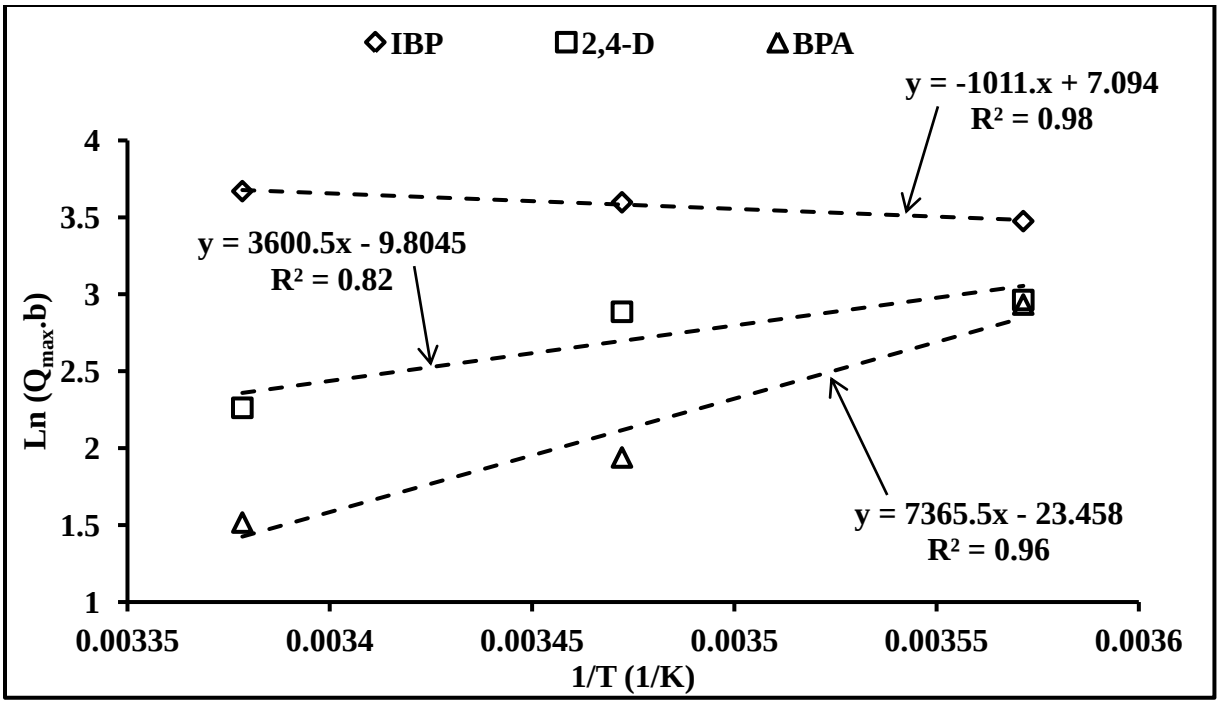

Figure D-2. Van't Hoff Plot for thermodynamic analysis of adsorption of IBP, 2,4-D, and BPA on CS in temperature range of 280-296 K